

MIE 243: Design Project

Conceptual Design of Robotic Arm for Hobbyist
Cinematographers

Group 18

Tulgar Ilhan 1010908163

Zeynep Elif Olmez 1010909055

João De Campos Carvalho 1010858519

Alek Adis Kilicyan 1011075765

1.0 Executive Summary	5
2.1 Problem Statement	6
2.2 Target Audience	6
2.3 General Overview	6
3.0 Research	7
3.1 Materials	7
3.2 Drive Mechanisms	8
3.3 Rotational Drive Motors	8
3.4 Camera mount	9
3.5 Customizability	9
3.6 Safety Features	10
4.0 Engineering Specifications	10
5.0 Candidate Designs	15
5.1 Idea Generation	15
5.2 Idea Selection	18
5.2.1 Candidate Design 1 Description	19
5.2.2 Candidate Design 3 Description	19
5.3 Final Design Selection	20
5.3.1 Objectives pair-wise comparison	20
5.3.2 Weighted Decision Matrix	21
6.0 Design Analysis and Description	22
6.1 Modelling Assumptions	22
6.1.1 Static + Dynamic Torque Requirements	22
6.1.2 Joint Speed Requirements	23
6.1.3 Power Estimation	24
6.1.4 Motor and Gear Ratio Selection	24
J2 – Shoulder (High Torque Joint)	24
J3 - Elbow	25
J5 - Wrist Pitch	25
6.1.5 Module Selection	26
Fatigue and stress limits assumptions	27
Contact limit	27
Module selection for stages of J2	28
6.2 Final Design Overview	28
6.2.1 Hexapod frame	29
6.2.2 Hexapod Legs	29
6.2.3 Base Rotation Planetary gearbox	29
6.2.4 Base Motor	30
6.2.5 Shoulder Rotation Planetary gearbox	30
6.2.6 Shoulder Motor	31
6.2.7 Forearm Rotation Planetary gearbox	31

6.2.8 Elbow Motor	32
6.2.9 Wrist Pitch Rotation Planetary gearbox	32
6.2.10 Wrist pitch Motor	33
6.2.11 Wrist roll rotation Planetary gearbox	33
6.2.12 Wrist Roll Motor	34
6.2.13 Camera attachment housing	34
6.2.14 Camera attachment frame and screw	34
6.2.15 Electronics container and telescopic cable channel	35
6.2.16 Emergency stop button	36
6.2.17 Shoulder Casing and metal frame	36
6.2.18 Forearm Casing	37
6.2.19 Wrist mount	37
6.3 Materials Selection	37
6.3.1 Gear Materials	37
6.3.2 Structural Metal Components - Brackets and Hexapod Holder	38
6.3.3 External Shells and Covers - ABS	39
6.4 Load Analysis	39
6.5 Risk Analysis	40
6.5.1 Robot Mass Representation	40
6.5.2 Risk Evaluation	40
6.5.3 Mitigation Measures	41
6.6 Design Trade Offs	41
7.0 Drawings	42
7.1 Assemblies	43
7.2 Drive Motors	44
7.3 Hexapod Structure	46
7.4 Structural Components and Casings	49
7.5 Camera Mount	53
7.6 Gearboxes	54
7.7 Gears	57
7.8 Motion Support Components	58
7.9 Shaft Coupling	60
7.10 Connectors	61
7.11 Carriers	62
7.12 Emergency Stop	65
8.0 Cost and Feasibility Analysis	66
8.1 Cost Analysis	66
8.2 Feasibility Analysis	69
9.0 Conclusion	70
10.0 References	71
11.0 Appendices	77

Appendix A: Idea generation methods	77
Appendix B: Candidate Designs	81
Appendix C: Idea and Final Design selection and reiteration	82
Appendix D: Python Calculations	83
Appendix E: Load Analysis	88

1.0 Executive Summary

This report presents the complete mechanical design of a long-reach, low-cost robotic arm developed for hobbyist cinematographers in the sports industry. The design addresses key limitations in current motion-control solutions such as high price and complexity by prioritizing affordability, stability, smooth motion, portability, and ease of assembly. The resulting system provides a reliable tool for dynamic pre-game sports cinematography, enabling users to achieve controlled pans, tilts, low-angle and high-angle shots, Dutch tilts, and repeatable 3D motion paths.

Extensive research was conducted to establish engineering requirements that reflect both industry standards and the needs of amateur filmmakers. Key topics included drive mechanisms, gear reduction systems, material selection, motor selection, camera-mounting interfaces, and safety features. This research informed a robust set of engineering specifications, ensuring the final design meets performance expectations for reach, stiffness, vibration limitation, motion precision, structural durability, and user safety.

The ideation phase produced multiple candidate concepts through structured brainstorming methods, including Black Box modelling, Blue-Sky Thinking, Morph Chart development, and SCAMPER iteration. Seven design concepts were generated and evaluated using multivoting, pair-wise objective comparison, and a weighted decision matrix. Design 6, a multi-DOF robotic arm employing planetary gear transmissions, was selected for final development due to its strong balance of stability, workspace size, dynamic capability, and feasibility. Subsequent refinement led to a 5-DOF configuration supported by a redesigned hexapod base that enhances stability and portability.

The finalized mechanical design integrates a series of stepper motors working in conjunction with custom planetary gearboxes, each optimized for joint-specific torque demands derived from dynamic modeling, gravity loading with safety factors, and worst-case workspace analysis. Structural components are manufactured from 6061 aluminum for strength and machinability, while ABS housings provide lightweight protection for internal components. Gear trains are fabricated from 42CrMo4 steel, which exceeds bending and contact stress requirements while minimizing cost.

A detailed kinematic and dynamic model validated torque and speed requirements for all joints, confirming that gearbox-motor combinations provide significant safety margins, including a $2.65\times$ margin at the most heavily loaded joint. Load simulations, material checks, and stress analyses ensure reliability across the entire workspace.

The projected cost established during the engineering specifications phase was \$5,000 CAD. Our calculated cost of \$3,713.52 CAD falls well within this budget, allowing for the affordability of hobbyist cinematographers. Overall, the final robotic arm design is well prepared to advance into the detailed design phase, meeting the needs of hobbyists while offering a competitive and innovative solution in the sports cinematography market.

2.0 Introduction

2.1 Problem Statement

There is a gap of relatively low cost and easily accessible robotic arms in the cinematography industry for hobbyists. This project aims to construct a robotic arm for cinematography, that is low cost and long reach, and is designed to produce smooth, consistent moving shots for users who cannot afford the high end professional equipment. Currently in the industry there are professional camera movement equipment that are often large in size, heavy, expensive and they demand several skilled operators, which makes them beyond the reach of amateur filmmakers. Some examples of these systems include track mounted dollies and Steadicams. Consequently, the hobbyists need a practical solution that offers steady camera positioning, regulated motion routes, and a broad enough working range to produce sweeping dramatic motions.

The aim of this project is to build a robotic arm that is relatively inexpensive compared to current industry standards, provides a large range of motion for long reach abilities, and offers smooth and reliable motion while remaining stable. The robotic arm is also designed to be easy to assemble and compatible with hobbyist users. The robotic arm must allow individuals to configure repetitive camera trajectories in three dimensions and produce high-quality motion. Thus, the final design must establish a balance between reach, rigidity, weight, and cost while making sure the arm can be produced utilizing accessible prototyping techniques and realistically built from inexpensive, commercially available materials.

2.2 Target Audience

The target audience is defined as hobbyist cinematographers and beginner professionals that aim to create promotional shots for sports and the players, as well as the pre-game content. This audience is unable to justify the expense of a professional robotic arm for filming, however they require a design solution that can film dynamic shots such as slow motion walks, rotational hero shots, high and low angle shots, and dramatic poses, and that is reliable and controlled. They need a system that is easy to use without special training and to assemble with lightweight cameras, and that can create high quality visuals with smooth motion routes.

Filming that is focused specifically on sports is usually conducted in wide indoor and outdoor environments, thus the intended users of the robotic arm prioritize portability and long reach capabilities. Large movement range, stable framing and smooth shots are essential for these users. The system offers a significant improvement over handheld equipment for creating sports advertising shots, since it is more cost-effective, secure, and relatively easy to operate.

2.3 General Overview

The aim of the project is to design a multi axis robotic arm for hobbyist cinematographers that need smooth and consistent motion for sports focused filming. In order to guide the

design process, significant research was conducted regarding currently available motion-control systems and professional robotic arms to discover the operational qualities desired by film makers. The research included common joint and drive mechanisms, material choices and motor-gearbox configurations used in commercial robotic arms. Additionally, the mechanical requirements, such as torque demands for every joint, structural integrity of the design and vibration control, for a stable and long reach motion were inspected. The research was used as a benchmark to guarantee that the final design could provide dependable cinematic shots. Furthermore, comparisons of production techniques, casing elements, and affordable drivetrain alternatives guided decisions that kept the system inexpensive without losing durability. According to the patterns seen in current engineering products, safety considerations, ease of assembly, and upgrade compatibility were also included. Overall, the data gathered creates a basis for a robotic arm design that mixes practicality, cost, and visual performance, giving a readily available tool for filmmakers wishing to upgrade their sports-focused work.

3.0 Research

This section gives an overview of the features and mechanisms found in a robotic arm.

3.1 Materials

When researching robotic arms for different applications, hobbyists and industrial applications, the materials for structural members, casings and bases were inspected. The comparisons were made by utilizing the most common commercially available robotic arms like the Universal Robots UR5/UR10, Franka Emika Panda, and Kinova Gen3 [1]. These options mainly rely on 6061-T6 or 6063-T5 aluminum extensions for their arm links and joint housings as they effectively balance machinability and strength while also being low weight. Aluminium provides enough stiffness to minimize vibration during movement, a vital requirement in ensuring smooth camera footage, while also having easy machinability using workshop tools compared to other metals like steel [2] . Other materials such as polycarbonate (PC), ABS, or nylon outer casings are used to improve aesthetics and provide lower weight and a low cost solution for protecting internal wiring and motors. These materials are commonly found in consumer and research robotics as they are durable, impact resistant and inexpensive to mold or 3D print [3].

Furthermore, after assessing existing robotic bases and mounting structure, it was concluded that the most stable designs use steel or reinforced aluminium for internal load bearing components as they provide high stiffness and effective vibration damping that prevent camera shake [4]. Given the requirements of the robotic arm being designed of low cost, portability, rigidity, vibration reduction and easy manufacturability, the design will use a steel insert reinforced base, aluminium 6061 for the castings, and ABCS/PC for cosmetic housings and cable covers. Using aluminium allows structural links to remain low weight but still strong, while ABS and polycarbonate reduces costs and simplifies manufacturing. Overall,

the materials chosen align with industry standards while being a viable and accessible option for hobbyists, providing durability, smooth motion and easy assembly.

3.2 Drive Mechanisms

A robotic arm's drive mechanisms enable precisely controlled movement at the base, shoulder, elbow, and wrist by generating and transmitting rotating motion at every joint. Proper camera routes need smooth rotation, reliable torque output, and repeatable alignment for lightweight robotic arms intended for cinematography. Thus the most suitable mechanism options for our design include rotating actuators combined with mechanical gear reduction systems. Planetary gearboxes specifically are frequently utilized in robotic joints as they enhance motor torque, lower output speed, and offer reliable performance under a variety of loads [5]. To ensure steady, vibration free camera motion, planetary gearboxes transmit torque amongst many gears that promote endurance and decrease slippage [6].

The advantages of planetary gears are lower backlash in comparison to normal spur gear reductions. This provides improved point to point accuracy of the motion and smoothness, as well as less camera shake due to slight directional shifts at the joints. Additionally, these features support the tracking and pan shots [7]. The disadvantages of this mechanism are that they are more costly and complicated than standard spur gear trains, and they need careful construction to preserve the precise positioning of the internal gear stages [8]. Although this mechanism might be more expensive due to its compact size, stable output and high torque density, the planetary gearbox mechanisms are a more practical choice for a robotic arm since it has a better price-performance ratio for a hobbyist robotic arm.

Harmonic drive is another mechanism found in robotic arms that is utilized to optimize precision. It is a form of strain-wave gearing notable for its exceptionally minimal backlash and great positional precision. Harmonic drives are suitable for joints like wrist or elbow joints that need precise positioning adjustments since they can accomplish gear reductions of 50:1 to over 160:1 in a small footprint using an adaptable spline and elliptical wave generator [9]. The camera stabilization is enabled by the close to zero backlash that creates smooth and consistent motion. Compared to planetary gearboxes, this mechanism is more expensive and it might reduce efficiency at elevated speeds [10]. They are mostly used in high-end robotic arms, however for hobbyist cinematographers their cost and specialized production needs make them less suitable.

3.3 Rotational Drive Motors

Rotary actuators allow for there to be precise motion at each joint of the robotic arm, meaning that during cinematography practices the camera position can be modified. When looking at currently existing actuator configurations, such as used in the Universal Robots UR5/UR10, Franka Emika Panda, Kinova Gen3, and KUKA LBR iiwa designs, it was found that these systems scale the amount of torque that a joint can output by utilizing varying motor size, gearing, and transmission methods [1]. Larger actuators are placed where the torque demands are highest, at the base and shoulder, while smaller motors are used toward

the wrist as this reduces inertia and improves responsiveness [11]. This usage aligns closely with the usage in our design, which integrates three different stepper motor frame sizes, NEMA 34, NEMA 23, and NEMA 17, to meet the various requirements of each joint. The NEMA 34 motor provides high holding torque that is needed for the base rotation joint that works to counteract the full leverage and mass of the arm [12]. The shoulder and elbow joints use NEMA 23 motors, as it delivers moderate torque and great repeatability. This is similar to the mid joint actuators found in many lightweight robotic manipulators commercially available [13]. Finally, a compact NEMA 17 motor is used at the wrist, where the reduced load allows for smaller actuators, ensuring precise and smooth camera movements [14].

Although servo motors tend to operate at higher efficiencies and lower noise levels, stepper motors offer better positional accuracy at lower speeds and higher holding torque without the need for complex feedback systems [15]. This characteristic is incredibly valuable for cinematography as slow, deliberate movements and stable fixed positions are more important than high speed motion. By selecting motors of different sizes at each joint, our design replicates torque scaling strategies that are used in professional robotic arms while still having easy manufacturability and being affordable for hobbyist users.

3.4 Camera mount

The main end-effector of the robotic arm is the camera mount mechanism, which holds the camera stably and permits accurate alignment during operation. The camera mount must have features, such as being lightweight, stable and compatible with conventional camera gear, to ensure smooth motion that minimizes vibration for cinematography applications. Standardized $\frac{1}{4}$ "-20 and $\frac{3}{8}$ "-16 threaded plate interfaces or Arca-Swiss style quick-release clamps are used in the majority of consumer and specialized camera accessories, such as those from DJI, Freefly, SmallRig, and Manfrotto. This enables users to attach DSLRs, mirrorless systems, and compact film cameras without the need for customized hardware [16][17]. Our design adheres to these same guidelines, guaranteeing widespread compatibility with typical filmmaking tools and attachments.

The camera mount is connected to the wrist of the robotic arm allowing smooth and controlled shots. Many stabilization components and gimbal systems utilize rubber isolation bushings, elastomer damper elements, or soft-mounted plates to absorb vibrations with high frequencies while maintaining structural rigidity given that even minor vibrations can deteriorate quality of the shots [18]. This arrangement provides rigid support avoiding exerting excessive load on the wrist motor by using lighter mechanical parts.

3.5 Customizability

The ability to customize aspects of a robotic arm is an important feature because it allows users to improve the arms functionality and adapt it to different conditions. The majority of modern robotic arms emphasize the importance of modularity and enable users to alter the robot to a wide range of tasks, by changing the following features [19][20][21]:

- Replaceable camera mounts
- Camera control components (wired or wireless)
- Extra stabilization components
- Interchangeable end-effectors
- Wireless safety stop component

3.6 Safety Features

The power isolation switch and emergency stop button are the two crucial safety measures that are always present nowadays in robotic arms, and they both need to be readily available to the operator of the machine. Current industry robots, such as the Universal Robots UR5, Franka Emika Panda and KUKA LBR iiwa, utilize visible emergency stop systems to instantly cease motion in case of unexpected motion, mechanical malfunctions and possible operator injuries [22][23][24]. Clear vision and unhindered access to the emergency stop are essential for cinematography applications, since users regularly operate in close range to the moving arm. Furthermore, torque limitations, and joint recognition are often integrated into robotic arms in order to avoid the machine from operating beyond safe areas or applying excessive force [25]. While adhering to current robotic safety regulations, these precautions guarantee that the robotic arm functions dependably and protects the operator and the robot while in operation.

4.0 Engineering Specifications

The design specifications for our robotic arm design for hobbyist cinematographers, shown in Tables 1 and 2, were developed by studying the latest product designs and suggesting necessary additional features. The design specs were adjusted for increased quality of life of the users, and were established to ensure our robotic arm would be competitive with existing solutions and offer unique advantages targeted to user demands.

Table 1. Engineering Specifications

Specification	Metric	Justification
Endpoint Payload Capacity	$\leq 1.3 \text{ kg}$	When combined with a tiny setup, a hobbyist-level cinematography camera such as the Sony A7 III weighs no more than 1 kilogram. Setting the endpoint payload to 1.3 kg provides a 30% safety margin for dynamic operational loads. [26]

Must keep vibration frequencies low enough to avoid apparent jitter during video capture.	≤ 10 Hz	Human hand-held camera shake is typically observed in the 10-20 Hz range. The optical image-stabilization devices are designed to correct camera motion predominantly between 0.5 and 20 Hz. Vibrations over \sim 10 Hz are at the top limit of the correction range and often appear as high-frequency jitter in film [27].
Camera Attachment	The threaded interface must have 1/4-20 UNC (\approx 6.35 mm major diameter) and 3/8-16 UNC (\approx 9.52 mm major diameter).	Photography-gear guides confirm 1/4-20 UNC is common for most consumer cameras, and 3/8-16 UNC is for heavier/professional equipment [28].
All motors must operate with the same encoding system.	SDM32G431	Using a single encoder system ensures constant position feedback, simplifies motor-controller connections, reduces calibration errors, and enables uniform control algorithms across all joints [29].
Must have a static base while in operation.	The base must remain immobile during all actuator motion, with no translational movement (0 m/s) and no rotation $> 1^\circ$ under full payload and maximum arm speed.	A static base prevents inadvertent camera motion, reduces transmitted vibration, and provides constant framing during cinematic shots, all of which are crucial for stability when capturing athletes in pre-game conditions [30].
Must have ≥ 3 degrees of freedom.	The arm must at least provide yaw, pitch, and roll to enable 3-DOF motion.	Pans require yaw control, allowing the camera to rotate horizontally [31]. Dutch tilt requires roll rotation (wrist roll) to tilt the frame diagonally [32]. Tilts, high-angle and low-angle shots require vertical pitch motion at the shoulder and forearm joints [31].

Operation Height	Must be able to reach up to 1.7 m high for eye-level shots.	Ergonomic anthropometric data lists the mean standing eye height for men as 1.635 m. [L 33].
Must support multiple camera motion and framing modes: static shots, pan, eye level, high angle, low angle, and Dutch tilt.	Static shots, pan, eye level, high angle, low angle, Dutch tilt	These shots are standard cinematic framing techniques required for pre-game athlete coverage, allowing for dramatic overheads, tight low-angle "hero" shots, and upright portrait framing. Range flexibility allows the arm to position the camera without adjusting the base or tripod [34].
Weight	The total mass of the robot system (base + arm + motors + electronics, excluding camera and external accessories) must be \leq 24 kg.	Under ideal conditions, the NIOSH lifting equation defines a maximum recommended manual lifting load of about 23 kg for a healthy worker [35].
Must support smooth horizontal motion suitable for walking-pace tracking shots.	Maximum translational speed is 1.5 m/s	Healthy adults typically walk at around 1.31 m/s outdoors [36]. Setting the robot's speed slightly higher than this ensures it can comfortably track normal pre-game walking movements without requiring excessive speed capability.
Rotational motion (camera/arm yaw or pan speed).	Rotational motion must be \geq 120 degrees per second.	Professional robotic camera arms and gimbals often offer rotational speeds in the range of 120–200°/s to facilitate smooth pans and dynamic camera movements for cinematic effect [37].
Must be assembled with screws.	All structural joints and panels must use standard machine screws (e.g., M3/M4/M5 or 1/4"-20), no adhesives or welds.	Educational robotic kits commonly rely on screws for assembly because screws enable easy disassembly, maintenance, and component replacement [38].

Must be assembled with tools in a standard toolbox.	To assemble and service the robot, a basic household/DIY toolkit, such as screwdriver bits, hex/Allen keys, pliers, driver handles, and hex keys from the Hi-Spec 24-piece Household/DIY Tool Kit, must be enough [39].	Designing the robot in such a way that allows the hobbyist to assemble/service it using a standard toolbox reduces maintenance complexity, lowers cost, and ensures accessibility for users.
Total hardware cost	< 5,000 CAD	Budget constraints set by design requirements; all components (structure, motors, electronics, etc.) must be selected so that the total BOM stays under 5,000 CAD. The current industry robotic arm prices range between 5000 - 9000 USD [40][41].
Reach radius	$\geq 1.0 \text{ m}$	A 1.0 m reach is considered long for compact and low-cost robotic arms, as many desktop and small collaborative robots operate in the 0.3–0.6 m range (e.g., Meca 500: 0.33 m reach); therefore, a $\geq 1.0 \text{ m}$ envelope positions this system at the upper end of the compact-robot workspace class [42].
Lifetime	$\geq 10,000$ operating hours	Stepper motors such as NEMA 17 typically have lifetimes up to 20,000 hours [43]

Table 2. Engineering Safety Specifications [44][45][46]

SAFETY SPECIFICATIONS		
Specification	Metric	Justification
Emergency Stop Function	Stop time ≤ 1.0 s (Cat 1) OR immediate power removal ≤ 0.2 s (Cat 0)	Stop behaviour and categories formally defined in IEC 60204-1.
Risk Assessment Requirement	All hazards identified; residual risk $<$ Medium (Risk Index $\leq 3 \times 3$)	Mandatory structured risk analysis per ISO 12100.
Power & Force Limiting (PFL)	Transient contact force ≤ 140 N; Quasi-static force ≤ 65 N	Human-robot contact biomechanical limits defined in ISO 15066.
Speed & Separation Monitoring (SSM)	Minimum protective distance ≥ 250 mm at 1.5 m/s robot speed	Protective distance calculation method defined in ISO 13855.
Collaborative Workspace Design	Gap width ≥ 25 mm OR ≤ 4 mm at all joints	Crushing and trapping hazard dimensions defined in ISO 13854.
Functional Safety – PL Assignment	Minimum Performance Level = PL d	Safety-related control system classification defined in ISO 13849-1.
Safety Control System Validation	MTTFd ≥ 30 years; DCavg $\geq 90\%$	Safety validation methodology defined in ISO 13849-2.

5.0 Candidate Designs

This section outlines the idea generation and selection process that led to our final design. The methods used for idea generation are shown in Appendix A. The initial candidate designs are represented in Appendix B and the idea selection process is represented in Appendix C.

5.1 Idea Generation

Several engineering techniques were used throughout the project's ideation stage to make sure the suggested design solutions matched our engineering specifications and catered to the needs of hobbyist users. The ideation techniques include Black Box Method, Blue Sky Thinking, Free Brainstorming, Morph Chart, and SCAMPER method. Each technique was used to come up with different design aspects of our robot and by combination and optimization of these aspects the 3 initial candidate designs were generated. After determining the initial candidates, iterations were made by team discussion, and a total of 7 other improved candidate designs were produced.

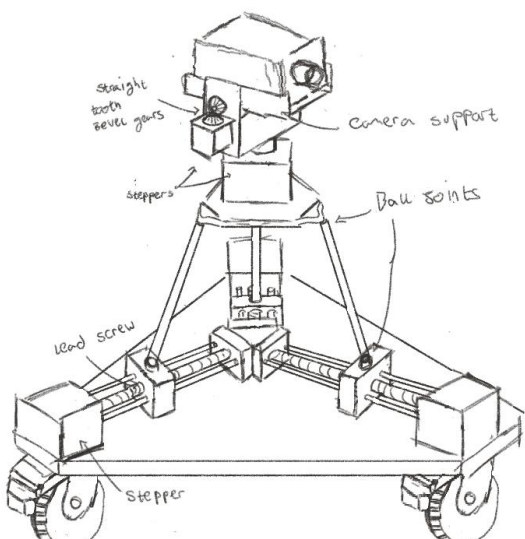
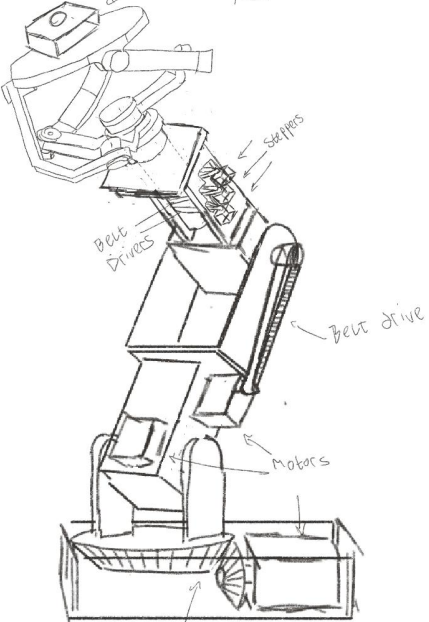
In order to define the mechanical scope of the project the Black Box Method, shown in Figure 78, was used. The method determined the inputs of the system to be the power supply of the system, human operations regarding the robotic arm, payload and materials. The system was described as the base, arm linkages, rotational joints, stabilization features during operation, camera attachment to the wrist and safety features. The aim of the system was to move the camera by placing it onto the proper attachment, and achieve the desired shots described in the design specifications by having long-reach. It highlighted the importance of multiple joint movements thus the need for multiple degrees of freedom, such as at least 3, while also keeping the robot dynamic when not in operation for ease of use purposes.

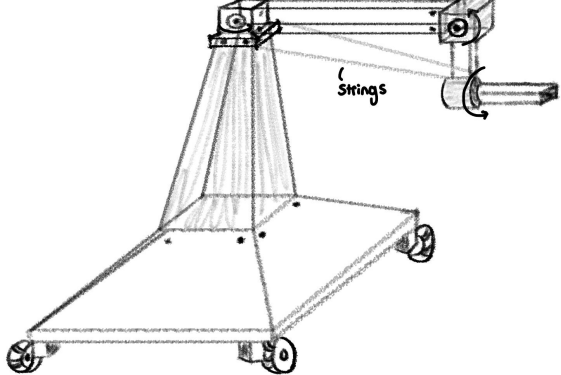
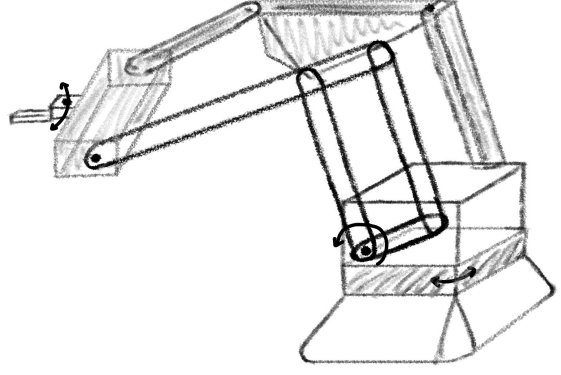
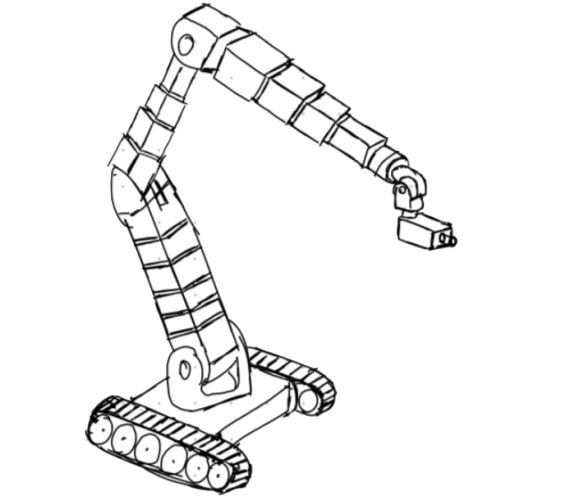
Both the Blue Sky Thinking and Free Brainstorming methods were used to generate 22 ideas in total regarding the motion mechanism of the robot, as well as base, forearm and wrist designs that allow motion that match with our specifications. The Blue Sky thinking method was utilized since it allowed idea generation without restrictions and the Free Brainstorming method allowed us to generate mostly feasible ideas. The ideas generated through these methods are shown in Tables 11 and 12. These ideas were then further evaluated to eliminate the duplicates and non-feasible ideas, and with the remaining ideas a Morph chart was created.

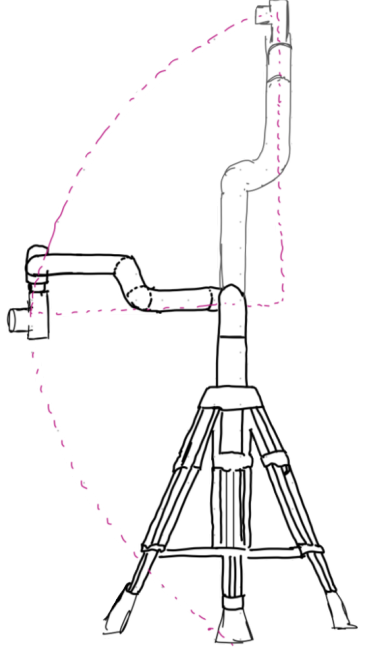
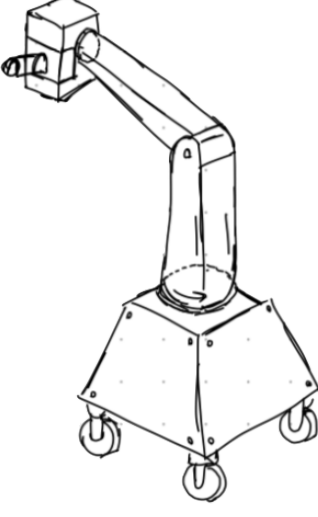
The Morph chart, shown in Table 13, aimed to group the existing ideas from different categories and turn them into candidate design solutions. The categories, also known as the functions, in the table included; the base, robotic arm mechanism type, shoulder joints, safety features, stabilization of the robotic arm, and camera orientation. By this categorization, our 3 initial candidate designs were formed, as represented in Figures 79, 80, 81.a and 81.b in Appendix B.

Initial candidates were iterated for further differentiation by team discussion, and using the SCAMPER method. All aspects of the design were reconsidered and changed if found necessary. This method allowed us to substitute, combine, adapt, modify, put to another use, eliminate and reverse different mechanisms within the designs. It was performed 2-3 times for each candidate design, shown in Tables 14 - 20. Consequently, 7 candidate designs were produced and the final designs are presented in Table 3.

Table 3. Candidate design drawings and description (final 7)

Design #	Conceptual Design Drawings	Description
1	 <p>Figure 1. Isometric view of Design 1</p>	<p>A 5 DOF robot that utilizes a parallel linear actuator mechanism on the base with attachable lockable caster wheels. The motion supports are provided with metal ball joints. Includes multiple steppers and a screw in camera mount. The rotation of the camera is provided by a perpendicular straight tooth bevel gear pair.</p>
2	 <p>Figure 2. Isometric view of Design 2</p>	<p>A spherical orbital system is created for rotation of the camera, by a spherical parallel manipulator. At the end of the manipulator there is a screw in camera mount. The base movement is performed using a straight tooth bevel gear pair and the forearm movement is performed by a belt drive mechanism.</p>

3	 <p>Figure 3. Isometric view of Design 3</p>	<p>A 3 DOF robot that has removable string attachments for payload support. Utilizes a heavy base to counterweight the moment generated by the arm movement. The motion supports in the system include a thrust bearing for the base yaw, a roller bearing for the forearm pitch, and a ball bearing for the wrist roll.</p>
4	 <p>Figure 4. Isometric view of Design 4</p>	<p>A 3 DOF robot that utilizes a parallel four-bar mechanism for forearm pitch. Provides a 360-degree base yaw utilizing pulley mechanisms and a thrust bearing for motion support. The wrist includes a standard camera attachment with screws, and the wrist roll is provided by a perpendicular straight tooth bevel gear pair with ball bearings as motion support.</p>
5	 <p>Figure 5. Isometric view of Design 5</p>	<p>A telescopic arm mechanism is used to adjust the reach of the robot. The movement of the robot is performed by utilizing tank tracks that also stabilize the robot. Overhead reach is performed by reversed joint orientation. The rotational movement of the forearm is provided by planetary gears.</p>

6	 <p>Figure 6. Isometric view of Design 6</p>	<p>A 6 DOF robot that has a tripod base for stability and adjustability of the height. A thrust bearing and a gearbox mechanism are used for the base yaw. For forearm pitch and shoulder pitch, a belt drive mechanism is used, including a straight tooth bevel gear. The wrist motion is supported by a ball bearing, and the wrist has a standard screw camera attachment.</p>
7	 <p>Figure 7. Isometric view of Design 7</p>	<p>A 3 DOF robot that performs base yaw, shoulder pitch, and wrist roll. The mechanisms include roller bearings for motion support, planetary gears for motion conversion, and a gearbox for motion transformation. Multiple shafts are also used throughout the design for motion transmission.</p>

5.2 Idea Selection

After iterating through the seven candidate designs, our team held a discussion session to assess the feasibility of each candidate. Designs 2 and 4, shown in Figures 2 and 4, were deemed not worth pursuing after discussion due to not meeting the low budget constraint. Multi-voting was then employed to select the top three candidates from the remaining pool for further consideration in the idea selection process, as it allowed each team member to rank the designs based on their perceived alignment with the project's goals [Appendix C]. This resulted in selecting designs 1, 3, and 6.

5.2.1 Candidate Design 1 Description

Candidate Design 1, shown in Figure 8, is a 5-DOF system based on a 3-DOF linear parallel manipulator at the base, enabling complex camera-base motion, including full translational motion and limited pitch and roll. A second and third stepper motor in the camera base and on the side of the camera mount allow for camera yaw movement and 180 degrees of roll, enabling the robot to meet all the shot requirements. Due to the design's geometry, the end effector's height range was severely limited without affecting overall size constraints, which made it difficult to perform high- and low-angle shots efficiently.



Figure 8. Candidate Design 1 CAD

5.2.2 Candidate Design 3 Description

Candidate Design 3, shown in Figure 9, is a 3-DOF system that uses string supports to account for camera weight and allow for more budget-friendly motors. Among the selected candidate designs, Candidate 3 is estimated to be the least expensive to manufacture due to its simplicity. While limited in the number of camera shots it allows, the large base enables stable filming, and its simplicity enables a more reliable final product.

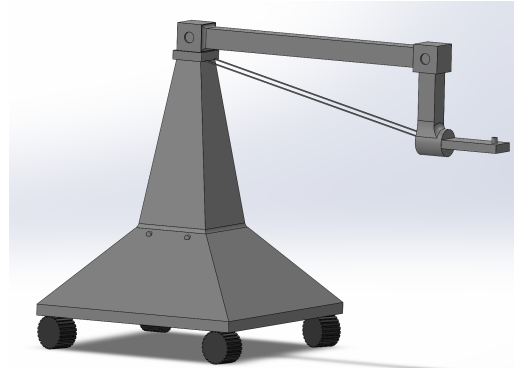


Figure 9. Candidate Design 3 CAD

5.2.3 Candidate Design 6 Description

Candidate Design, shown in Figure 10, is a 6-DOF design that uses belt drives to move the internal mechanism's weight closer to the motors and leverages planetary gearboxes to enable the selection of cheaper motors, accounting for the high degree of motion the robot can perform. The high number of motors required also increases the overall cost of this design. The tripod base offsets the high costs of this robot design and enables easy transportation and height adjustment before filming; however, concerns remain about the design's stability during operation.



Figure 10. Candidate Design 6 CAD

5.3 Final Design Selection

After selecting the top 3 candidates that met the project requirements, a pairwise comparison of our objectives yielded a weight decision matrix that enabled selecting the optimal design within our specifications.

5.3.1 Objectives pair-wise comparison

To objectively assess our final candidate designs, the project objectives were compared to determine their relative importance to the final design. A pairwise comparison was chosen for this process because it used information from every team member to evaluate our selected objectives mathematically. 8 Objectives were selected, and their importance was compared with all other objectives through team discussion using the 1-9 Relative importance scale [47]. The weighted average of the metric comparisons for each objective is then used to establish the final weights and rankings, as shown in Table 4.

Table 4. Results of Pair-Wise comparison of objectives

OBJECTIVE WEIGHTS			
#	Objective	Weight	Rank
1	Must remain stable on both smooth and rugged surfaces	6.48%	7
2	Must have options for 3/8" screw and 1/4" screw attachments for camera attachment to the endpoint of the arm	6.50%	6
3	Must have an endpoint reach within a ≥ 1 meter radius semisphere	22.23%	2
4	Must be able to be assembled with tools in standard toolbox	1.29%	8
5	Translational motion should be ≥ 10 kph.	10.14%	4/5
6	Rotational motion should be ≥ 120 degrees per second.	10.14%	4/5
7	Must have Base Yaw (360 degrees), Shoulder Pitch(180 degrees), Forearm Pitch (180 degree), Wrist Roll(360), Camera Yaw (360 degrees) = 5 degrees of freedom	28.13%	1
8	Must have vibrational frequencies ≤ 3 Hz during operation	15.09%	3

5.3.2 Weighted Decision Matrix

The Data from the Pair-Wise comparison were then used to evaluate the 3 final candidate designs in a Weighted Decision Matrix. Each team member rated each design's performance on each objective on a scale of 1-10, based on their personal understanding of the design's capabilities. The voting averages were imputed into the matrix and multiplied by each objective's weight to produce the final design. This output is a numerical metric on how each design fulfilled the project objectives. Resulting in Candidate Design 6 having the best score and being selected as the final candidate design based on objective qualifications. Demonstrated in Table 5.

Table 5. Weighted Decision Matrix results.

Weighting Factor Applied			
Objective #	Candidate 3	Candidate 6	Candidate 6
7	16.17%	28.13%	26.72%
3	20.01%	20.01%	11.67%
8	10.56%	10.56%	11.32%
5	6.84%	6.84%	6.84%
6	8.11%	8.11%	7.86%
2	6.50%	6.50%	6.50%
1	4.54%	4.86%	3.89%
4	0.77%	0.77%	1.19%
Totals	61.70%	73.66%	64.41%

5.4 Final design reiteration and development

After selecting Design 6 as the final candidate, a team meeting was held to evaluate the specific mechanisms and direct further development of the design. A 5-DOF design was deemed optimal because 6-DOF was redundant for the particular shots the camera robot was expected to perform. The first reiteration of the final design is detailed in Appendix C. As the development process continued, concerns about the stability of the robot base led to the development of a Hexapod base, with six legs instead of three, to ensure stable motion during operation. The size constraint of the robot, along with the weight of electronic components, led to the design of an electronics casing underneath the robot to avoid overloading the motors and to facilitate the robot's movement while lowering the center of mass, further improving stability. The size limitation of the robot's stage casings also prevented the use of belt drives, as the extra weight and space they required were not optimal for this project's specific constraints.

6.0 Design Analysis and Description

This section analyses the actuators, transmissions, and mechanical components of the robot. A full kinematic and dynamic model was implemented in Python using the principle of exponentials(POE) formulation. The model evaluates gravity loads and joint speed requirements across the robot's workspace. These results are used to select motors, gear ratios, gear modules and structural materials. Python calculations can be seen in Appendix D.

6.1 Modelling Assumptions

To obtain conservative torque calculations, the following modelling assumptions were made:

- All link masses and payload are treated as a single effective mass located at the wrist.
- The effective mass used in the simulations is:
$$m_{eff} = m_{arm} + m_{payload} = 17kg + 1.35kg$$
- End-effector acceleration = $a_{des} = 3m/s^2$
- Gravity torques include 1.5x design safety margin to account for modelling errors.
- All joint limits were included in the workspace sampling to identify worst-case configurations.

These assumptions intentionally overestimate loads, ensuring safe motor and gearbox selection.

6.1.1 Static + Dynamic Torque Requirements

The model finds both the gravity torques and the dynamic torques. The final design torque is the sum of both, and can be seen in Table 6.

Table 6. Torque Calculations

Joint	Gravity Torque	Dynamic Torque	Design Torque(Total) $\tau_{total} = \tau_{gravity} + \tau_{dynamic}$
J1 - Base Yaw	0N.m	45. 9 N.m	45. 9 Nm
J2 – Shoulder Pitch	225 N·m	45. 893 N.m	271 Nm
J3 – Elbow Pitch	86. 46N.m	17. 63 N.m	104. 1 Nm
J4 – Wrist Roll	negligible	small/friction only	0 Nm
J5 – Wrist Pitch	14.85 N.m	3 N.m	19.7 Nm

Notes:

- J4 rotates about its own axis and experiences almost no gravity loading; only frictional and inertial effects matter.
- J2 is the dominant joint and drives the torque requirements of upstream components. This is the shoulder pitch

6.1.2 Joint Speed Requirements

The workspace scan (this is a section in the code) also computed the worst-case joint velocities needed to achieve a 1.5 m/s end-effector speed.

Theoretical max from Jacobian is:

$$|q'|_{max} = [0, 9.55, 12.60, 9.27, 21.36] rad/s$$

The Jacobian scan returns very high joint speeds because it includes configurations close to kinematic singularities, where tiny end-effector motions mathematically require extremely large joint velocities. These values are not physically achievable and do not represent real operating conditions.

Real robots avoid singularities, and motors cannot reach those theoretical speeds once gearbox friction, inertia, torque-speed limits, and thermal limits are considered.

Therefore, instead of using the singularity-driven values (9–21 rad/s), realistic design speeds were chosen:

$$\begin{aligned} J2 - J3: 1.7 \text{ rad/s} &\rightarrow 97^\circ/\text{s} \\ J4 - J5: 3.2 \text{ rad/s} &\rightarrow 183^\circ/\text{s} \end{aligned}$$

6.1.3 Power Estimation

Power is approximated using: $P = \tau_{joint} \cdot q \dot{\cdot}_{design}$

Table 7. Power Estimations

Joint	Torque	Speed	Power
J_2	271 N.m	1.7 rad/s	460.7ω
J_3	104.1 N·m	1.7 rad/s	177ω
J_4	19.7 N.m	3.2 rad/s	57.28ω

These results from Table 7 confirm that selected motors operate within realistic thermal and continuous power limits.

6.1.4 Motor and Gear Ratio Selection

Only J_2 , J_3 , and J_5 were used for motor and gearbox sizing because these joints experience the dominant torque loads and define the actuator requirements of the system. J_1 has negligible gravity loading, and J_4 is a pure roll joint with minimal torque demand. Therefore, J_2 (shoulder), J_3 (elbow), and J_5 (wrist pitch) represent the actual load-bearing joints that dictate motor torque, speed, and gear ratio selection.

A gearbox efficiency of $\eta = 0.8$ is assumed.

General formula:

$$\begin{aligned} G_{req} &= \frac{\tau_{joint, desired}}{\eta \tau_{motor, cont}} \\ \omega_{motor} &= G_{required} \omega_{joint, des} \\ rpm &= \omega_{motor} \frac{60}{2\pi} \end{aligned}$$

J_2 – Shoulder (High Torque Joint)

Required joint torque: 271N.m

Selected motor to check values: NEMA 34, ~4.5 N·m, ~2700 rpm max

$$G_2 = \frac{\tau_{joint}}{\eta \times \tau_{m2}} = \frac{271}{0.8 \times 4.5} = 76:1 \quad (4.5: holding torque)$$

Motor speed at design joint speed:

$$\omega_{m2} = G_2 \omega_2 = 129.2 \text{ rad/s} = 130 \text{ rad/s}$$

$$130 \times \frac{60}{2\pi} = 1240 \text{ rpm} \rightarrow \text{well below } 2700 \text{ rpm threshold of } 2700 \text{ rpm}$$

Therefore, since rpm is below the motor's specifications, it has been finalized to use a 76:1 gear ratio.

$$\rho_{joint} = \omega_2 \tau_{joint} = 271 \times 1.7 = 461 J$$

$$\rho_{m2} \approx \frac{\rho_{joint}}{\eta} \approx \frac{461}{0.8} = 461\omega$$

J3 - Elbow

Required torque: 104.1 N.m

Selected motor: NEMA 23, 4.24 N·m, 1300 rpm max

$$G_3 = \frac{\tau_{joint}}{\eta \times \tau_{mg}} = \frac{104.1}{0.8 \times 4.24} \approx 31:1$$

Motor speed:

$$\omega_{m3} = G_3 \cdot \omega_3 = 30.7 \times 1.7 \approx 52.1 \text{ rad/s}$$

Power:

$$\rho_{joint} = 104.1 \times 1.7 = 177\omega$$

$$\rho_{m3} \approx \frac{\rho_{joint}}{\eta} \approx \frac{177}{0.8} = 221\omega$$

Motor comfortably within limits so **NEMA 23 + 31:1** works.

However, since 31 is a prime number the gear ratio will be increased to 36:1.

J5 - Wrist Pitch

Required torque: 19.7 N·m

Selected motor: NEMA 17, 0.6 N·m, 975 rpm max

$$G_5 = \frac{\tau_{joint}}{\eta \times \tau_{mg}} = \frac{17.9}{0.8 \times 0.883} \approx 26:1$$

$$\omega_{m5} = G_5 \cdot \omega_5 = 25.35 \times 3.2 \approx 81.1 \text{ rad/s}$$

$$rpm_5 = 81.1 \frac{60}{2\pi} \approx 755 \text{ rpm}$$

Therefore, the rpm requirements for the NEMA 17 is good.

$$\rho_{joint} = 17.9 \times 3.2 = 57.3W$$

$$\rho_{m5} \approx \frac{\rho_{joint}}{\eta} \approx \frac{573}{0.8} \approx 71.6W$$

The power requirements for NEMA 17 is 100W therefore, NEMA 17 is suitable.

6.1.5 Module Selection

This step calculates the module for J2 as it is the joint that needs to apply the highest torque.

4.5Nm from NEMA34:

$$\tau_1 = 4.5 \times 5 = 22.5 \text{ Nm}$$

$$\tau_2 = 22.5 \times 5 = 112.5 \text{ Nm}$$

$$\tau_3 = 112.5 \times 3 = 337.5 \text{ Nm}$$

Tangential Force at J2

$$F_T = \frac{2\tau}{dp} = \frac{2\tau}{mz_s} \text{ (mz}_s\text{: module x number gear sum)}$$

5:1 stage (1,2)

$$z_s = 12$$

$$z_p = 18 \text{ (planet teeth #)}$$

3:1

$$z_s = 16$$

$$z_p = 16$$

$$z_r = 48$$

$$\text{Stage 1: } F_{t1}(m) = \frac{2 \times 22.5}{m12} = \frac{3.75}{m}$$

$$\text{Stage 2: } F_{t2}(m) = \frac{2 \times 112.5}{m12} = \frac{18.75}{m}$$

$$\text{Stage 3: } F_{t3}(m) = \frac{2 \times 337.5}{m12} = \frac{42.1875}{m}$$

This force is the load shared all around across planets, but the bending stress must be checked on the sun gear, which sees the full tangential force per planet.

$$F_{tooth} = \frac{F_t}{n_p} \rightarrow \frac{42.1875}{3m} = \frac{14.0625}{m} \rightarrow \text{Bending stress: } S_b = \frac{F_{tooth}}{bmY}$$

Fatigue and stress limits assumptions

We want something that has high wear resistance so something “quenched-tempered” or “carburized” be a great choice

Table 8. Fatigue and Stress Limit Assumptions

	Bending limit	Contact limit
4140/42CrMo4	500-700 MPa	1300-1700 MPa
Carburized	900-1100 MPa	1600-2200 MPa

According to Table 8, carburized material seems better but we also have budgetary constraints. Therefore, first we will check in with 42CrMo4 to see if it is applicable to us.

Where $m=2.5$ (we are guessing if module of 2.5 applicable):

$$\gamma = 0.296 \approx 0.3 \text{ for } 16 \text{ teeth } 20^\circ \text{ angle pressure}$$

$$S_b = \frac{14.0625}{(2.5)^2 \times 16 \times 0.3} = 0.468 \text{ MPa}$$

$$m=3 \rightarrow S_b = 0.325 \text{ MPa}$$

These values are way lower then the allowable limit so we don't really have a constraint in the module selection.

Contact limit

$$S_c = c_p \sqrt{\frac{F_{tooth}}{bdp}} \rightarrow c_p \approx 1500 \text{ MPa}$$

$$dp = 16 \times 2.5 \times 40 \text{ mm}$$

$$S_c = 1500 \sqrt{\frac{14.0625}{256m^2}} \approx \frac{442.97}{m}$$

$$m = 2.5 = 442.97/2.5 \rightarrow 177.19$$

$$m = 3 \approx 147.66$$

We are not even close to the range we are good at module selection. As J2 was successful for the module selection, the other joints will be given a module ratio accordingly.

Module selection for stages of J2

- Low torque, level 1 → $m=2$ → $m=1.5$ could have been selected but for ease of manufacturing $m=2$ is selected
- Medium torque, level 2 → $m=2$
- High torque level 3 → $m=2.5$

Since J2 represented the highest torque condition in the arm, it was used as the baseline for sizing. Once the J2 stage was shown to be safe with module $m=2.5$, the remaining joints were assigned smaller, more efficient modules in the range of $m=2.0$, and $m=1.5$. This ensures adequate strength while minimizing size, weight, and machining cost for the lighter-loaded joints.

6.2 Final Design Overview

The final design is represented in Figure 11. This section pertains to explaining the importance and description of each major component



Figure 11. Final Design CAD Render

6.2.1 Hexapod frame

The frame of the supporting hexapod was designed to connect the legs to the robot's main body. It ensures the legs are positioned in a hexagonal pattern and supports the entire structure during any tipping motion. The leg attachments keep them fixed and prevent wobble or accidental dismounting of the robot. Due to the heavy loads it must support, the frame is made of ABS, ensuring the whole structure remains stable.

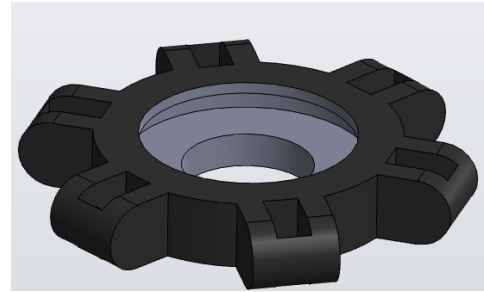


Figure 12. Hexapod Frame CAD

6.2.2 Hexapod Legs

The robot's base contains six telescoping legs that ensure height adjustment and prevent tipping. Each leg segment includes a locking mechanism that maintains the leg's height and supports the weight of the entire structure. In addition, the base of the legs has rubber padding that minimizes slip during operation, which involves constant movement.

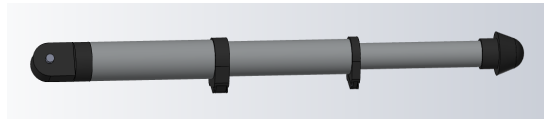


Figure 13. Hexapod Leg CAD

6.2.3 Base Rotation Planetary gearbox

The single-stage planetary gearbox for the base rotation enables high-torque motion of the robot's entire body. Its 5.884:1 reduction ratio enables the NEMA 24 Stepper motor to deliver a constant operating torque of 18 Nm for rotational yaw motion at the robot's base. The gearbox's housing(transparent) positions all the components and enables smooth operation while allowing it to be fixed to the hexapod frame. The gearbox itself consists of three 35-tooth planetary gears, an 18-tooth sun gear, and an 88-tooth ring gear. The reduction motion output is transmitted by a gear shaft that contains a

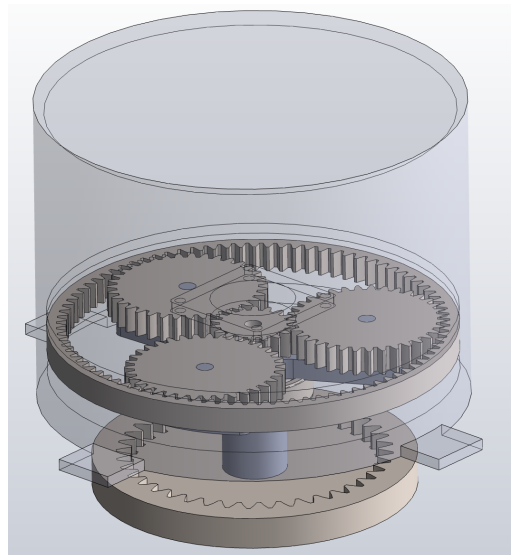


Figure 14. Base Planetary Gearbox CAD

40-tooth spur gear that couples with a ring gear attached to the base of the robot, allowing rotation.

6.2.4 Base Motor

A stepper motor powers the Base yaw movement. This allows for more precise and reliable control of Joint 1 in the robot, resulting in higher-quality video. The NEMA 24 431 in.-oz stepper motor was selected because its high torque rating is essential for maintaining stable, constant movement of the robot during operation.

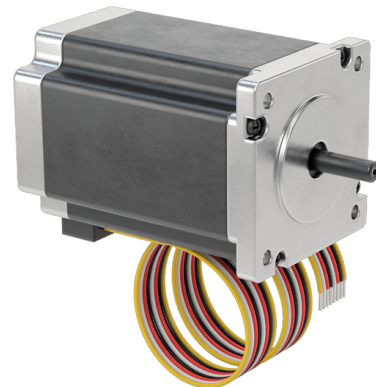


Figure 15. Base Motor CAD

6.2.5 Shoulder Rotation Planetary gearbox

The triple-stage planetary gearbox for shoulder rotation enables high-torque motion of the robot's shoulder, forearm, and wrist. Its 76:1 reduction ratio enables the NEMA 34 Stepper motor to deliver a constant operating 271 torque of Nm in rotational pitch motion at the robot's Joint 2. The gearbox's housing (transparent) positions all the components and enables smooth operation, while allowing it to be fixed to the Shoulder casing. The gearbox itself consists of three stages of planetary gear sets. The first stage has four 16-tooth gears acting as planetary and sun gears; the second and third stages are comprised of three 18-tooth planetary gears and a 12-tooth sun gear. All three stages work within three 48-tooth ring gears. The reduction motion output is transmitted by a gear shaft that contains a 24-tooth bevel gear, which couples with a horizontal gear

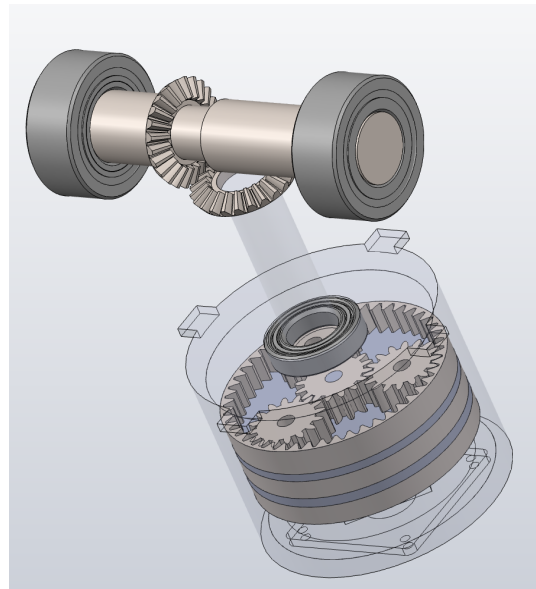


Figure 16. Shoulder Planetary Gearbox CAD

shaft attached to the shoulder joint of the robot and allows rotation.

6.2.6 Shoulder Motor

A stepper motor powers the shoulder pitch movement. This allows for more precise and reliable control of Joint 2 in the robot, resulting in higher-quality video. Due to the high loads needed on the joint, the NEMA 34 467 in.-oz stepper motor was selected because its high torque rating is essential for maintaining stable, constant movement of the robot during operation.

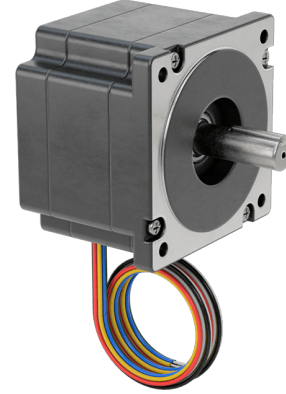


Figure 17. Shoulder Motor CAD

6.2.7 Forearm Rotation Planetary gearbox

The double-stage planetary gearbox for forearm rotation enables high-torque motion of the robot's forearm and wrist. Its 36:1 reduction ratio enables the NEMA 23 Stepper motor to deliver a constant operating torque of 105 Nm in rotational pitch motion at the robot's Joint 3. The gearbox's housing (transparent) positions all the components and enables smooth operation, while allowing it to be fixed to the forearm casing. The gearbox consists of two stages with 24-tooth planetary gears, a 12-tooth sun gear, and a single 60-tooth ring gear encompassing both stages. The reduction motion output is transmitted by a gear shaft that directly attaches to the robot's forearm and allows rotation.

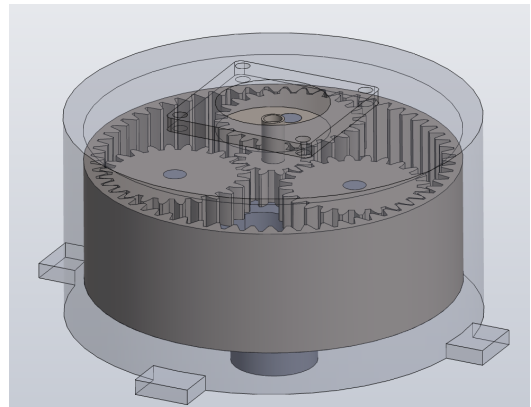


Figure 18. Forearm Rotation Planetary Gearbox CAD

6.2.8 Elbow Motor

A stepper motor powers the forearm pitch movement. This allows for more precise and reliable control of Joint 3 in the robot, resulting in higher-quality video. Due to the high loads needed on the joint, the NEMA 23 600.4 in.-oz stepper motor was selected because its high torque rating is essential for maintaining stable, constant movement of the robot during operation.



Figure 19. Elbow Motor CAD

6.2.9 Wrist Pitch Rotation Planetary gearbox

The single-stage planetary gearbox for the wrist pitch rotation enables high-torque motion of the robot's wrist. Its 26:1 reduction ratio enables the NEMA 14 Stepper motor to deliver a constant operating torque of 19.7 Nm in rotational pitch motion at Joint 4 of the robot. The gearbox's casing (transparent) positions all the components and enables smooth operation, while allowing it to be fixed to the wrist casing. The gearbox itself consists of three 24-tooth planetary gears, a 12-tooth sun gear, and a 60-tooth ring gear. The reduction motion output is transmitted by a flexible coupling, which allows rotation of the wrist and roll motion of the camera attachment simultaneously.

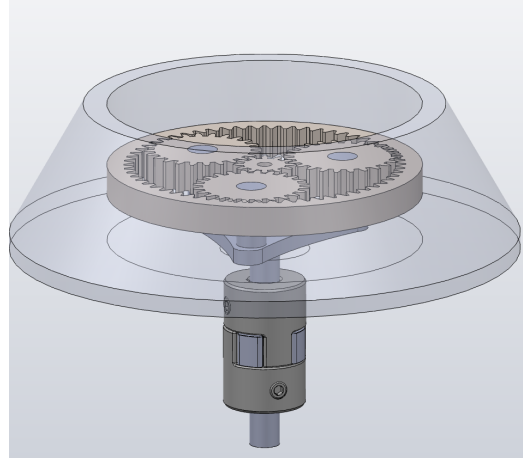


Figure 20. Wrist Pitch Rotation Planetary Gearbox CAD

6.2.10 Wrist pitch Motor

A stepper motor powers the wrist pitch movement. This allows for more precise and reliable control of Joint 4 in the robot, resulting in higher-quality video. The NEMA 14 15.5 in.-oz stepper motor was selected for maintaining stable, constant movement of the robot during operation.



Figure 21. Wrist Pitch Motor CAD

6.2.11 Wrist roll rotation Planetary gearbox

The double-stage planetary gearbox for the wrist roll rotation enables high-torque motion of the robot's end effector. Its 26:1 reduction ratio enables the NEMA 23 Stepper motor to deliver a constant operating torque of 17.9 Nm for rotational roll motion at the robot's Joint 5. The gearbox's housing (transparent) positions all the components and enables smooth operation, while allowing it to be fixed to the Camera attachment housing. The gearbox consists of two stages: the first with 24-tooth planetary gears, a 12-tooth sun gear, and a 60-tooth ring gear, and the second with 14-tooth planetary gears, a 12-tooth sun gear, and a 40-tooth ring gear. The reduction motion output is transmitted by a shaft that directly attaches to the robot's camera attachment housing and allows rotation.

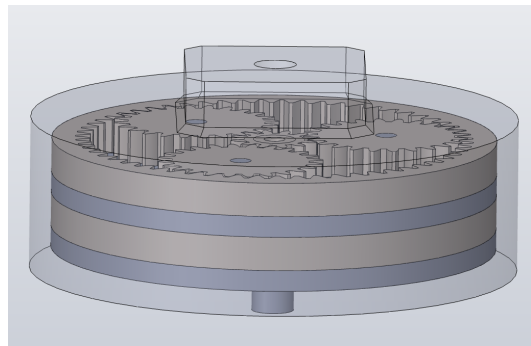


Figure 22. Wrist Roll Rotation Planetary Gearbox CAD

6.2.12 Wrist Roll Motor

A stepper motor drives the wrist roll movement. This allows for more precise and reliable control of Joint 5 in the robot, resulting in higher-quality video. Due to the high loads needed on the joint, the NEMA 17 125 in.-oz stepper motor was selected because its high torque rating is essential for maintaining stable, constant movement of the robot during operation.



Figure 23. Wrist Roll Motor CAD

6.2.13 Camera attachment housing

This housing was designed to allow for the secure attachment of the camera attachment frame and house the wrist roll gearbox and motor. The divot on the housing surface accommodates the camera attachment frame and contains a screw hole for attaching the camera to the robot's end effector.

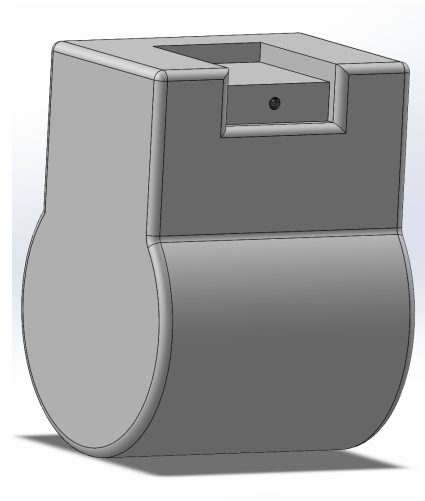


Figure 24. Camera Attachment Housing CAD

6.2.14 Camera attachment frame and screw

The camera frame was designed to allow easy attachment of a variety of camera or cellphone mounts to the robot's end effector. Its shape fits within the divot of the camera attachment housing, and it includes a $\frac{1}{4}$ in screw with 20 threads per inch, as it follows the standard for most camera mounts [48]. The mounting screw enables easy hand attachment of the camera frame, with an

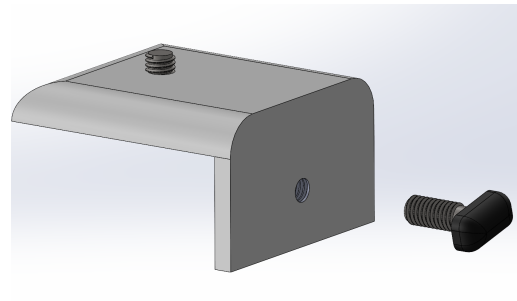


Figure 25. Camera Attachment Frame and Screw CAD

ergonomic plastic head that allows the user to secure a camera or phone mount to the robot without external tools. In addition, it provides for the attachment of multiple camera dimensions, as the frame is first secured to the camera and subsequently to the robot end effector.

6.2.15 Electronics container and telescopic cable channel

The electronics container was designed to remain beneath the robot and tripod, housing all electronic components, including the microcontroller, battery, and motor drivers. It enables the robot to operate without the extra weight of the control electronics, resulting in more reliable movement and more cost-effective motors. The telescopic cable channel was designed to allow the motor wires to safely connect to the motor drivers and the power system without affecting the hexapod base's height-changing capabilities. The telescopic shafts allow for the height between the electronics container and the robot base to vary between 500mm and 100mm. They are made of Aluminum because they are not expected to support any relevant loads, as the hexapod base will sustain the robot's weight.

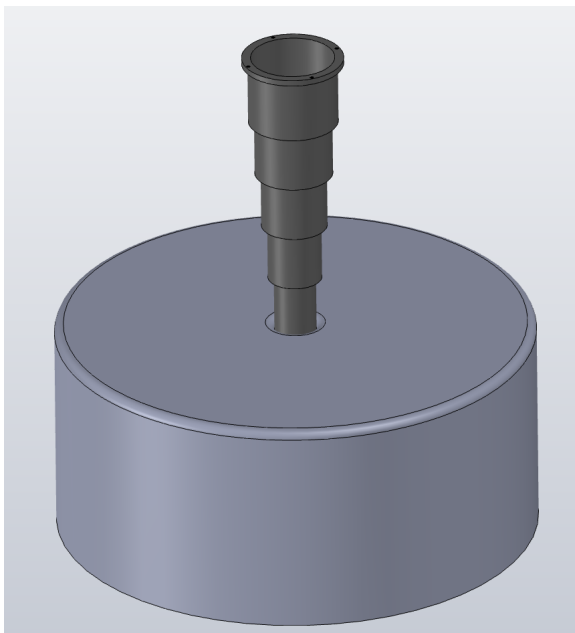


Figure 26. Electronics Container and Telescopic Cable Channel CAD

6.2.16 Emergency stop button

The emergency button was implemented as a safety feature to stop all movement in the robot upon pressing it. It was designed to be easily visible in bright red and detached from the robot via a wire, providing the user with easy access from a distance. It is also relatively large to ensure ease of pressing. The material used to make the emergency button is primarily plastic, with the internal mechanism that returns the button after pressing a metal spring, and the electrical switch that cuts off all current to the robot after pressing.

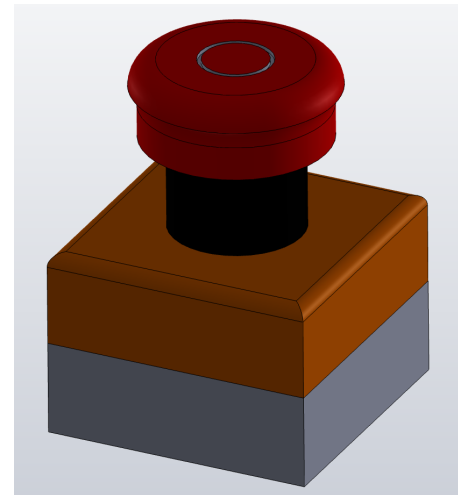


Figure 27. Emergency Stop Button CAD

6.2.17 Shoulder Casing and metal frame

The shoulder casing was designed to house both the shoulder and forearm gearbox and motors. It takes a cylindrical shape and features a 90° bend at one end, which aligns with the geometry of the planetary gearboxes and the robot's overall design language, and ensures linear movement by offsetting the bend in the forearm casing. It is attached to a turntable mechanism in its base, which supports axial loads from the robot's weight while allowing free rotation. The casing is made of plastic because it houses only components, and the internal metal frame fits within the casing and supports significant loads.



Figure 28. Shoulder Casing and Metal Frame CAD

6.2.18 Forearm Casing

The Forearm casing was designed to house the wrist gearbox and motors. It takes a cylindrical shape and features 90° bends at both ends, which align with the geometry of the planetary gearbox and the robot's overall design language, and ensure linear movement by opposing bends in the shoulder casing. The casing is made of plastic because it houses only components, and doesn't need to sustain any significant loads.

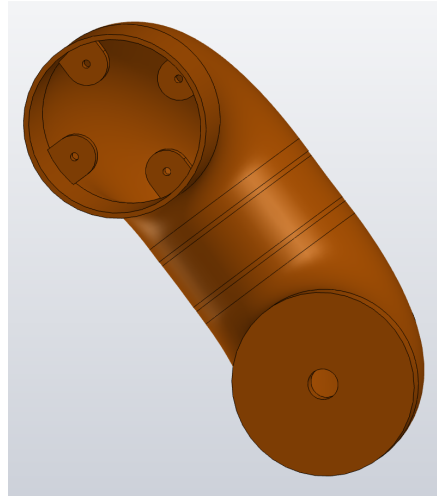


Figure 29. Forearm Casing CAD

6.2.19 Wrist mount

Allowing for both wrist pitch and end-effector roll rotation, the wrist mount was designed to support the camera attachment housing and to connect it to the end of the forearm casing. The geometry of this component allows free rotation along both axes and maintains camera stability. It is made from plastic due to its resistance and cost-effectiveness.



Figure 30. Wrist Mount CAD

6.3 Materials Selection

This section outlines the justification for the materials selected in the design.

6.3.1 Gear Materials

Two material options were evaluated for the gear stages, shown in Table 9:

Table 9. Material Comparisons

Material	Bending Limit	Contact Limit	Cost
42CrMo4 / 4140 (QT)	500–700 MPa	1300–1700 MPa	Low
Carburized Steel	900–1100 MPa	1600–2200 MPa	High

Bending stress:

$$S_b \approx 0.3 - 0.5 \text{ MPa} \ll 500 \text{ MPa (limit)}$$

Contact stress:

$$S_c \approx 150 - 180 \text{ MPa} \ll 1300 \text{ MPa (limit)}$$

Because both values are far below allowable limits, 42CrMo4 provides excellent margin at significantly lower cost. Therefore, all planetary stages use 42CrMo4 gears.

6.3.2 Structural Metal Components - Brackets and Hexapod Holder

The primary structural brackets, joint housings, and load bearing connections of the robotic arm are manufactured from Aluminum 6061. This material is a widely used aerospace and robotics grade alloy because of its balance of strength, machinability, and cost. The components need to withstand bending moments, shear forces, and torsional loads created during arm extension, fast camera movements, and repeated joint cycling. Aluminum 6061 has a yield strength of around 276 MPa, a sufficient amount to resist deformation under various cinematography payloads while still being a significantly lighter option than steel alternatives, reducing the overall torque requirements placed on the motors [49].

Aluminum 6061 is a great material choice for precision machined parts such as mounting brackets, gear interface plates, shoulder pivots, and the base attachment ring. Its ease of machinability allows for it to be milled or cut with a CNC machine to low tolerances, ensuring precise alignment of gearboxes, bearings, and motor shafts [50]. This is critical for repeatable robotic motion. The material also has great corrosion resistance due to its natural oxide layer which is beneficial for users operating the robotic arm indoors, outdoors, or in humid facilities. Additionally, Aluminum 6061's stiffness prevents flexing in long structural members, ensuring camera stability and minimizing vibration during fast motions.

Compared to other more expensive alloys such as Aluminum 7075, Aluminum 6061 is more affordable while still being rigid enough for hobbyist robotic systems. The alloy is also able to be anodized, allowing for protective or aesthetic surface finishes without compromising on

weight or durability [51]. This is why Aluminum 6061 is the best material choice as it balances structural performance, manufacturability, and cost effectiveness for the arm's brackets, housings, and other key mechanical components.

6.3.3 External Shells and Covers - ABS

The external shell and non-structural covers are manufactured from ABS (Acrylonitrile Butadiene Styrene). These components do not carry structural loads; instead, they protect internal mechanisms such as motors, wiring, and gear stages from dust and accidental contact, while also improving ergonomics by covering pinch points and providing a clean external appearance. ABS is well-suited for this role because it offers good impact resistance and toughness, is lightweight, so it does not increase joint torques, and is easily produced through FDM 3D printing—allowing rapid, low-cost iteration of covers, cable guides, and cosmetic elements. Its electrical insulation properties are beneficial around embedded electronics, and it maintains adequate dimensional stability when printed correctly. Since these parts experience only minor loads, ABS offers an ideal balance of manufacturability, cost efficiency, and functional performance [52][53][54].

6.4 Load Analysis

The load analysis was conducted using SolidWorks Simulation Add-In. [Appendix E]

Gear tangential load:

$$F_T = \frac{2\tau}{dp}$$

For J2's worst stage, forces are divided across multiple planets:

$$F_{tooth} = \frac{F_t}{n_p}$$

Stress checks in Section 6.1.6 confirms that:

- $m = 2.0$ is safe for low/mid torque stages (J3).
- $m = 2.5$ is safe for the high-torque J2 stage.
- $m = 1.5$ is sufficient for J5 due to high torque margins from upstream stages.

6.5 Risk Analysis

6.5.1 Robot Mass Representation

SolidWorks reports the robot's total mass as:

- 23.85 kg, with COM located 390 mm from the shoulder joint
- End-effector worst-case distance from base (J1 axis): 846 mm

Note: The end-effector was assumed to be the distance from the J1 to the base not from where the camera is actually to match the previous calculations.

The robot mass was converted into an equivalent end-effector mass to accurately model the gravitational torque on joints during extended configurations:

$$m_{eff} = m_{robot} \cdot \frac{d_{COM}}{d_{EE}} + m_{payload} = 23.85 \cdot \frac{0.390}{0.846} + 1.35 = 12.34 \text{ kg}$$

This ensures that torque predictions match the real robot geometry instead of assuming the entire mass is located at the end effector, which was done in the first phase for torque calculations. The workspace was sampled to determine worst-case joint torques under different operating conditions; one of them was the gravity of $1.5xg$. The required torques for the main load-bearing joints at 1 g are:

- **J2:** 100.96 N·m
- **J3:** 38.78 N·m
- **J5:** 6.66 N·m

The joint actuator capacities (motor \times gearbox) are:

- **J2:** 271 N·m
- **J3:** 104.1 N·m
- **J5:** 18 N·m

Given these values we can compute the safety factor ratio using the following basic algebra:

$$\frac{J_{calculated}}{J_{real}} = \frac{271 \text{ N.m}}{100.96 \text{ N.m}} \approx 2.65$$

6.5.2 Risk Evaluation

Using the safety factor results from Section 6.5.1, following risks are identified:

- Dynamic peak maneuvers: In addition to static gravity loading, the arm experiences dynamic torques due to acceleration. For the peak performance case ($1.5 \times g$ and high end-effector acceleration corresponding to 1.5 m/s tip speed), the safety factors at J2, J3, J5 remain around 1.5 relative to stall torque. These moves are safe as short

transients, but they are not suitable as a continuous operating mode due to heating and potential loss of steps in the steppers.

- Fatigue: Even though gear modulus were calculated using the knowledge obtained from materials science there are extremely high possibilities of fatigue. Operating frequently near the upper end of the torque values increases long-term fatigue risk in gear teeth, bearings, and structural interfaces. Although static factors are above 2.5, repeated dynamic loading and backlash can still cause wear or loss of precision over time.
- Collision Risk: At high speeds, the robot can reach a maximum speed of 1.5m/s that is equivalent to 375 J of kinetic energy and this could significantly injure a user or damage itself in a collision. The combination of relatively high joint torques and reduced control authority during step loss or saturation creates a safety risk.

6.5.3 Mitigation Measures

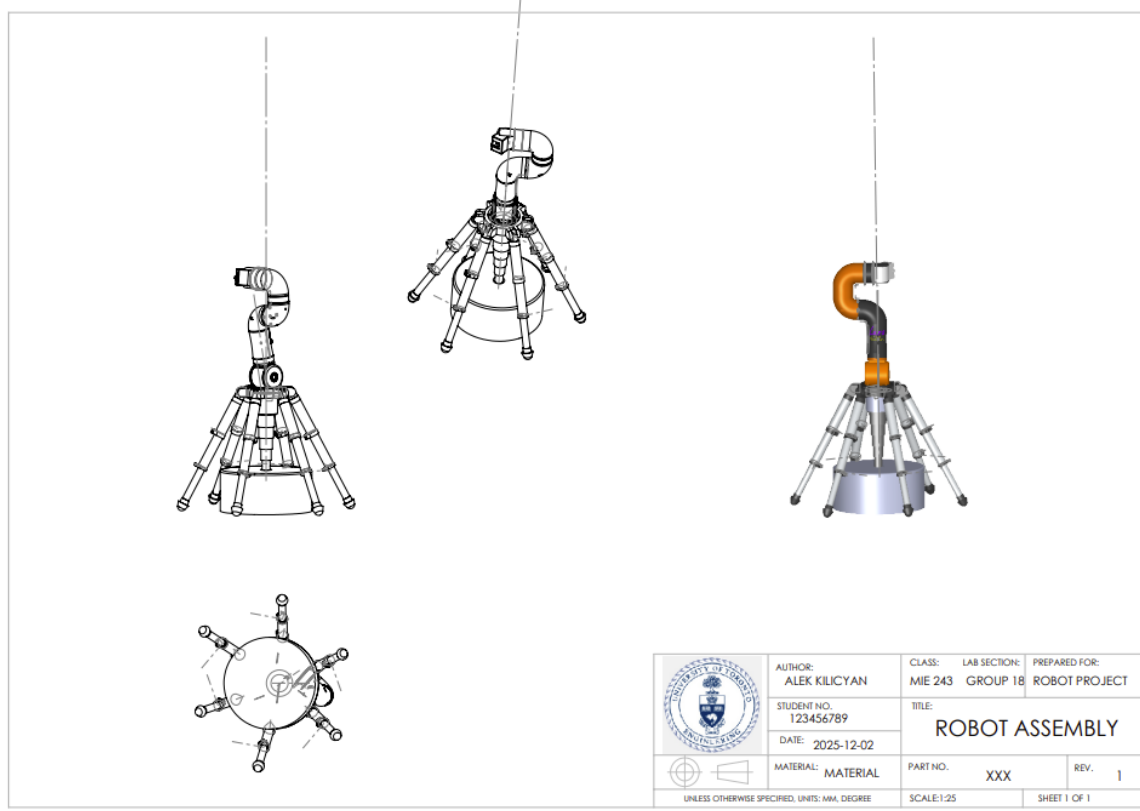
- Trajectory and acceleration limits/ speed options in the robot: The motion planner will limit normal operating accelerations to 0.5–1.0 m/s² at the end effector, reserving higher accelerations only for brief peak maneuvers. This keeps the joints within their continuous torque capability for typical motion and reduces thermal stress.
- Mechanical safety and guarding: Non-structural covers around moving joints and gears, as well as clear labelling of pinch points, will reduce the chance of accidental contact. The system will include an emergency-stop button away from the robot as well to immediately remove power to the actuators in abnormal situations.

6.6 Design Trade Offs

The design intentionally incorporates several trade-offs to balance cost, manufacturability, and functional requirements. Using stepper motors paired with external gearboxes instead of integrated actuators reduces cost, though they introduce limitations in efficiency, noise, and torque feedback. Conventional spur gear stages were selected over harmonic drives to keep the gearboxes easy to fabricate and replace, accepting higher backlash and lower precision as a consequence. ABS was chosen for the non-structural components because it is inexpensive, easy to print, and lightweight, despite offering lower stiffness and heat resistance than engineering polymers like PC or nylon. The adjustable hexapod base provides versatility and ease of mobility, but it is a compromise compared with more rigid base architectures that deliver superior stability at the expense of portability and complexity. Additionally, the robot arm uses a 5-DOF configuration rather than a full 6-DOF arrangement, which simplifies the mechanical arquitecture and reduces weight and cost but limits the range of possible movements and restricts the ability to execute more complex or fully articulated camera motions, limiting them to only a select few.

7.0 Drawings

All drawings are in millimeters and degrees.



SOLIDWORKS Educational Product. For Instructional Use Only.

Figure 31. Drawing of full assembly of final CAD (For ease of calculation, the robot was not centered; therefore, it appears tilted in the drawing.)

7.1 Assemblies

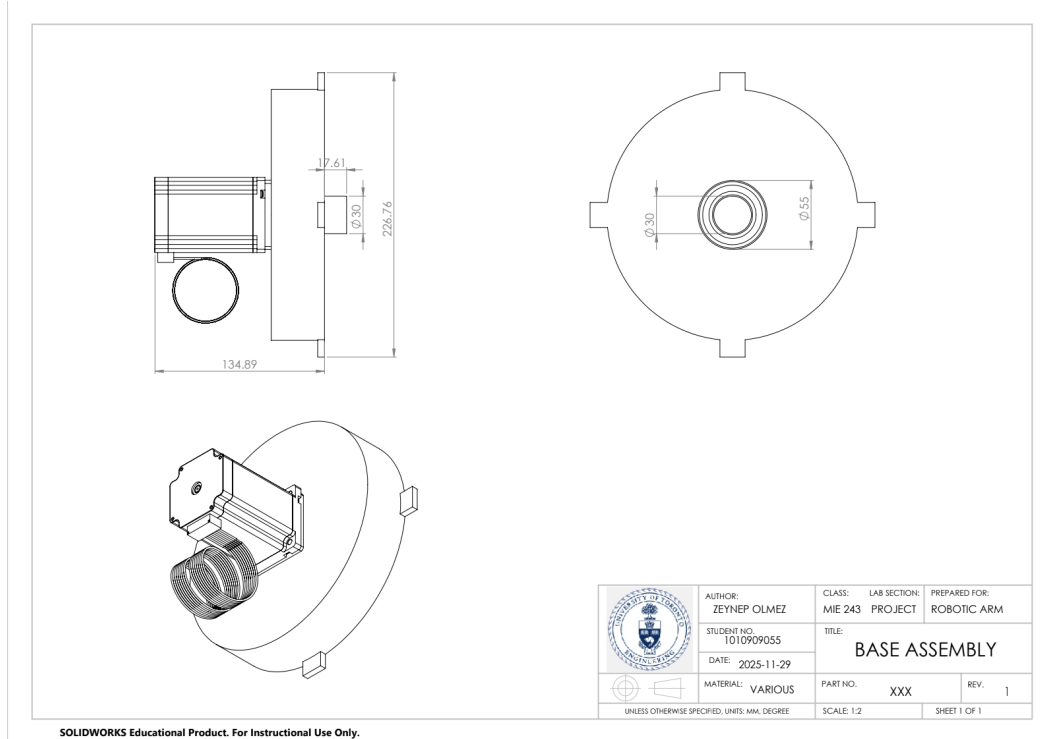


Figure 32. Drawing of Base Assembly

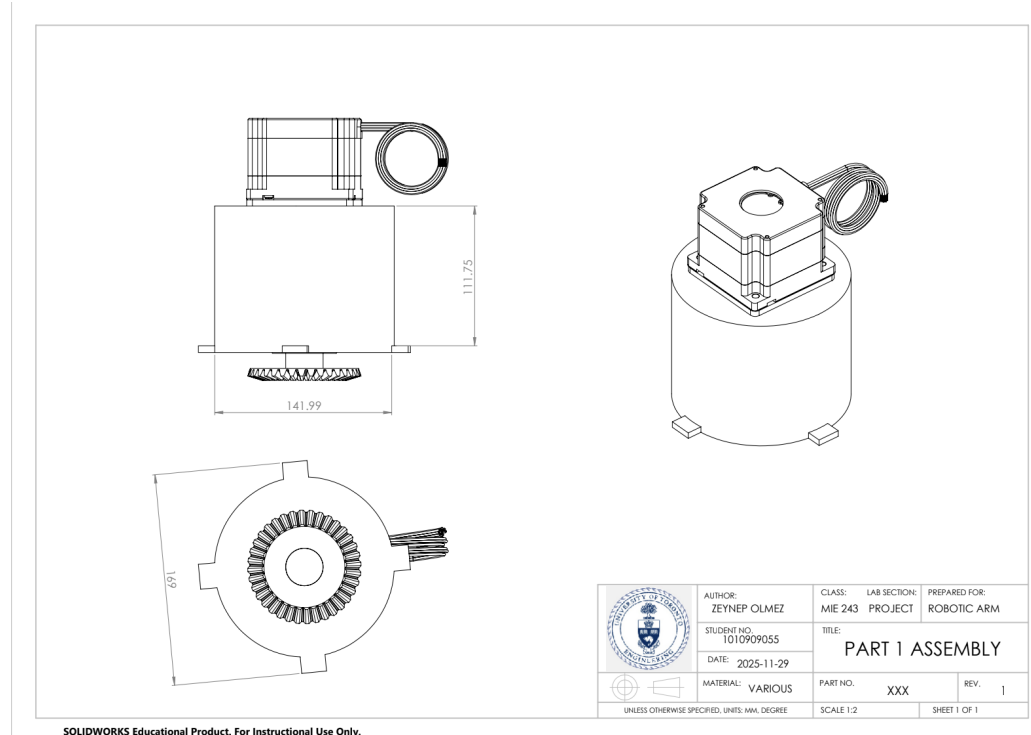


Figure 33. Drawing of Part 1 Assembly

7.2 Drive Motors

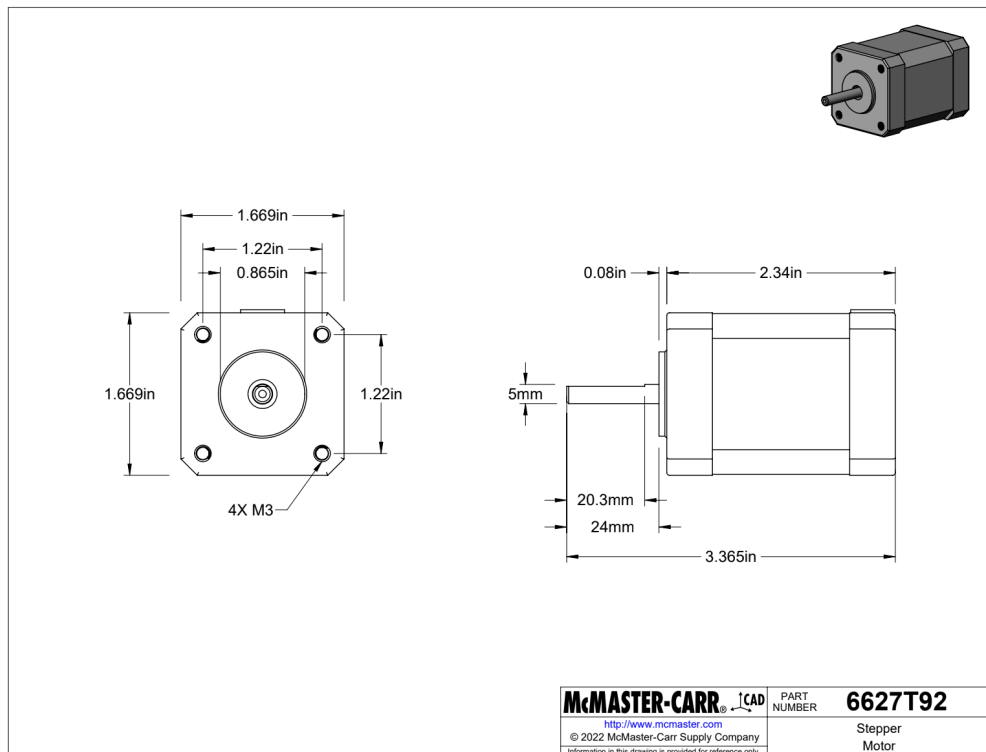


Figure 34. Drawing of NEMA 17 Stepper Motor

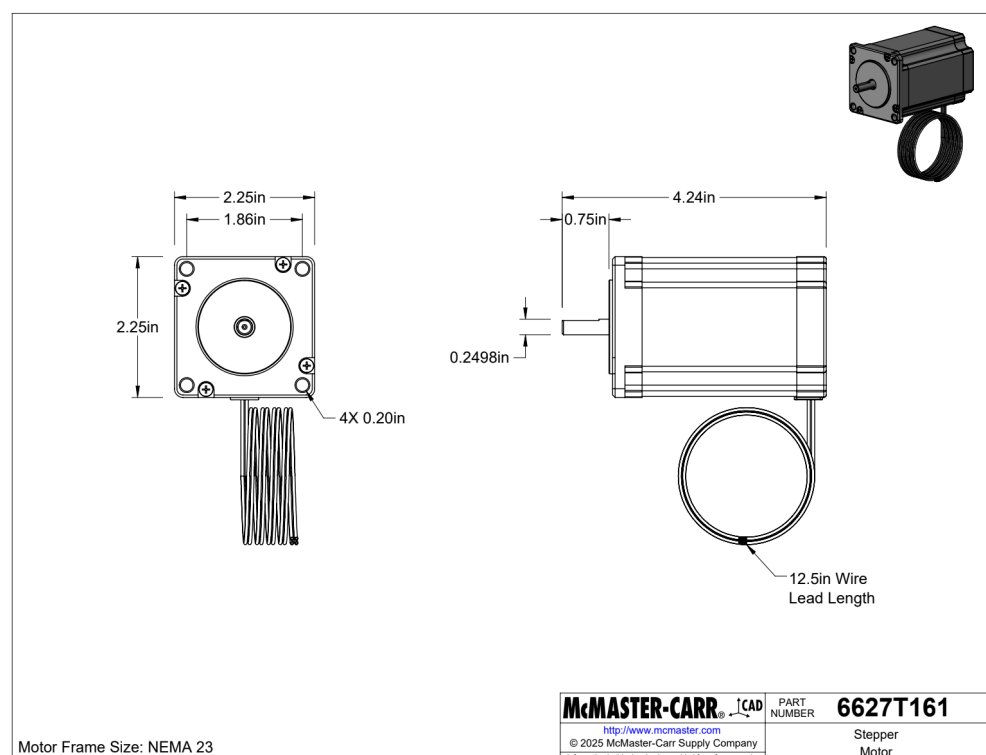


Figure 35. Drawing of NEMA 23 Stepper Motor

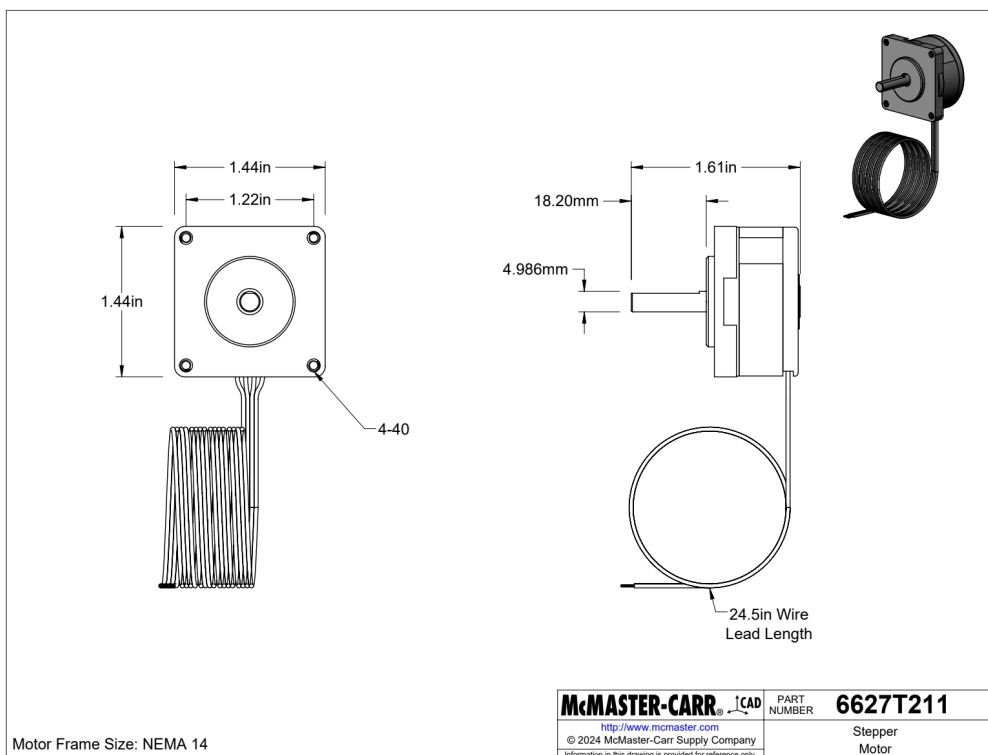


Figure 36. Drawing of NEMA 14 Stepper Motor

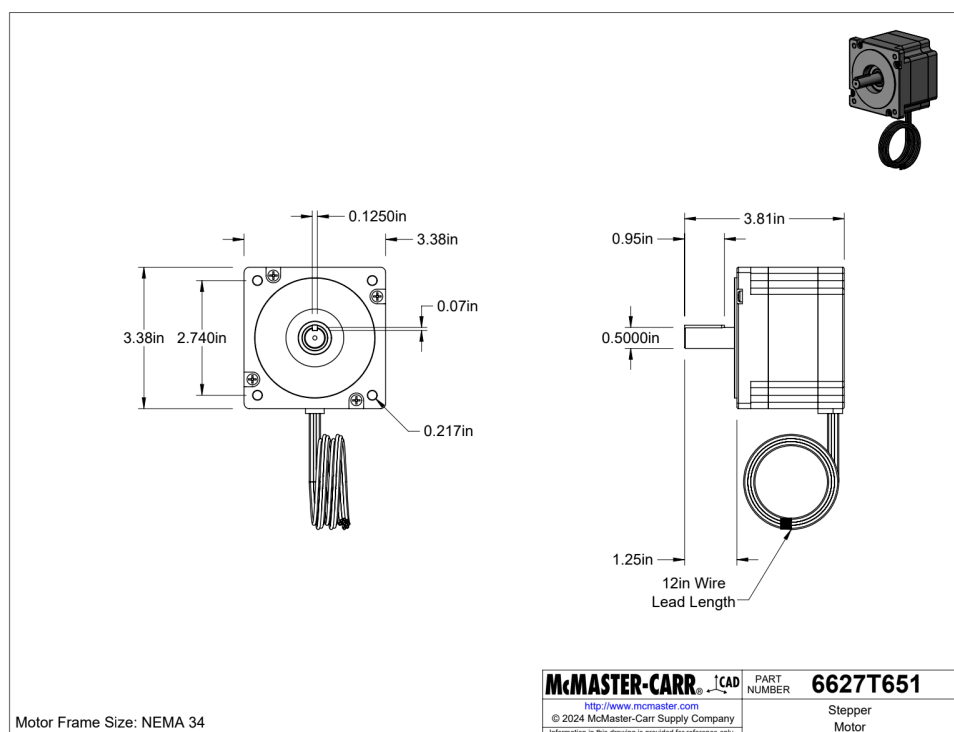
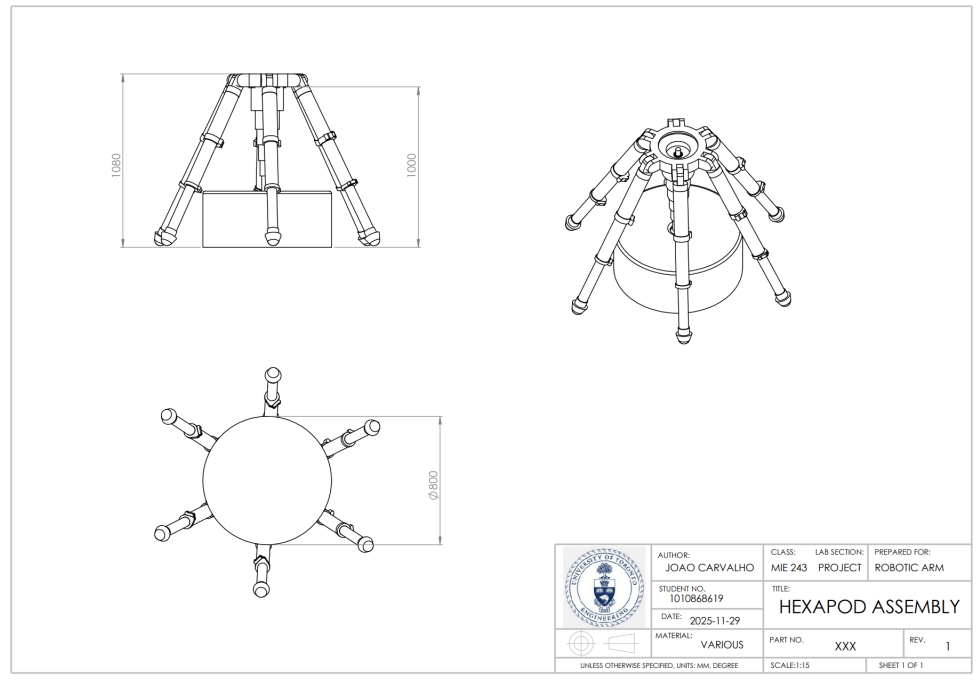


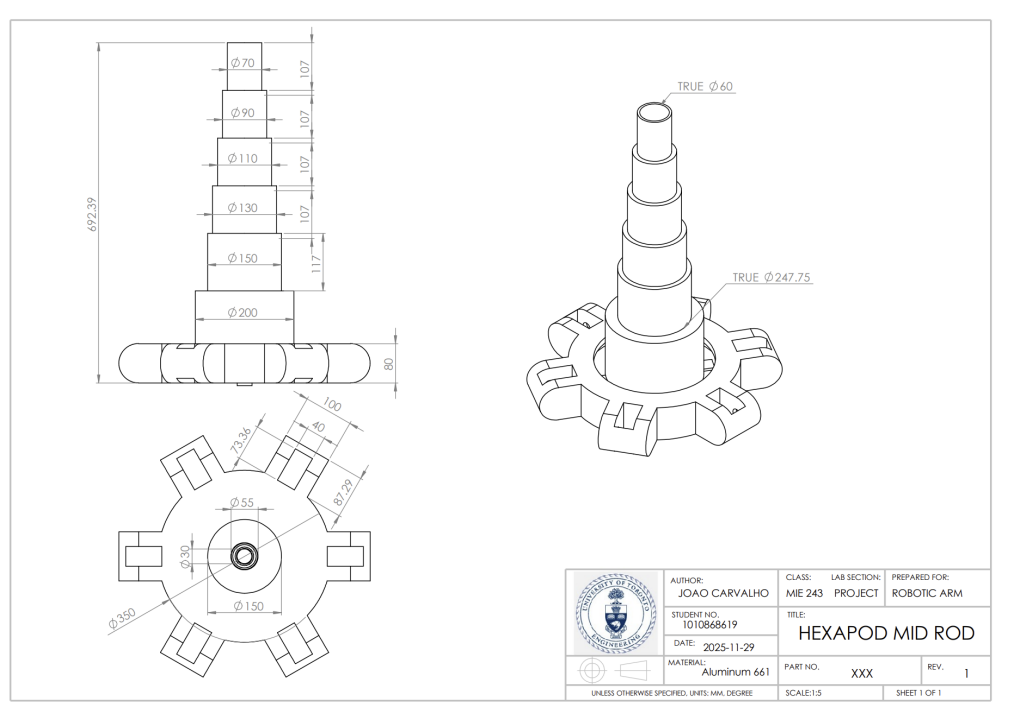
Figure 37. Drawing of NEMA 34 Stepper Motor

7.3 Hexapod Structure



SOLIDWORKS Educational Product. For Instructional Use Only.

Figure 38. Drawing of Hexapod Assembly



SOLIDWORKS Educational Product. For Instructional Use Only.

Figure 39. Drawing of Hexapod Mid Rod

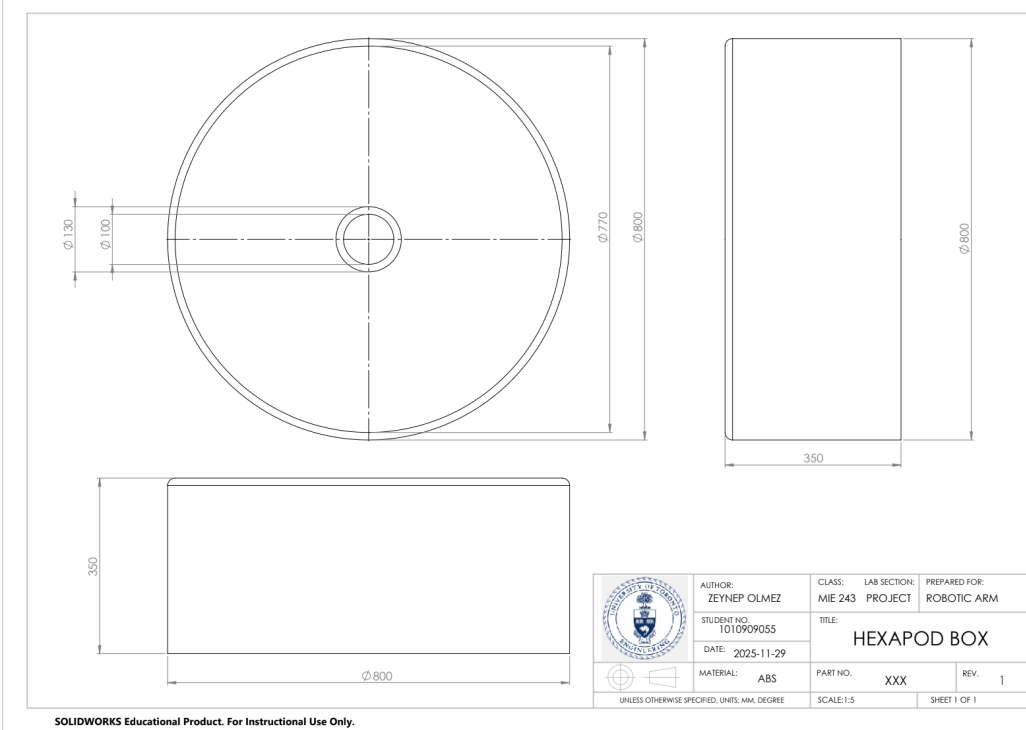


Figure 40. Drawing of Hexapod Box

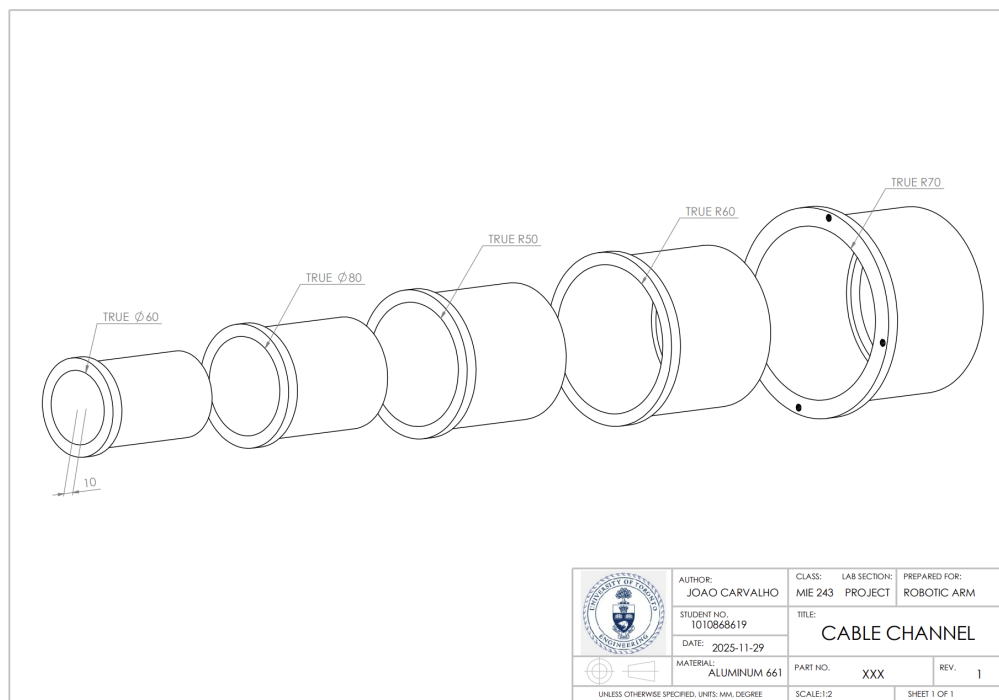


Figure 41. Drawing of Cable Channel Assembly

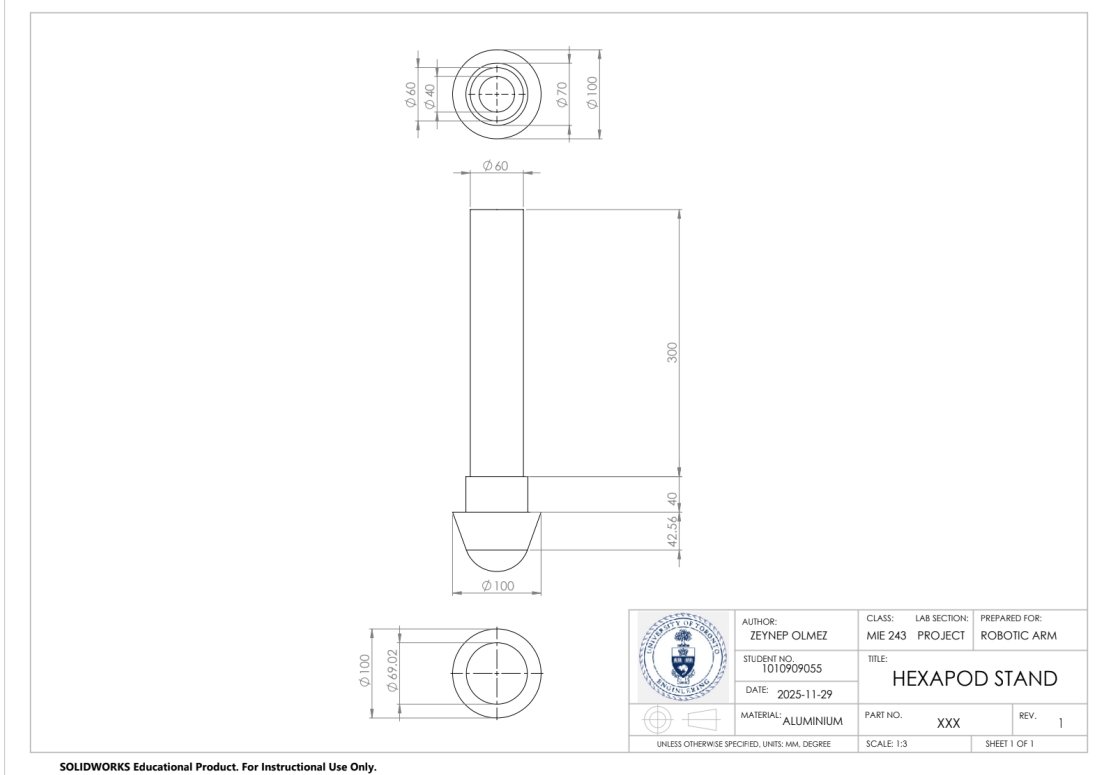


Figure 42. Drawing of Hexapod Stand 1

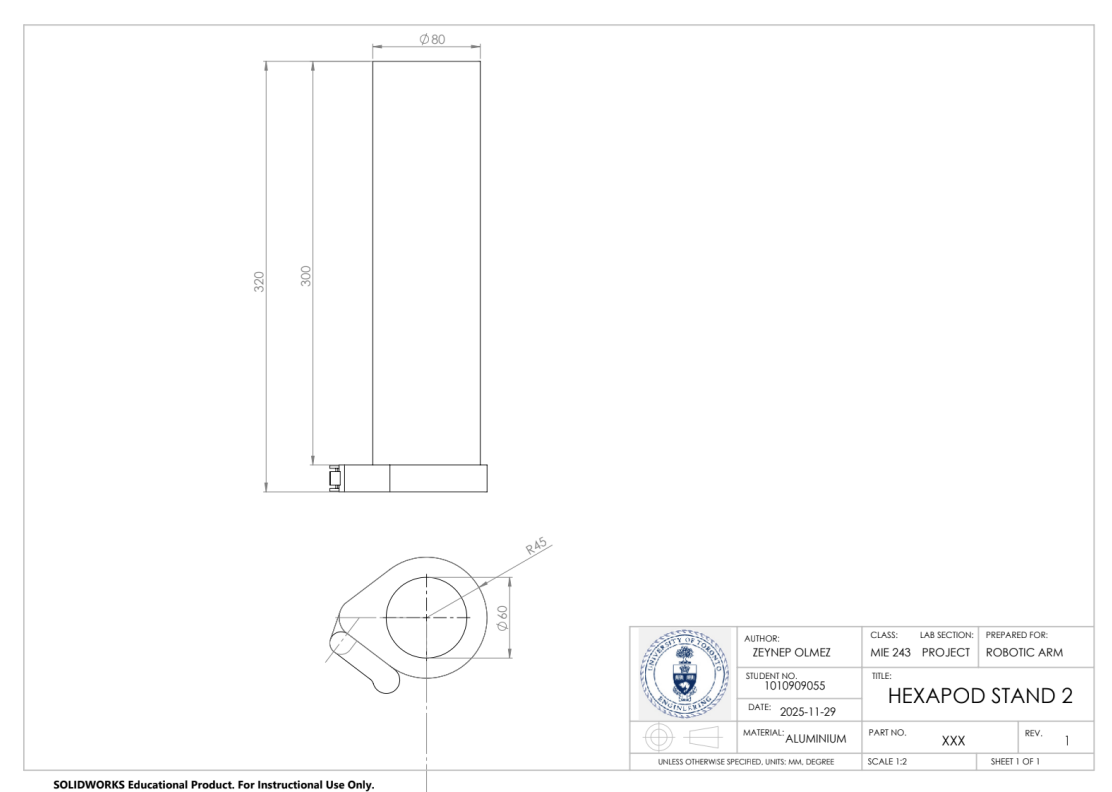


Figure 43. Drawing of Hexapod Stand 2

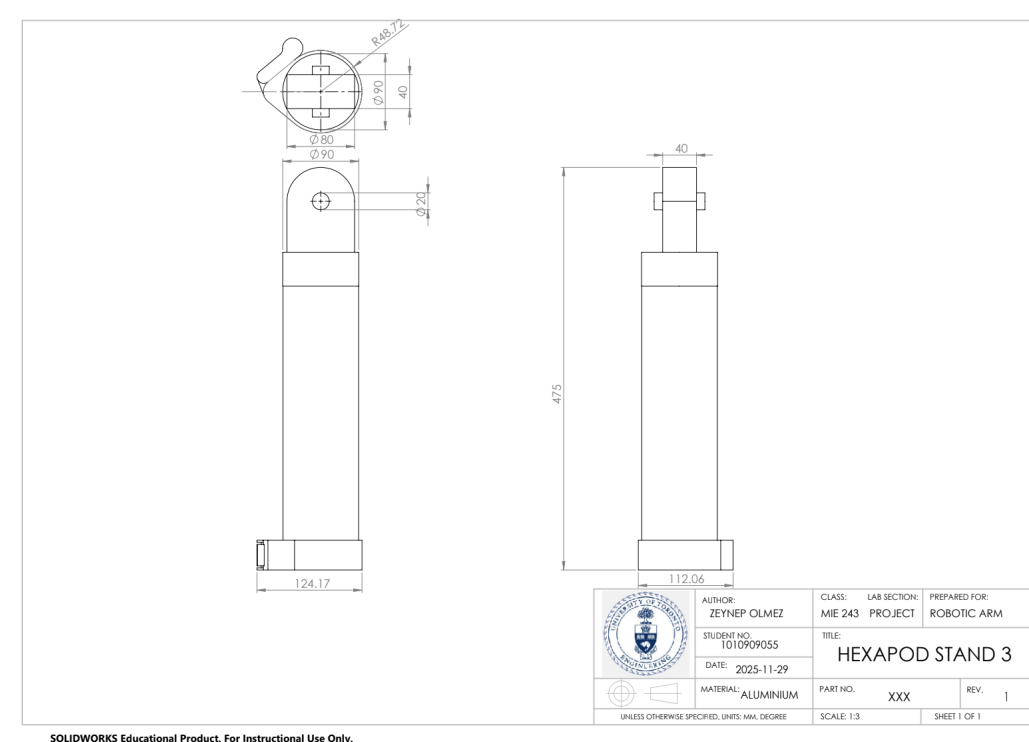


Figure 44. Drawing of Hexapod Stand 3

7.4 Structural Components and Casings

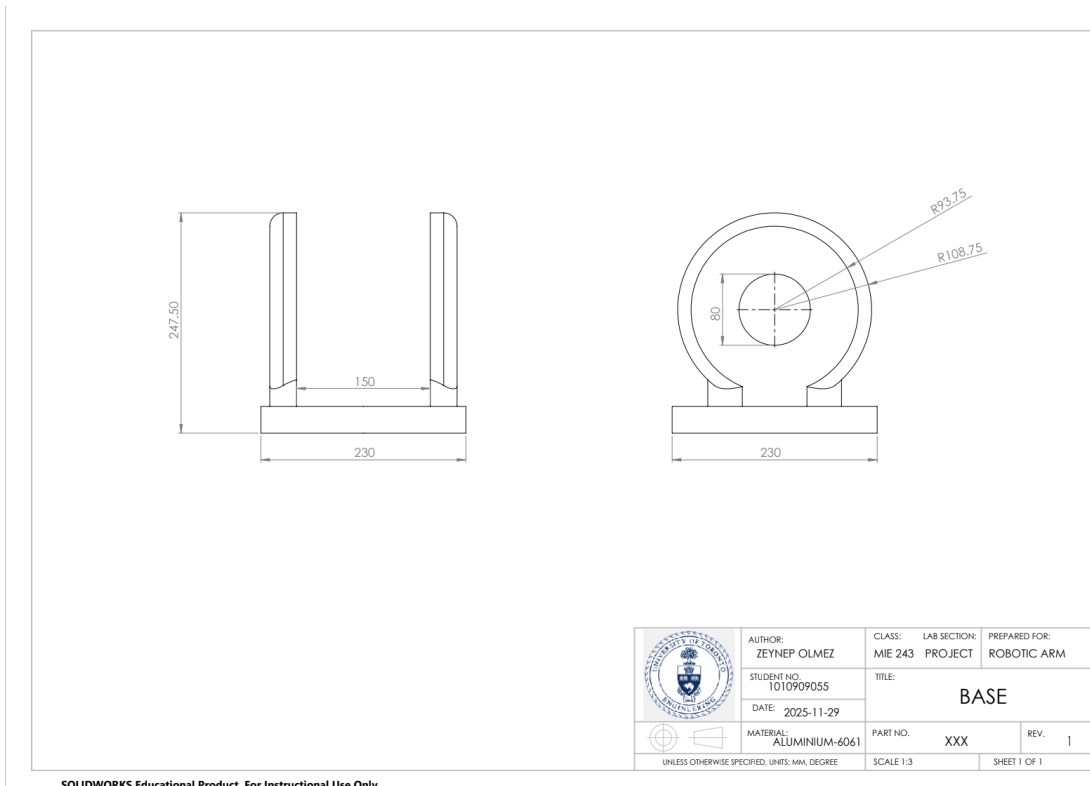


Figure 45. Drawing of Base Structure

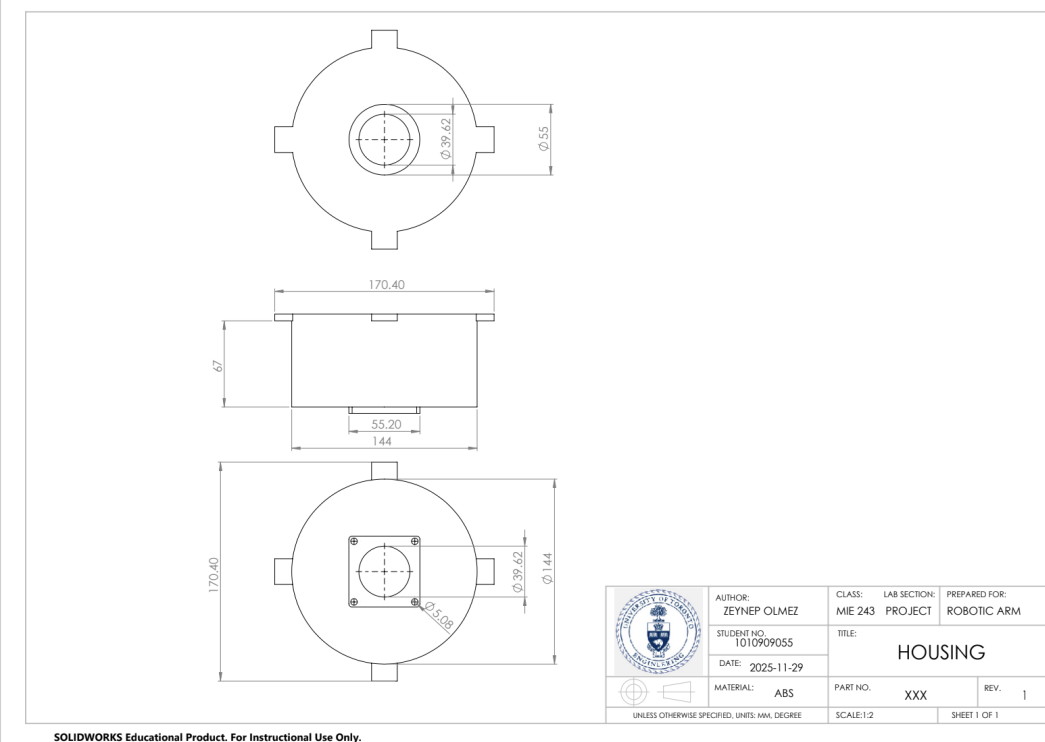


Figure 46. Drawing of Housing

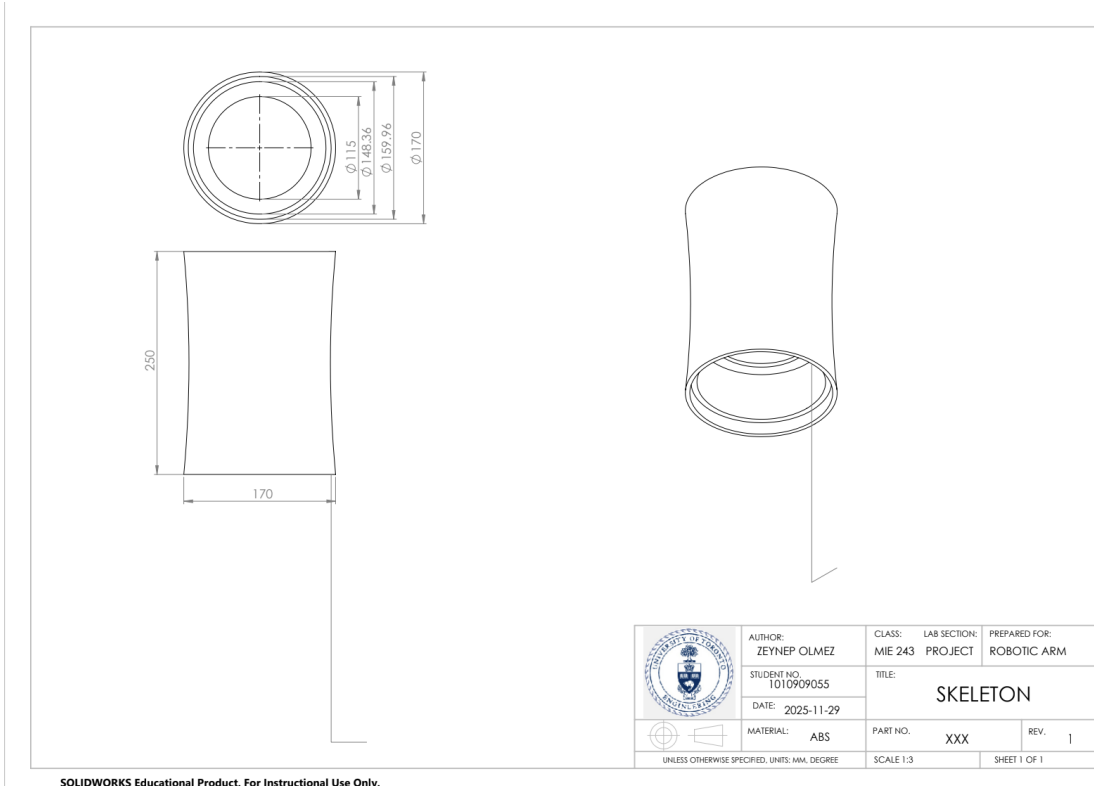


Figure 47. Drawing of Skeleton

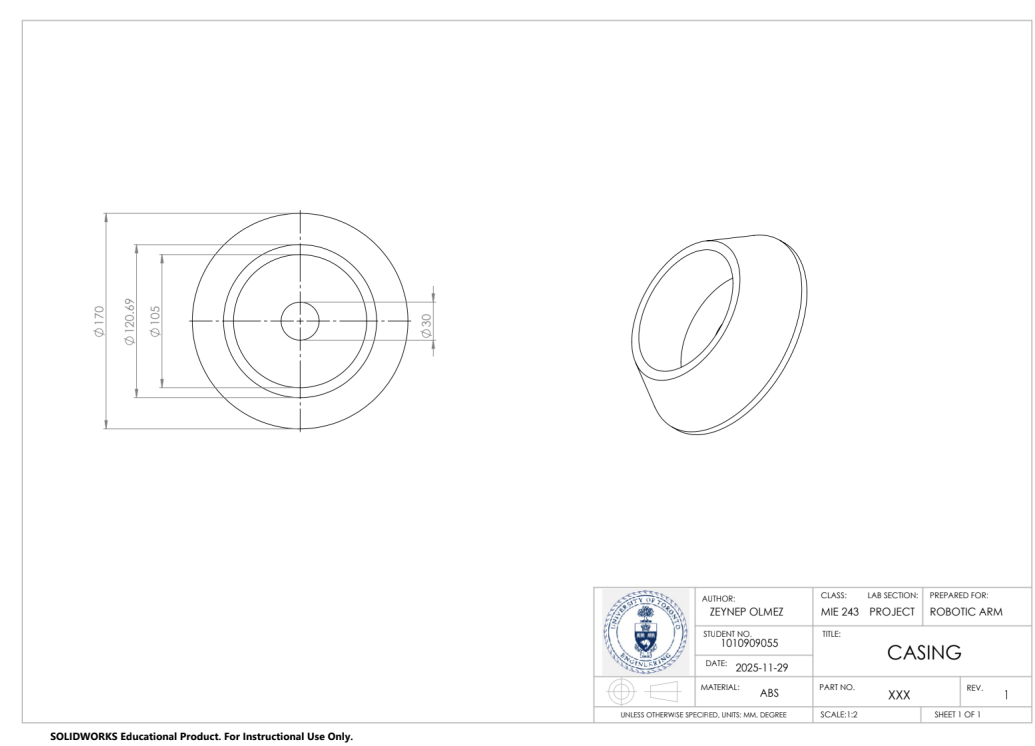


Figure 48. Drawing of Casing

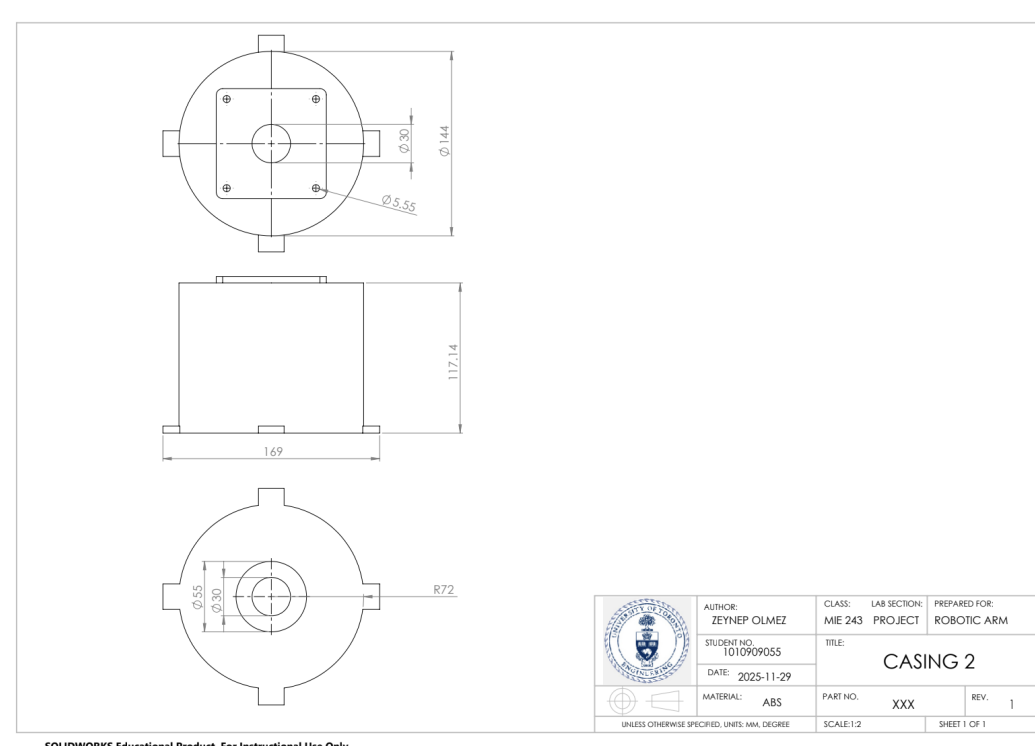


Figure 49. Drawing of Casing 2

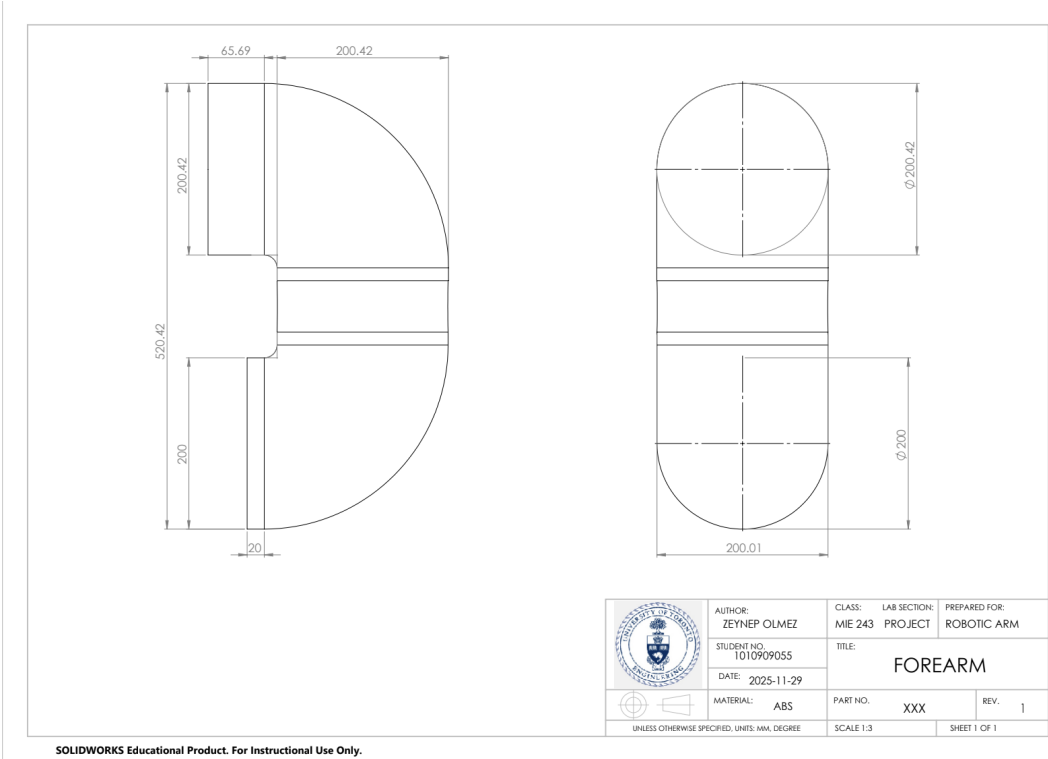


Figure 50. Drawing of Forearm

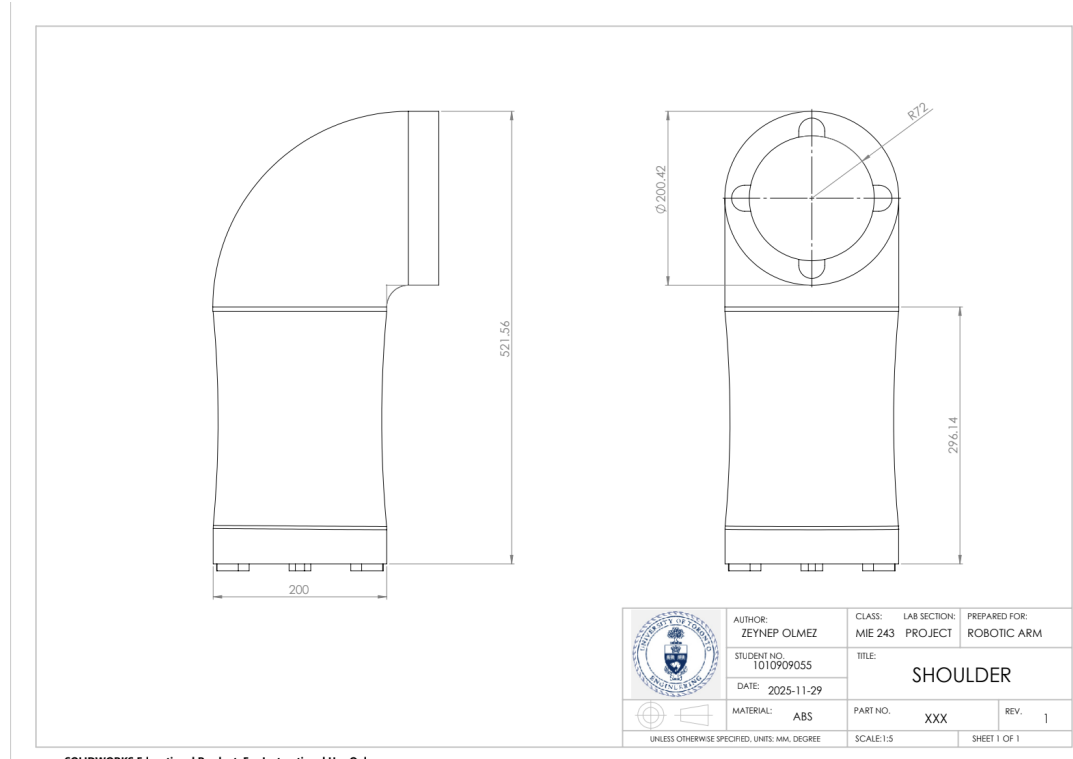


Figure 51. Drawing of Shoulder

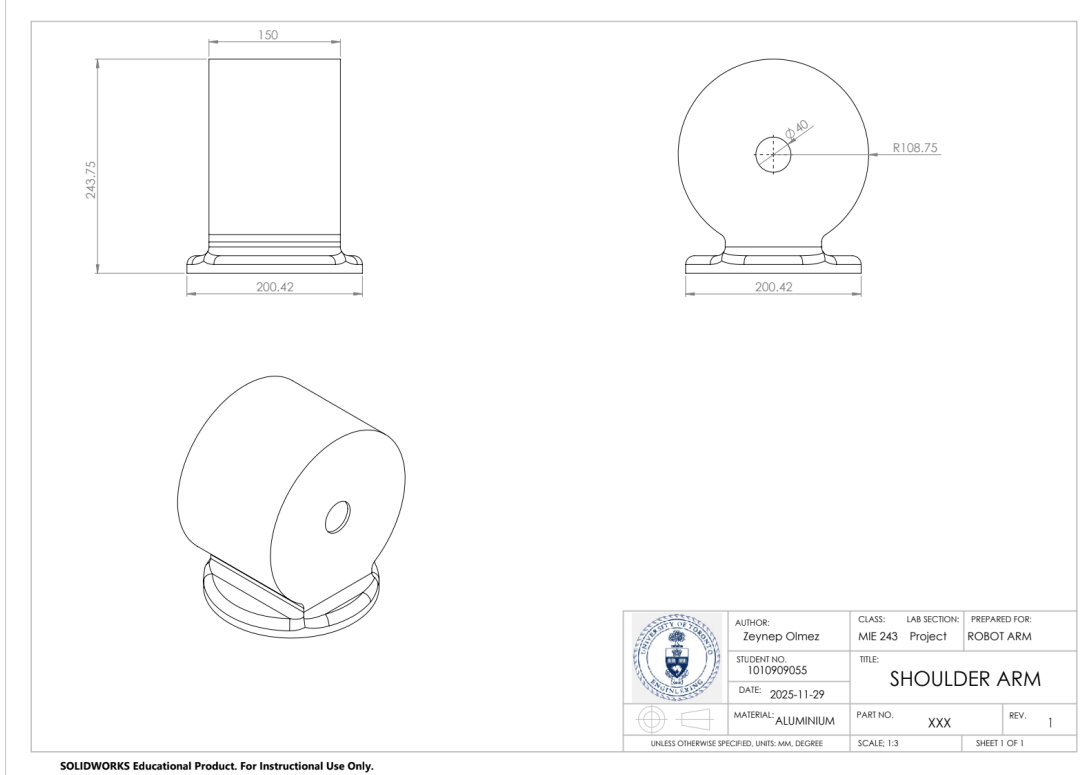


Figure 52. Drawing of Shoulder Arm

7.5 Camera Mount

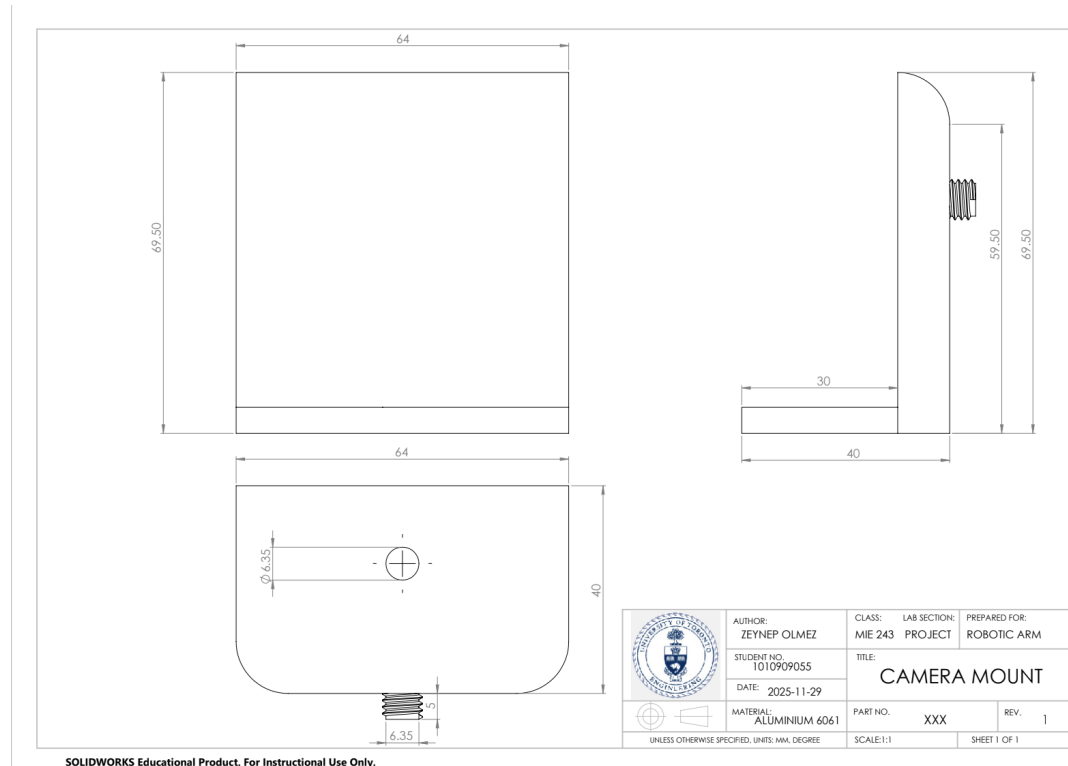


Figure 53. Drawing of Camera Mount

7.6 Gearboxes

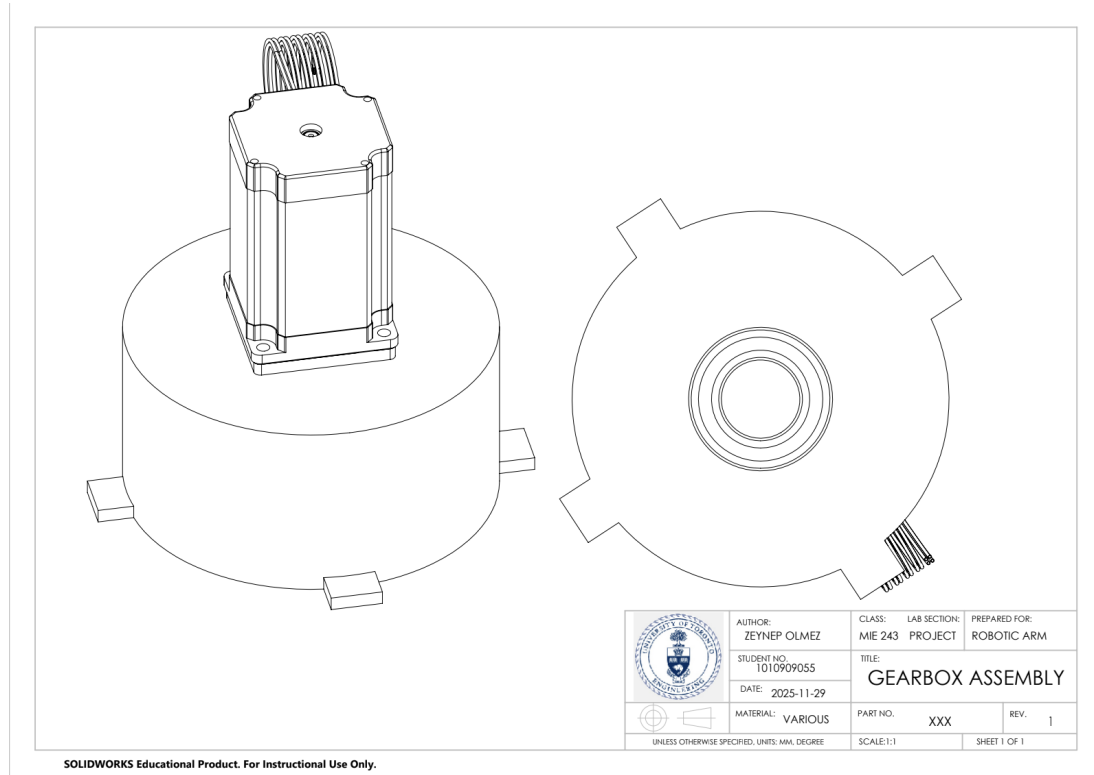


Figure 54. Drawing of Gearbox Assembly

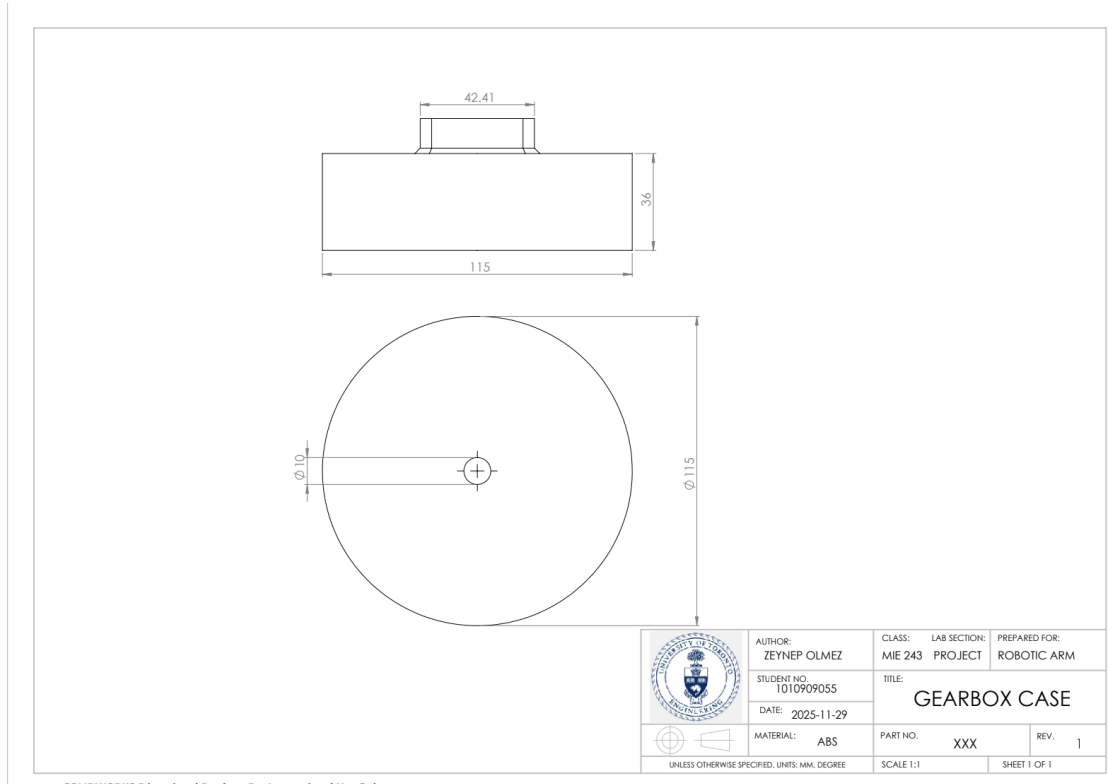


Figure 55. Drawing of Gearbox Case

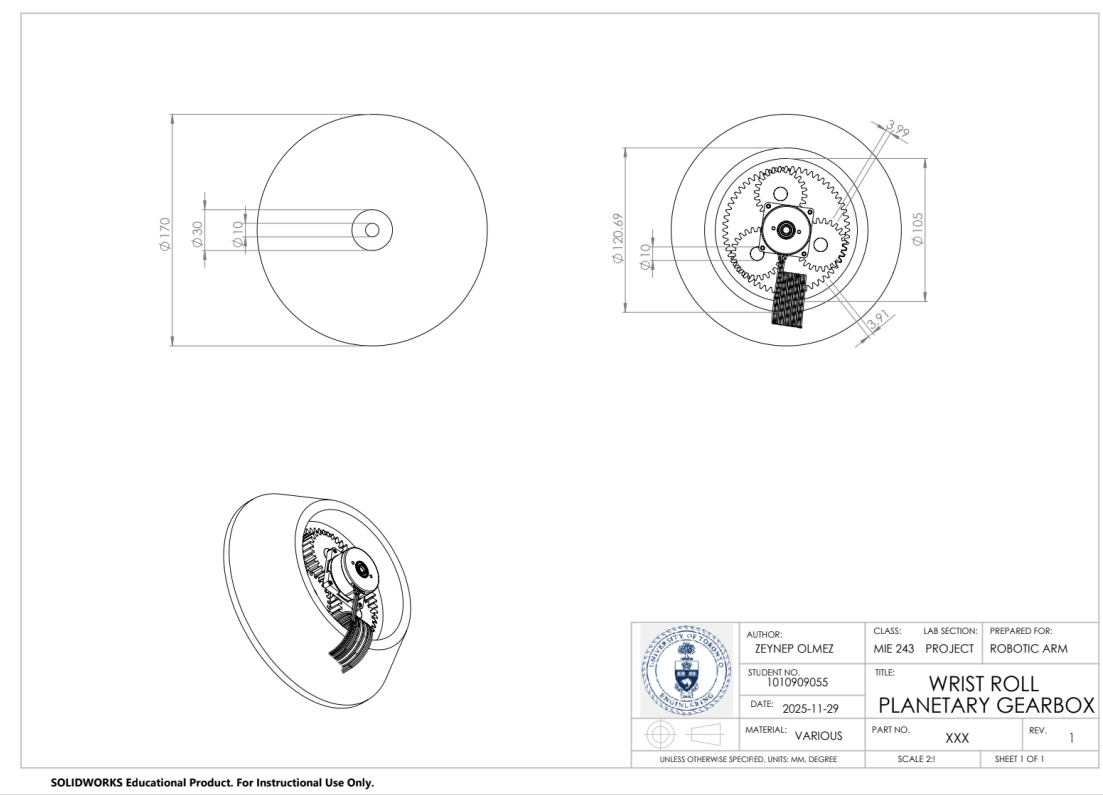


Figure 56. Drawing of Wrist Roll Planetary Gearbox

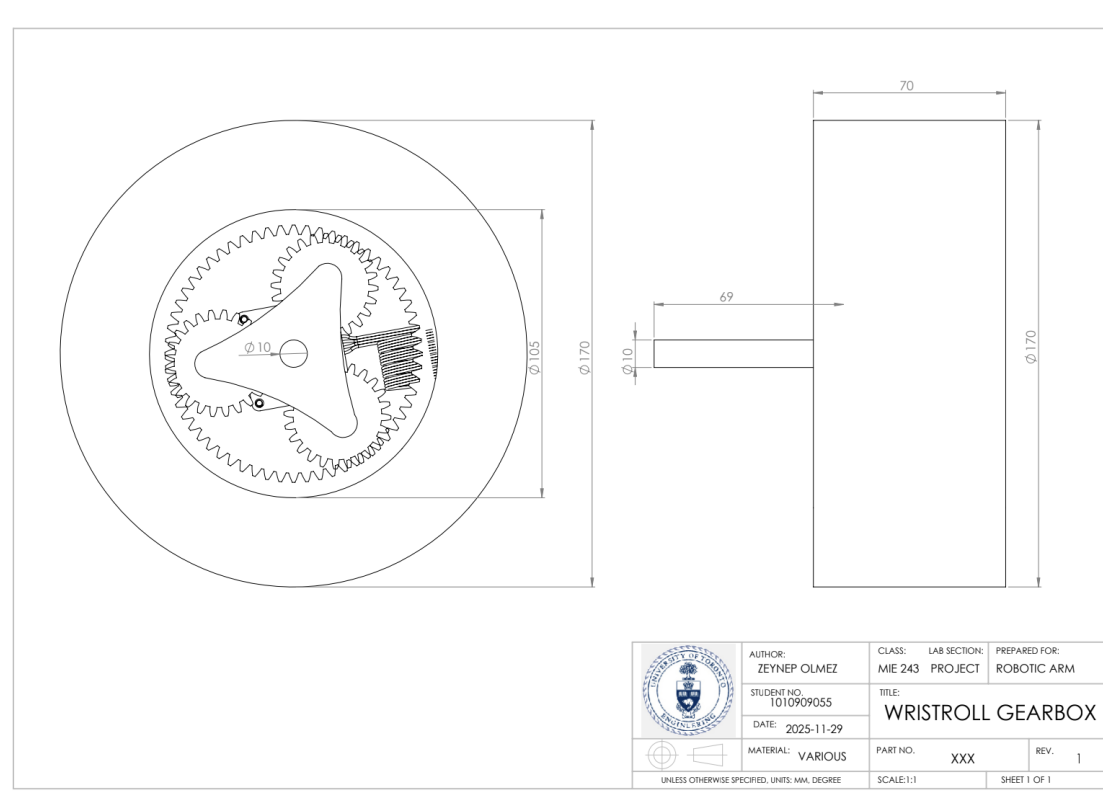


Figure 57. Drawing of Wristroll Gearbox

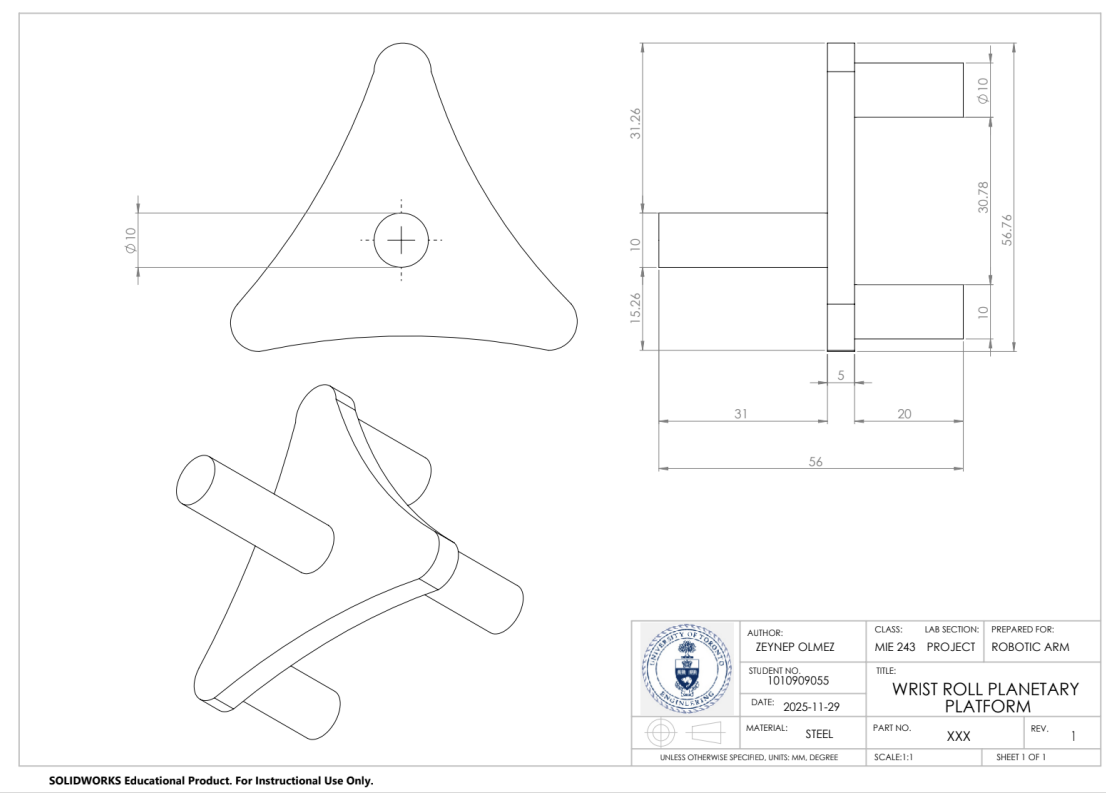


Figure 58. Drawing of Wrist Roll Planetary Platform

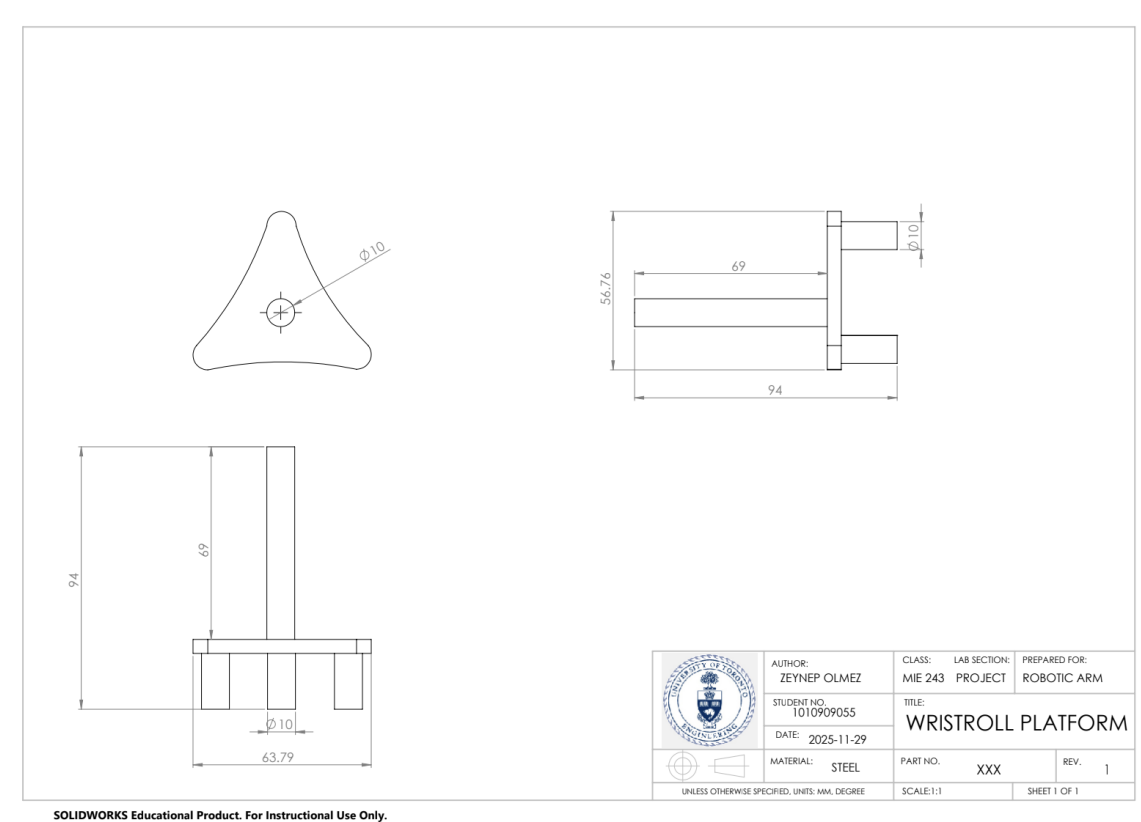


Figure 59. Drawing of Wristsroll Platform

7.7 Gears

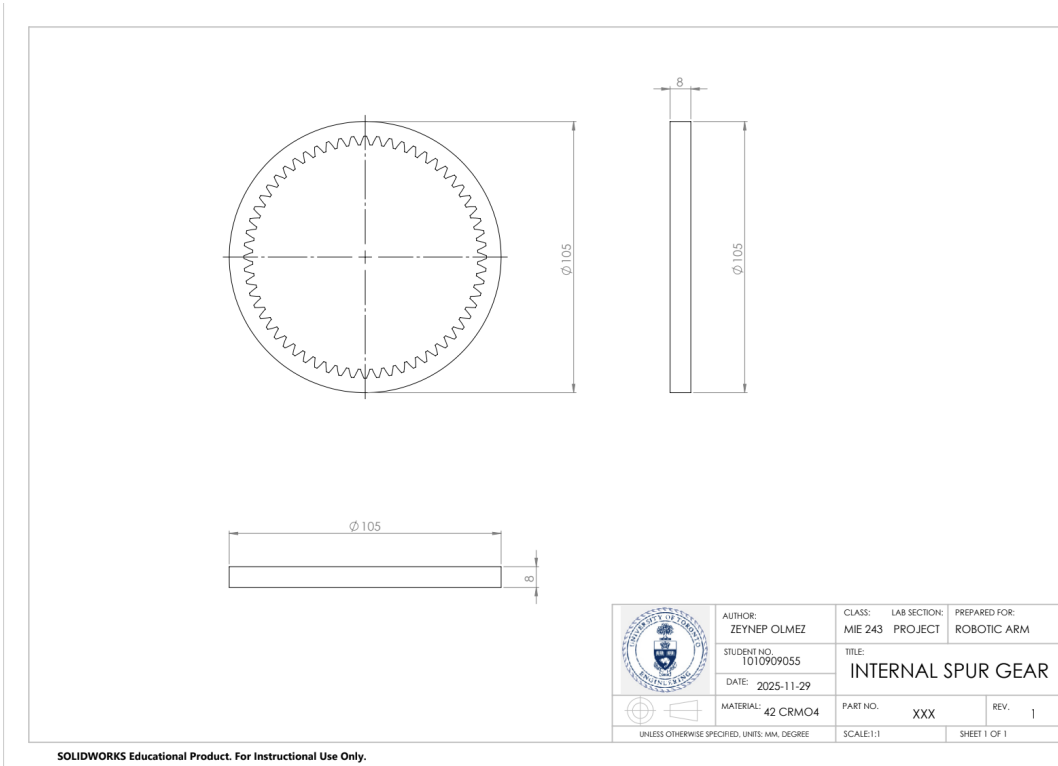


Figure 60. Drawing of Internal Spur Gear

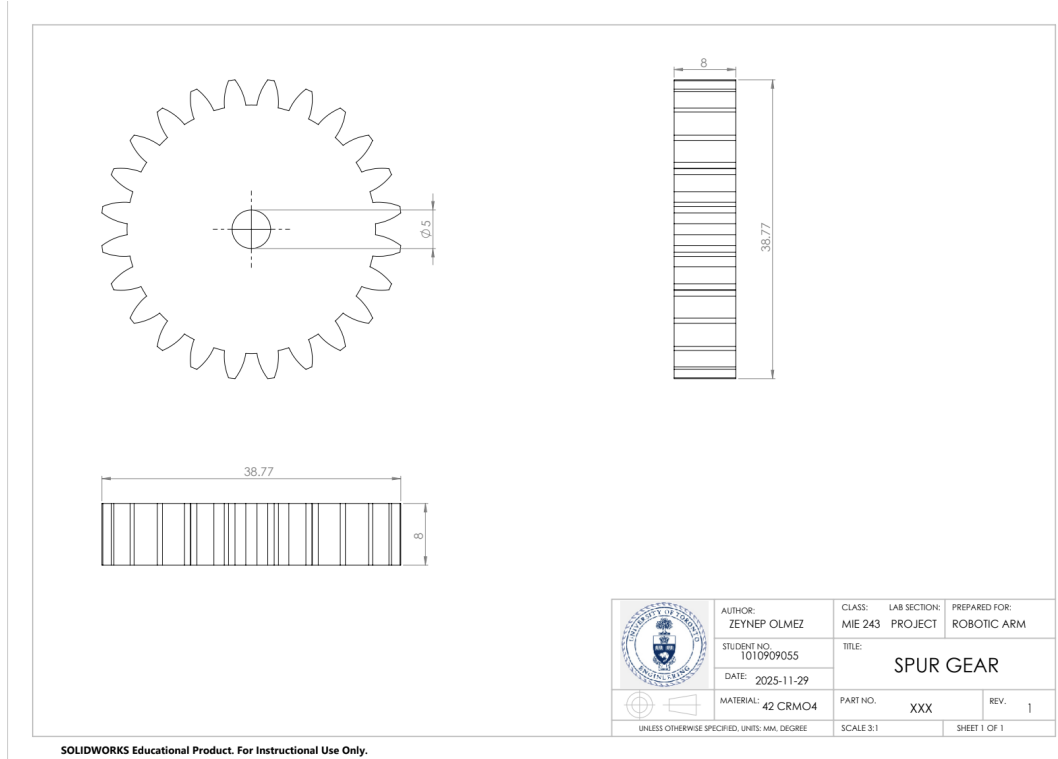


Figure 61. Drawing of Spur Gear

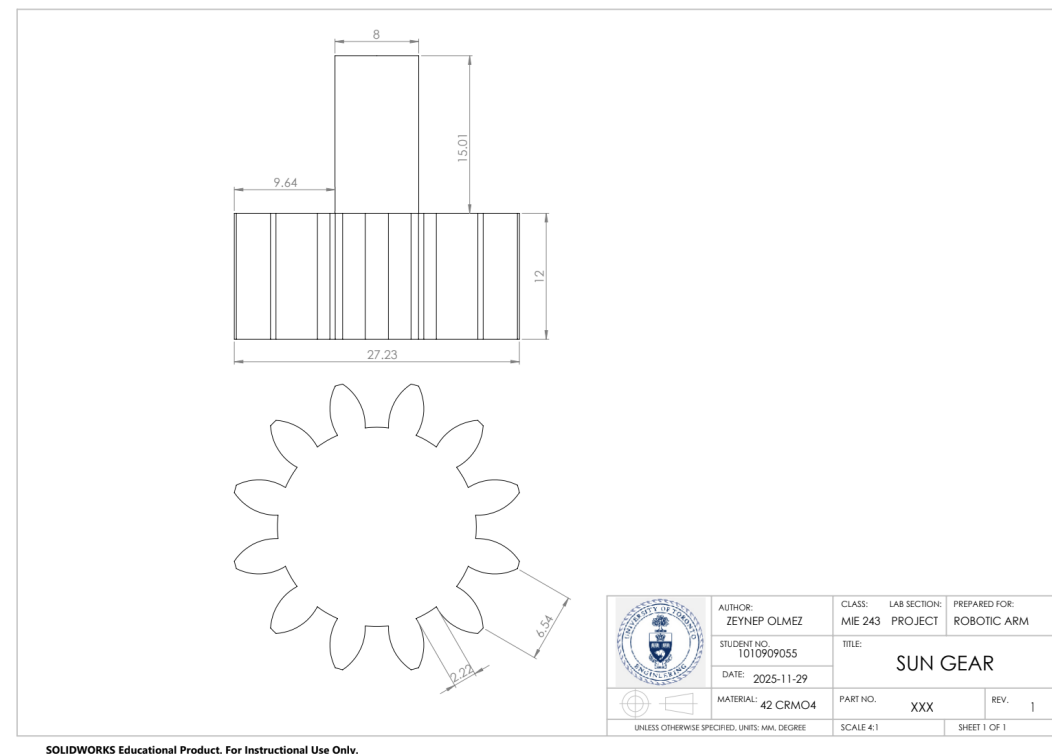


Figure 62. Drawing of Sun Gear

7.8 Motion Support Components

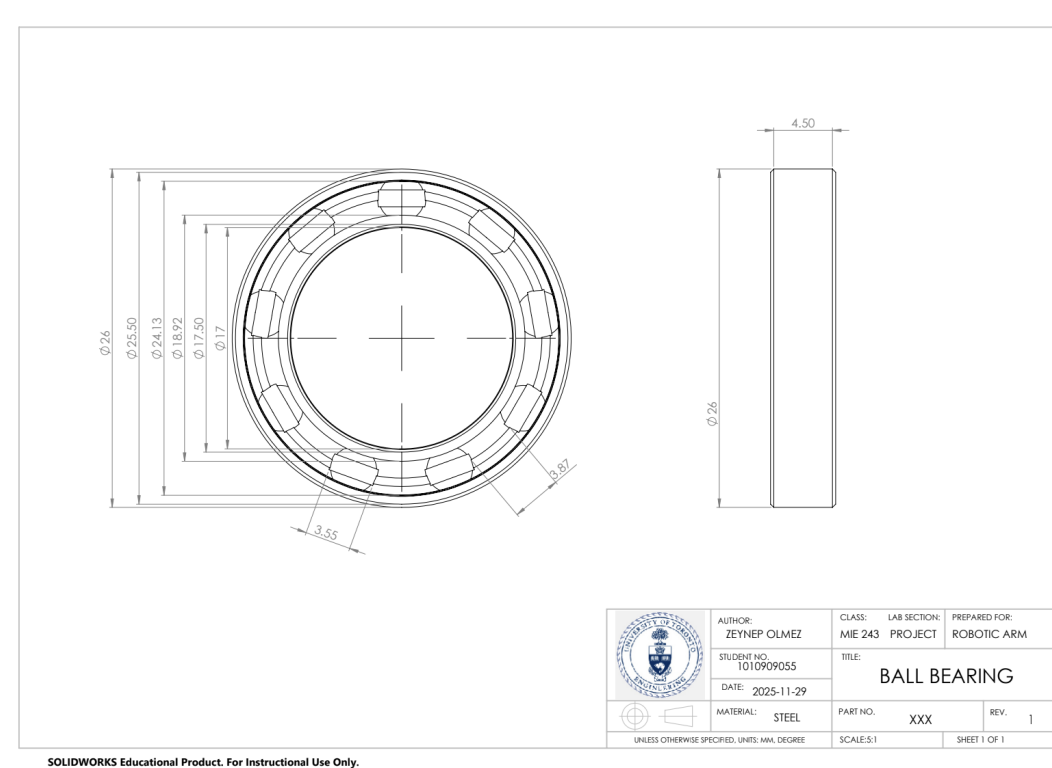


Figure 63. Drawing of Ball Bearing

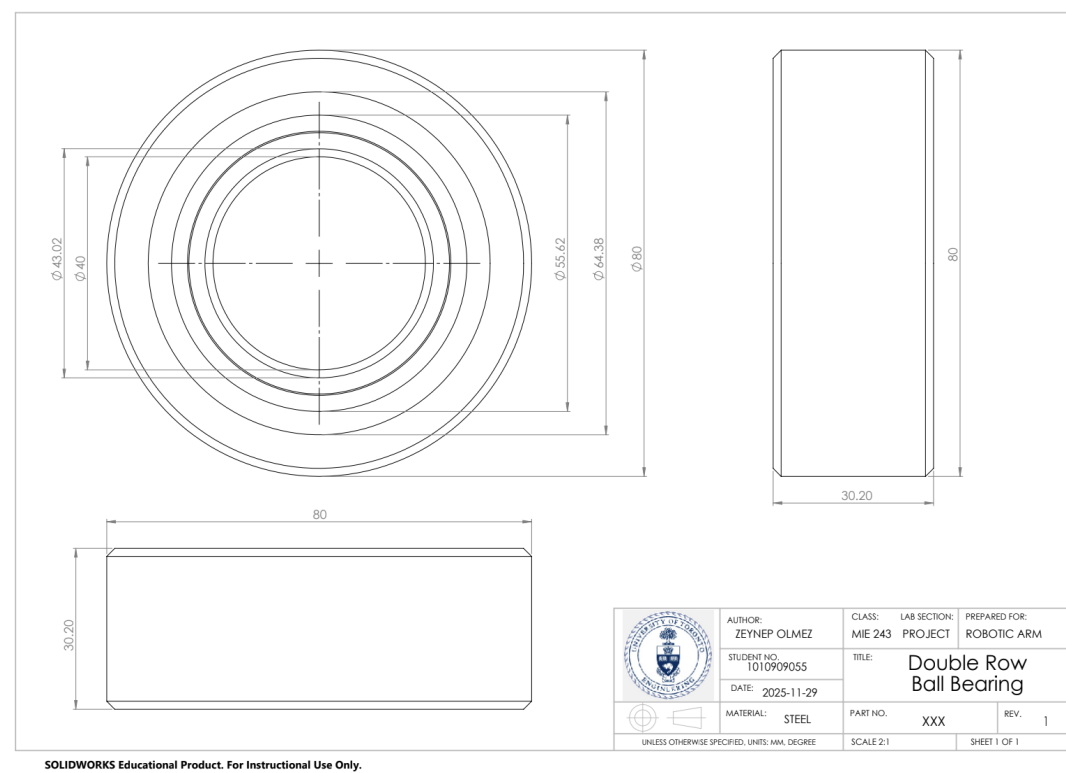


Figure 64. Drawing of Double Row Ball Bearing

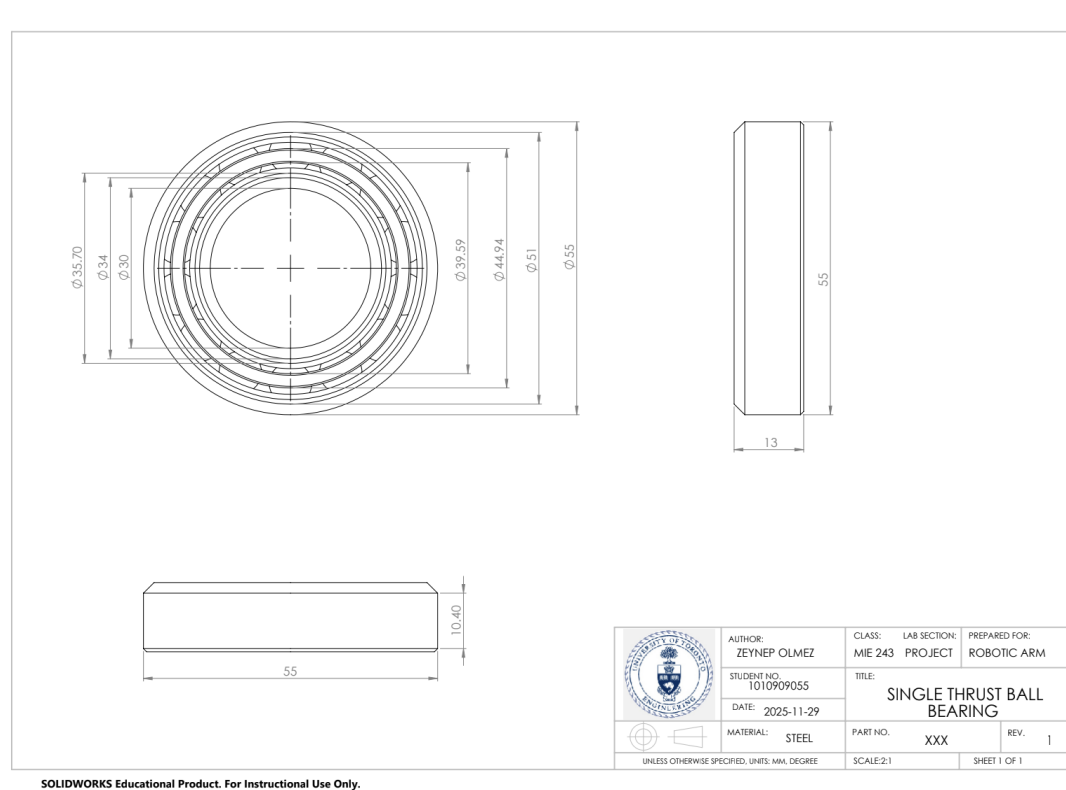


Figure 65. Drawing of Single Thrust Ball Bearing

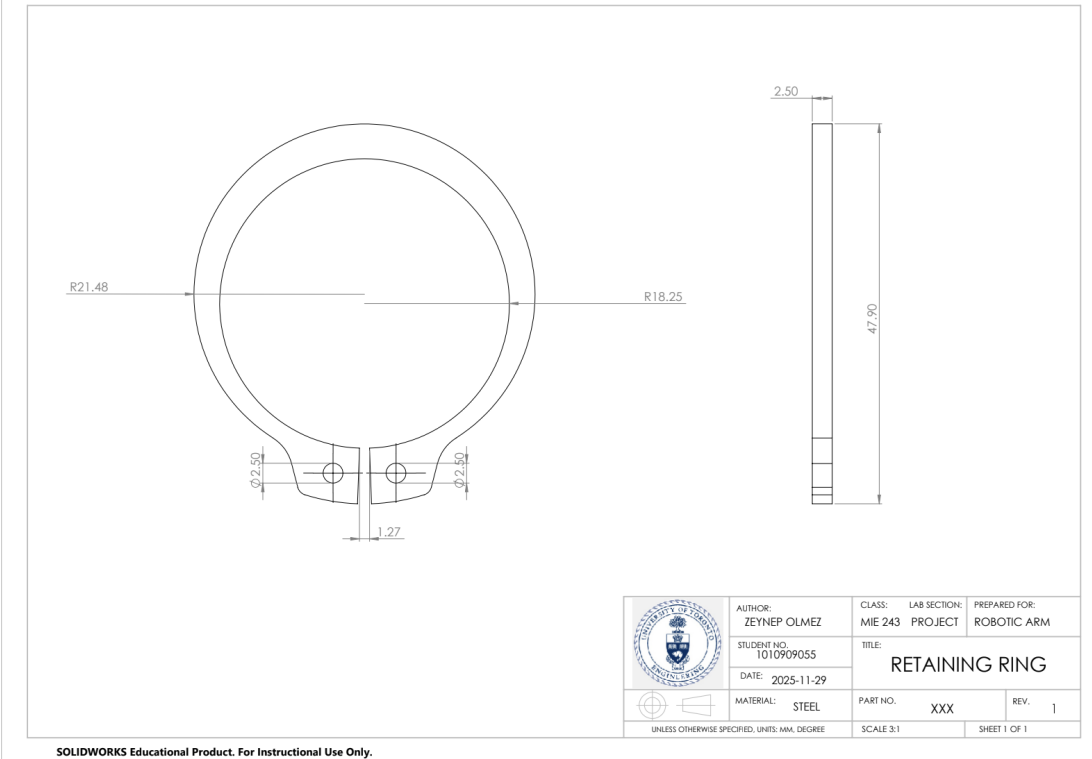


Figure 66. Drawing of Retaining Ring

7.9 Shaft Coupling

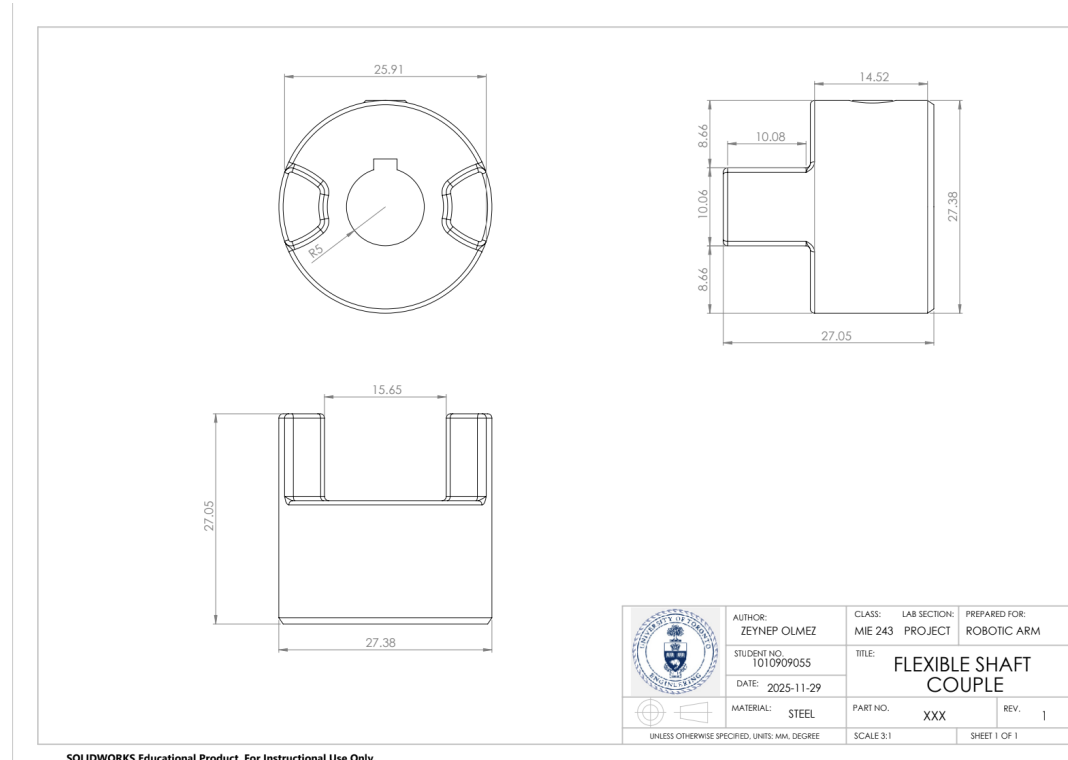


Figure 67. Drawing of Flexible Shaft Coupling

7.10 Connectors

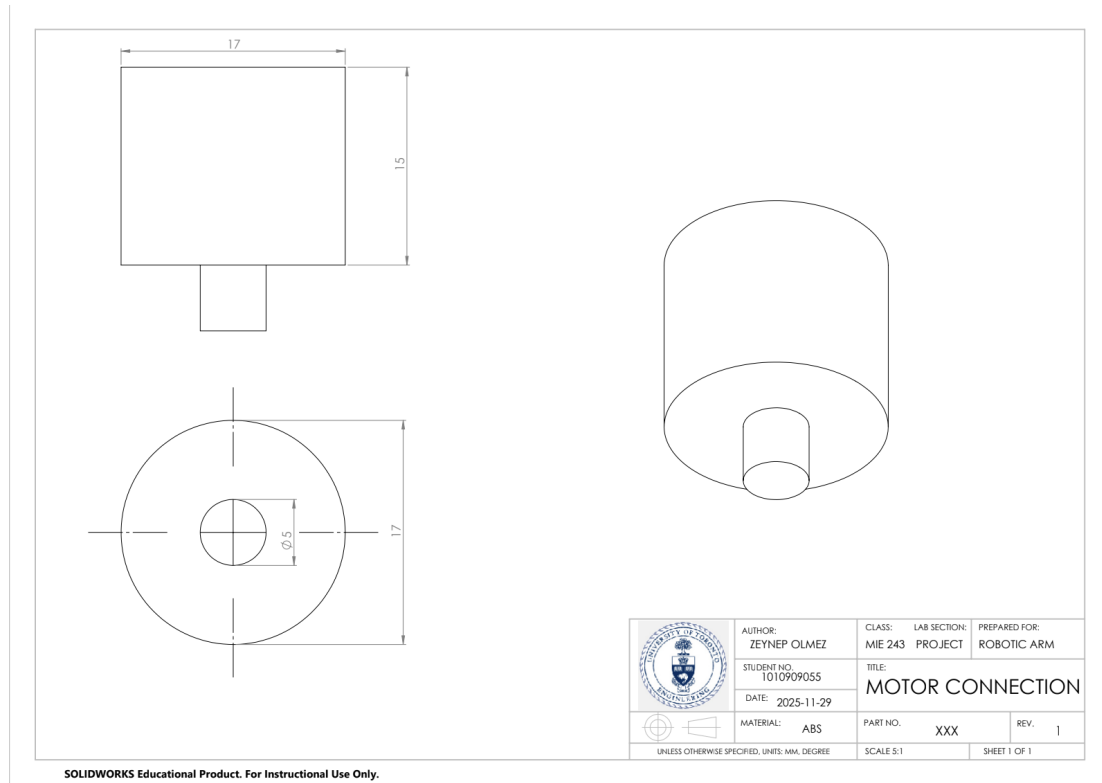


Figure 68. Drawing of Motor Connection

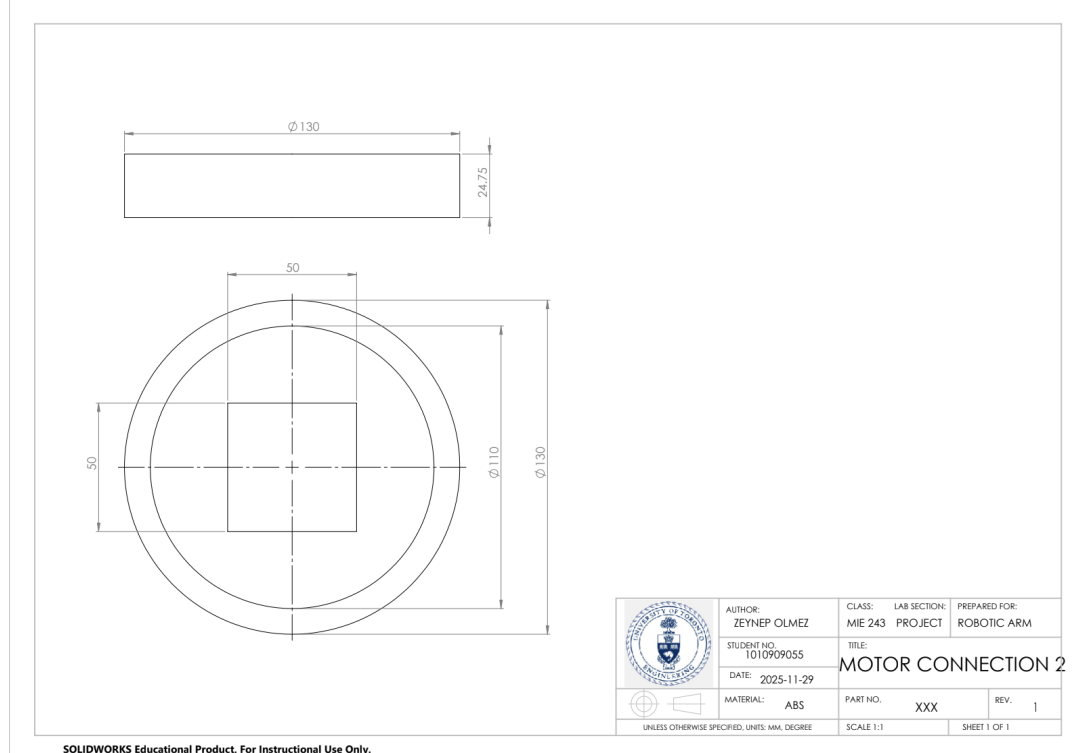


Figure 69. Drawing of Motor Connection 2

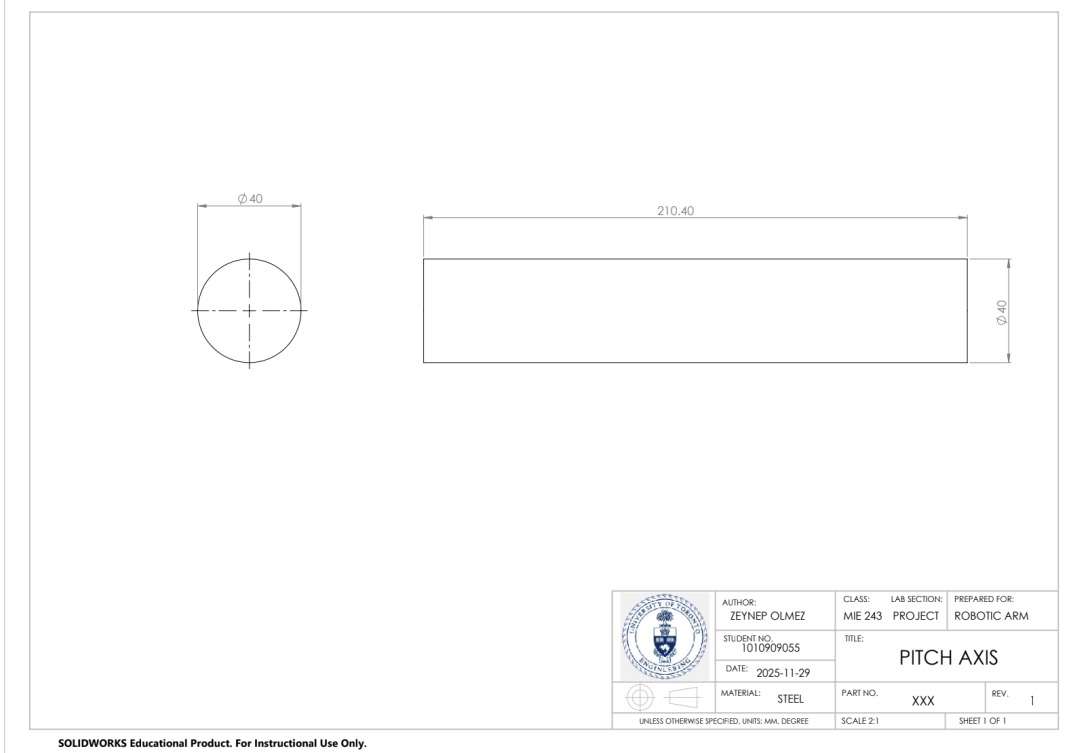


Figure 70. Drawing of Pitch Axis

7.11 Carriers

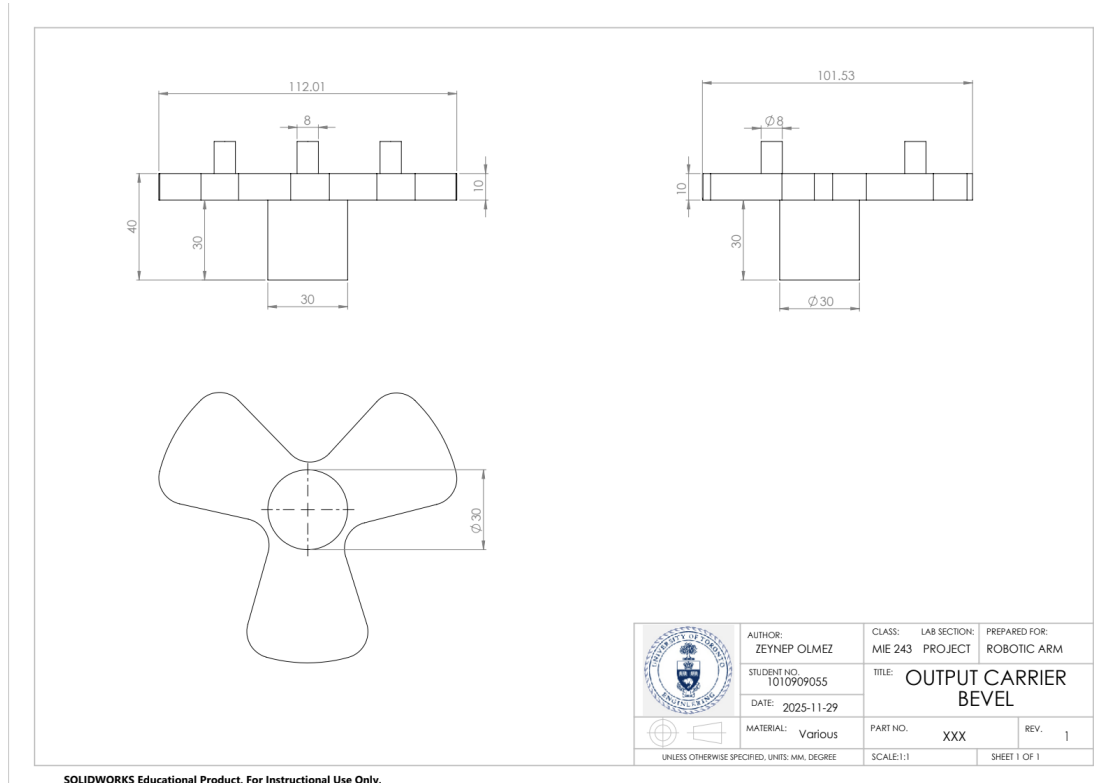


Figure 71. Drawing of Output Carrier Bevel

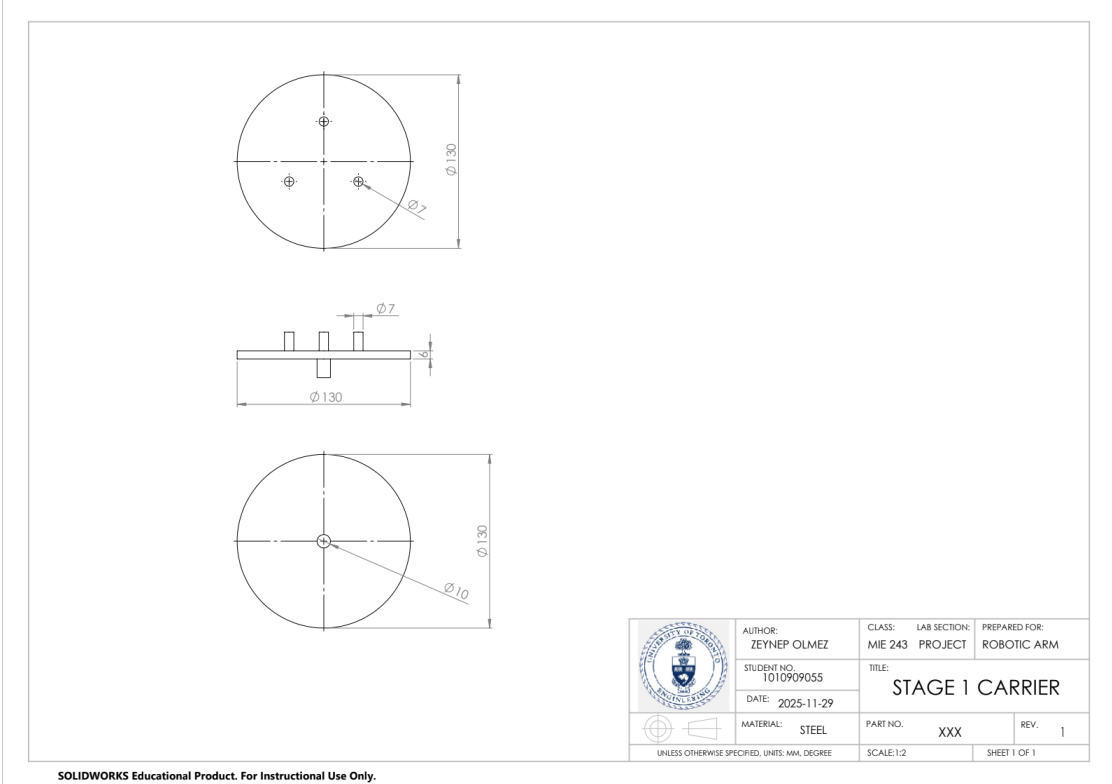


Figure 72. Drawing of Stage 1 Carrier

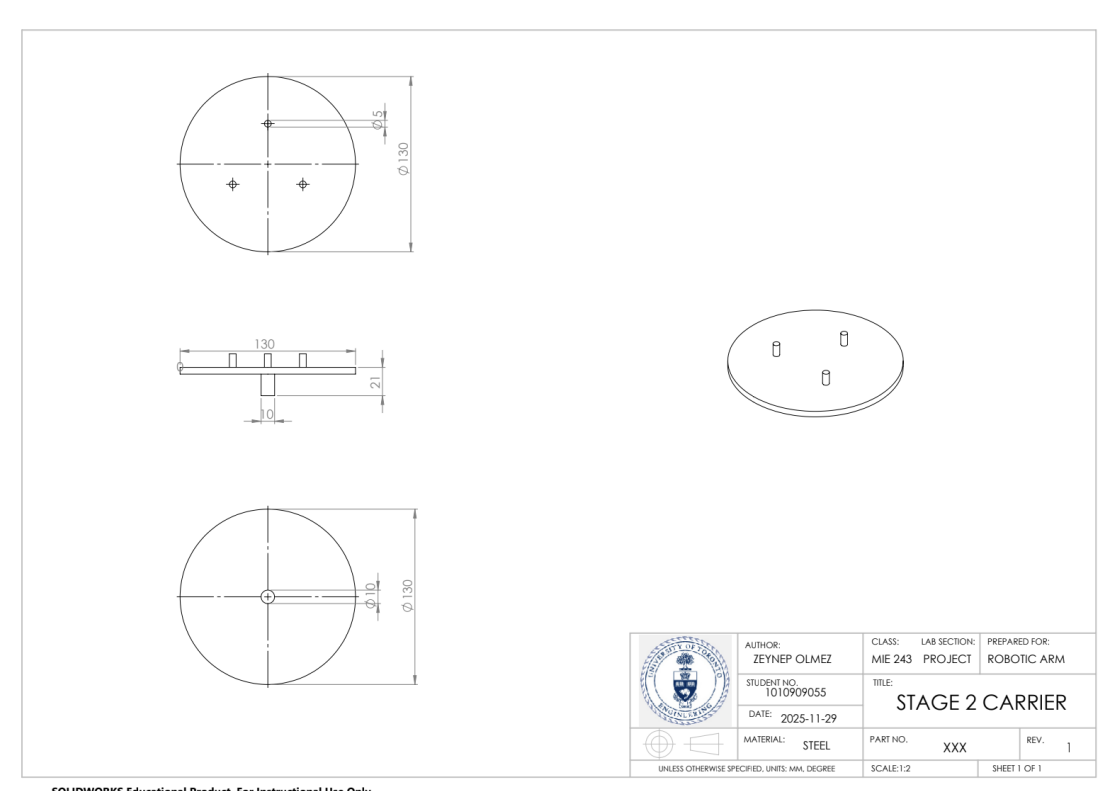


Figure 73. Drawing of Stage 2 Carrier

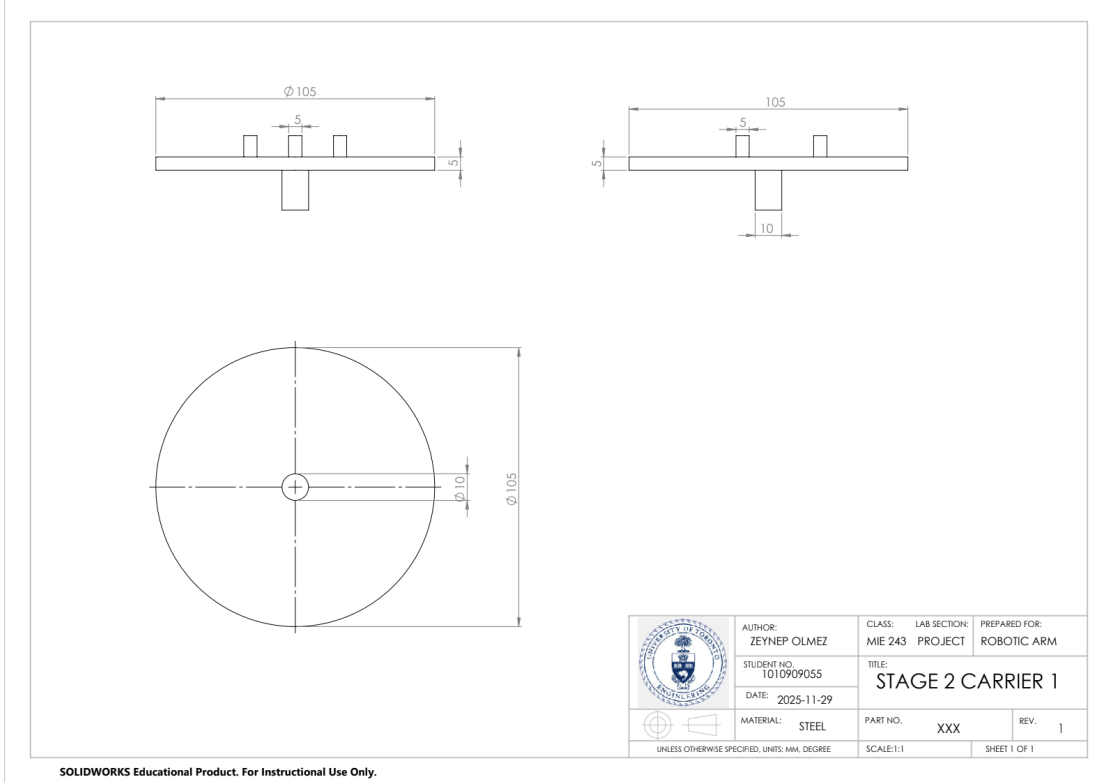


Figure 74. Drawing of Stage 2 Carrier 1

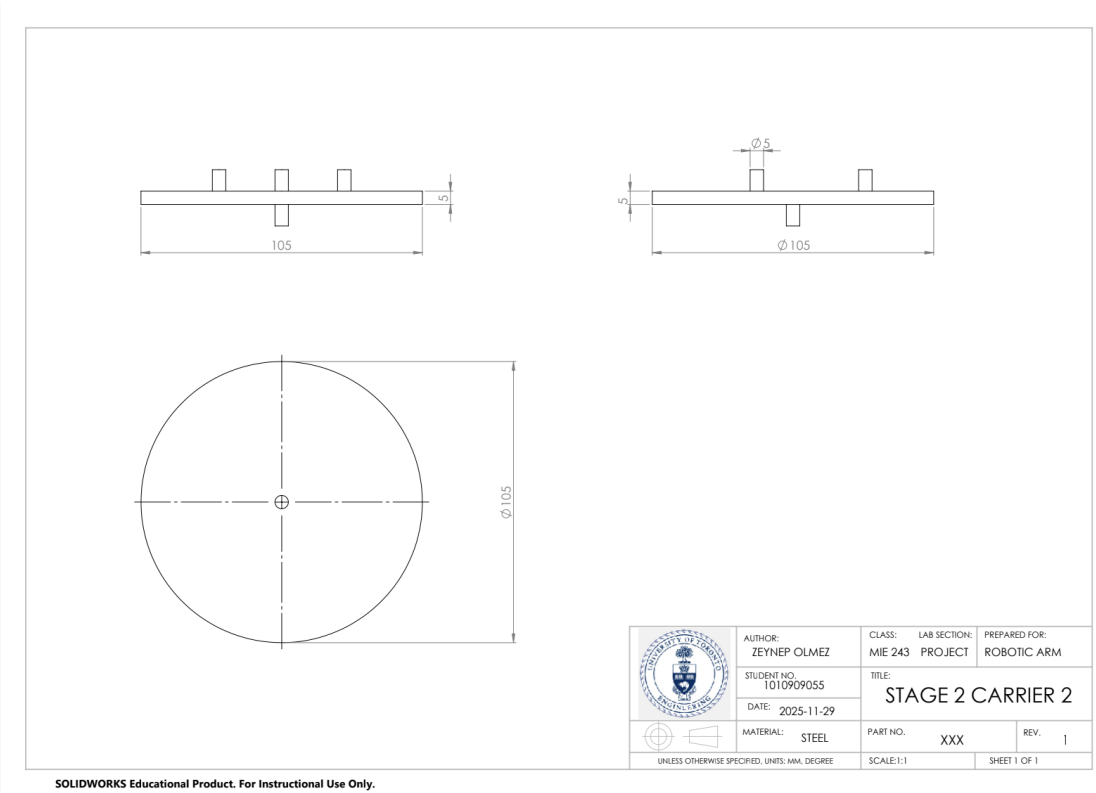


Figure 75. Drawing of Stage 2 Carrier 2

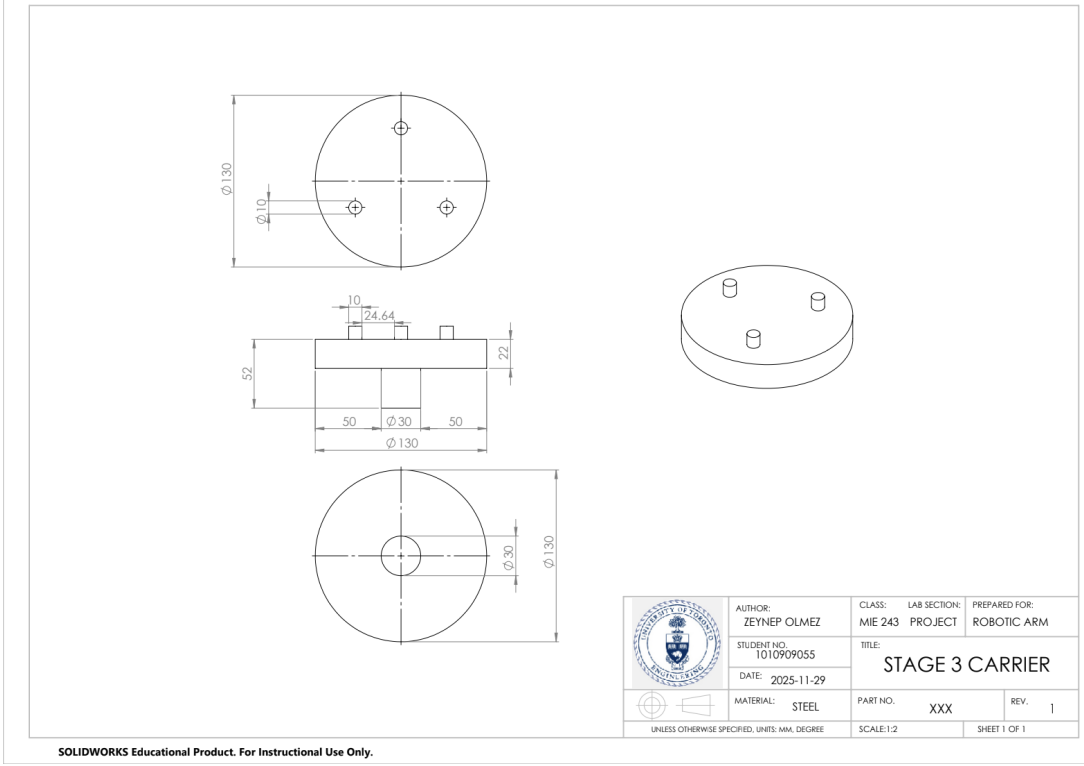


Figure 76. Drawing of Stage 3 Carrier

7.12 Emergency Stop

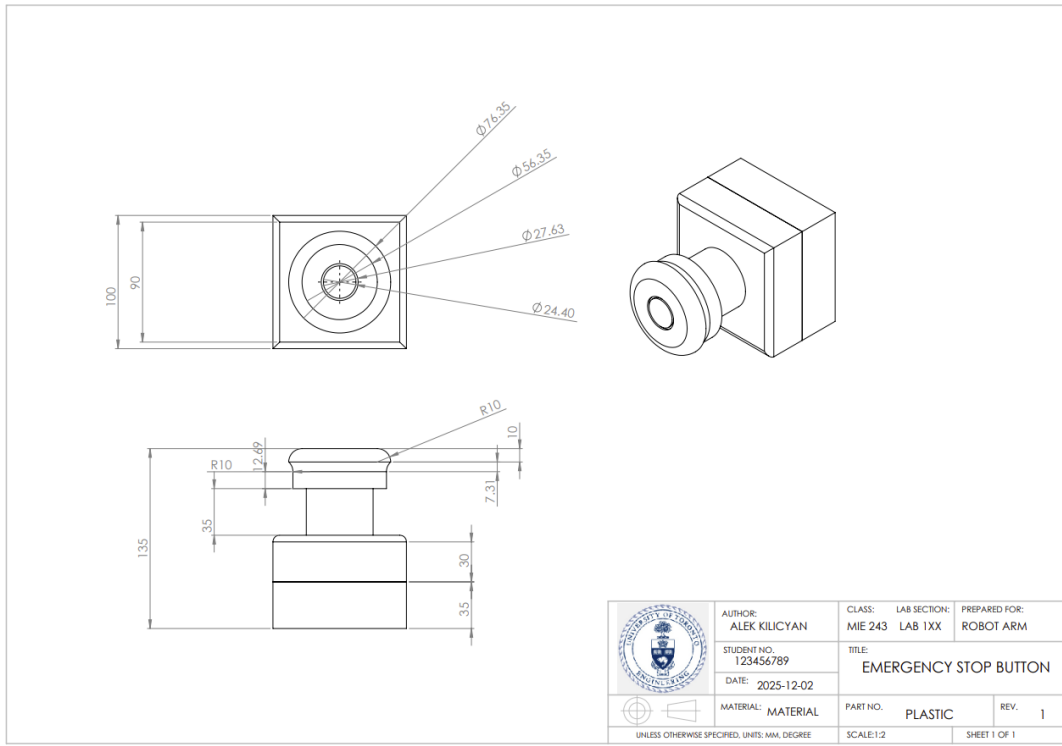


Figure 77. Drawing of the Emergency Stop Button

8.0 Cost and Feasibility Analysis

This section discusses the cost of the Robotic Arm design along with the feasibility of manufacturing and assembly.

8.1 Cost Analysis

This section addresses the Bill of Materials and the Cost of Each Part.

Table 10. Bill of Materials and Price

ITEM NO.	PART NAME / NUMBER	DESCRIPTION	QTY.	COST ea. (CAD)
1	6627T161	NEMA 23 Stepper Motor	1	240.37
2	6627T211	NEMA 14 Stepper Motor	1	86.14
3	6627T92	NEMA 17 Stepper Motor	1	87.69
4	6627T591	NEMA 24 Stepper Motor	1	152.00
5	6627T651	NEMA 34 Stepper Motor	1	128.33
6	6413K112	Set Screw Flexible Shaft Coupling, Iron Hub	2	7.29
7	8828T219	Angular-Contact Double Row Ball Bearing	2	171.68
8	5972K214	Ball Bearing	1	9.82

9	2664N16	Spur Gear, Module 1.5, 12 Teeth, 20° Pressure Angle, 1045 Carbon Steel	2	13.13
10	7880K26	Spur Gear, Module 1.5, 14 Teeth, 20° Pressure Angle	3	24.39
11	2664N18	Spur Gear, Module 1.5, 24 Teeth, 20° Pressure Angle, 1045 Carbon Steel	3	20.25
12	2664N16	Spur Gear, Module 2, 12 Teeth, 20° Pressure Angle, 1045 Carbon Steel	2	13.13
13	2664N17	Spur Gear, Module 2, 18 Teeth, 20° Pressure Angle, 1045 Carbon Steel	1	15.97
14	2664N1	Spur Gear, Module 2, 24 Teeth, 20° Pressure Angle, 1045 Carbon Steel	6	20.25
15	2664N19	Spur Gear, Module 2, 35 Teeth, 20° Pressure Angle, 1045 Carbon Steel	3	37.31
16	18635A52	Round Turntable, Lubricated, 175 lb Capacity, Aluminium	2	57.24
17	2696N16	Internal Ring Gear, 60 Teeth, Module 1.5, 20° Pressure Angle, Metal	6	57.74
18	2696N22	Internal Ring Gear, 100 Teeth, Module 1.5, 20° Pressure Angle, Metal	2	190.80

19	2696N33	Internal Ring Gear, 100 Teeth, Module 2, 20° Pressure Angle, Metal	1	300.06
20	J1-STRUCT	J1: Housing + Carrier + Shaft	1	387.32
21	J2-STRUCT	J2: Housing + Carrier + Shaft	1	36.12
22	J3-STRUCT	J3: Housing + Carrier + Shaft	1	132.45
23	J4-STRUCT	J4: Housing + Carrier + Shaft	1	17.57
24	J5-STRUCT	J5: Housing + Carrier + Shaft	1	24.67
25	M2-16-SHCS-BL KOX	Black-Oxide Alloy Steel Socket Head Screw, M2 × 0.4 mm, 16 mm Long, 100-Pack	1	13.03
26	Hexapod	Cameron T100BH Two Tripods	2	79.99
27	Shell	ABS Shell (11428 g) 24.99 CAD per 1000g	1	285.5
28	M5-20-HH-10.9-YZ	Zinc Yellow-Chromate Plated Steel Hex Head Screw, Class 10.9, M5 × 0.8 mm, 20 mm Long, 50-Pack	1	16.17
Total Cost = 3,713.52 CAD				

Based on the BOM given in Table 10, the total cost of the robot is \$3,713.52 CAD, which was significantly lower than the \$5,000 CAD goal budget mentioned in the Engineering Specifications. This will allow for flexibility for unexpected costs such as machining and wiring, which will leave a margin of about \$1,286.48 CAD.

Several design decisions enabled the system to be under budget. First, torque may be effectively matched to each joint by using stepper motors in a variety of NEMA sizes (14, 17, 23, 24, and 34), preventing needless overspending on large motors. Secondly, spur gears and internal ring gears were used rather than more expensive alternatives such as harmonic drives, which greatly decreases the transmission costs. Furthermore, additional cost savings were achieved by producing the ABS shell utilizing 3D printing material instead of machined aluminum or composite panels.

Finally, overall structural costs were controlled by the use of custom-fabricated housings and off-the-shelf bearings and turntables. It should also be emphasized that the overall cost reflects single-unit, not mass production. Therefore, this cost serves as the worst upper bound. Bulk purchases, supplier discounts, and more effective production techniques will be used when the robot is built in large quantities. As a result, the computed total of \$3,713.52 CAD should be regarded as the highest anticipated cost; further iterations or increased production are probably going to result in significantly reduced per-unit prices.

8.2 Feasibility Analysis

All of our team members in the design group have completed a Basic Machining Course at George Brown College, which provided us with essential experience on drill presses, lathes, and milling machines. As a result, the team possesses the required technical skillset to safely and accurately manufacture the custom components of the system.

The majority of the structural joint components can be fabricated from aluminum using manual milling and turning operations. Features such as bearing seats, motor mounting bores, shaft interfaces, and structural mounting faces can be produced through conventional machining. Threaded holes for fasteners and motor mounts can be created using a tap-and-die set, while shaft components can be manufactured on a lathe using standard facing and turning operations.

The ABS external shell is manufactured using 3D printing, eliminating the need for costly machining or tooling while allowing for prototyping and iterative design refinement. Furthermore, the base stability system, which utilizes commercial camera tripods, removes the need for large welded frames or custom support fabrication.

Overall, the robotic system is highly feasible to manufacture using a combination of off-the-shelf components and fundamental machining techniques. The design avoids complex manufacturing methods such as multi-axis CNC machining, casting, and welding, ensuring that the system can be realistically produced by the design team within both time and budget constraints.

9.0 Conclusion

The final design of our robotic arm delivers a cost-effective, efficient solution tailored to the demands of amateur cinematographers. It provides stable, repeatable motion through a 5-degree-of-freedom design, using stepper motors with multi-stage planetary gearboxes. It allows dynamic cinematic shots such as pan, tilt and heroic motion shots. The strength, stiffness, reduced weight and ease of use of the robotic arm is produced by appropriate material selection. The structural components such as brackets and hexapod holder are made of aluminum-6061, ABS is used for casings and housings, the motion support components are made up of steel, and lastly gears are specifically 42CrMo4.

A fundamental element of the design is its focus on stability and customizability. The hexapod base substantially enhances balance during long arm extensions and quick motions. In contrast, the electronics container, interchangeable camera mount, and replaceable attachments allow users to adjust the system to diverse filming demands. These features increase the portability, accessibility, and ease of assembly, making it a more feasible design for hobbyist cinematographers. Modeling assumptions and calculations were made to ensure the arm performs safely under worst-case scenarios and to validate the material selection for all components, the gear ratios, and the motor selection. The calculations include torque analysis, translational speed, and stress calculations. The 42CrMo4 steel planetary gear stages exhibited excellent fatigue resistance and large safety margins, ensuring long-term reliability under continuous use.

Even though the current robotic arm design is functional, further improvements can be made. Harmonic drives and additional stabilization sensors can be utilized as well as changes in material selection, such as using lighter composite materials, can be made to improve the performance of the design. However, these proposed changes are more expensive, making them harder to implement with our constraints of affordability and manufacturability. Currently, the robotic arm is an accessible motion-control solution that enhances the creative potential of amateur filmmakers and is ready for further prototyping and improvement.

10.0 References

- [1] "Trusted Robot Brands, One Platform," *Vention*.
https://vention.io/robot-arm?utm_adgroupid=161192374278&utm_adid=694982496449&utm_device=c&utm_source=google&utm_medium=ppc&utm_campaign=13059403350&utm_term=6%20axis%20robotic%20arm&hsa_acc=6710393722&hsa_cam=13059403350&hsa_grp=161192374278&hsa_ad=694982496449&hsa_src=g&hsa_tgt=kwd-308392105857&hsa_kw=6%20axis%20robotic%20arm&hsa_mt=p&hsa_net=adwords&hsa_ver=3&gad_source=1&gad_campaignid=13059403350&gbraid=0AAAAAADdnWDnEQ4bv2zpzUgzvephOKd7VU&gclid=Cj0KCQiAiqDJBhCXARIIsABk2kSIQXuAS8s4-pIyyZltL5v3_caFB9NAiNjzjHjAA8tMC2Z55uPKTAdsaAgFeEALw_wcB (accessed Dec. 02, 2025).
- [2] R. Kumar, "6061-T6 Aluminum Properties and its Uses," *Zetwerk.com*, Sep. 22, 2023.
<https://www.zetwerk.com/en-us/resources/knowledge-base/aluminum-extrusions/6061-t6-aluminum-properties-and-its-uses/>
- [3] "ABS vs PC vs Nylon: Choosing the Right Circuit Breaker Enclosure," *LAIWO Electrical Technology*, 2025.
<https://www.wosomelec.com/blog/abs-vs-pc-vs-nylon-choosing-the-right-circuit-breaker-enclosure> (accessed Dec. 02, 2025).
- [4] M. Alloys, "Steel vs Aluminum: Choosing the Right Material," *Millennium Alloys*, Oct. 16, 2023. <https://millenniumalloys.ca/steel-vs-aluminum-choosing-the-right-material/>
- [5] A. Cao, "Why Use Planetary Gear Motors in Robotics and Automation," *Ineedmotors.com*, Aug. 04, 2025.
<https://blog.ineedmotors.com/planetary-gear-motor-benefits-robotics-automation-precision/> (accessed Dec. 02, 2025).
- [6] "What Is a Planetary Gearbox And How Does It Work? | AssunMotor."
<https://assunmotor.com/blog/planetary-gearbox/>
- [7] Apex Dynamics, "What is backlash in a planetary gearbox?," *Apex Dynamics*, Nov. 04, 2025. <https://www.apexdyna.nl/en/gearboxes/backlash-planetary-gearbox> (accessed Dec. 02, 2025).
- [8] "Planetary Gear Motors vs. Spur Gear Motors," *ISL Products International*, 2022.
<https://islproducts.com/design-note/planetary-gear-motors-vs-spur-gear-motors/>
- [9] "Strain wave gears | NABTESCO," *Nabtesco.de*, 2025.
<https://www.nabtesco.de/en/products/strain-wave-gears> (accessed Dec. 02, 2025).
- [10] "Difference Between Planetary Gearbox vs Harmonic Drive - Shenzhen PICEA Motion Technology Co., Ltd," *Shenzhen PICEA Motion Technology Co., Ltd*, 2024.

<https://www.piceamotiondrive.com/difference-between-planetary-gearbox-vs-harmonic-drive.html> (accessed Dec. 02, 2025).

[11] Y.-J. Kim, “Design of Low Inertia Manipulator with High Stiffness and Strength Using Tension Amplifying Mechanisms,” presented at the 2015 IEEE/RSJ International Conference on Intelligent Robots and Systems (IROS), Accessed: Dec. 02, 2025. [Online]. Available: https://www.cs.cmu.edu/~cga/c/0749.pdf?utm_

[12] “68mm NEMA 34 Stepper Motor,” *Vention*.

https://vention.io/parts/68mm-nema-34-stepper-servo-motor-1161?utm_adgroupid=177640165627&utm_adid=732062309952&utm_device=c&utm_source=google&utm_medium=ppc&utm_campaign=22208168582&utm_term=&hsa_acc=6710393722&hsa_cam=22208168582&hsa_grp=177640165627&hsa_ad=732062309952&hsa_src=g&hsa_tgt=dsa-1646086090206&hsa_kw=&hsa_mt=&hsa_net=adwords&hsa_ver=3&gad_source=1&gad_campaignid=22208168582&gbraid=0AAAAAADdnWDkXFRI1VAzspwZr2BXXpSphq&gclid=Cj0KCQiAiqDJBhCXARIABk2kSkJ1ISJvwB3BjeIRhS41PkAwHTkZWbyUovmedgffcr9bPlyIchWAokaAn-CEALw_wcB (accessed Dec. 02, 2025).

[13] “NEMA 23 Stepper Motors – Mouser Canada,” *Mouser.ca*, 2023.

https://www.mouser.ca/c/electromechanical/motors-drives/stepper-motors/?frame%20size%20-%20nema=NEMA%2023&srsltid=AfmBOorQ91P7G4rMUM24xmJfQYmW1OaDdDzysOAT5wH5w_UvoFZEVBGa (accessed Dec. 02, 2025).

[14] “McMaster-Carr,” *Mcmaster.com*, 2025.

<https://www.mcmaster.com/products/motors/motor-frame-size~nema-17/> (accessed Dec. 02, 2025).

[15] admin, “Servo Motor vs. Stepper Motor: Choosing the Right Motor for Your Application | igus® Canada Blog & Toolbox,” *igus® Canada Blog & Toolbox*, Jul. 20, 2023.
<https://blog.igus.ca/2023/07/20/servo-motor-vs-stepper-motor/>

[16] “User Manual.” Accessed: Dec. 02, 2025. [Online]. Available:

https://dl.djicdn.com/downloads/DJI_RS_3_Mini/UM/20230105/DJI_RS_3_Mini_User_Manual_V1.0_en.pdf

[17] “Standard Configurations Catalog for Photo and Video Accessories Integrating Specifications and Dimensions for Open Ecosystem Development.” Accessed: Dec. 02, 2025. [Online]. Available: https://static.smallrig.com/mall/img/public/1721978727225_.pdf

[18] “How Does a Gimbal Work for Improving the Filming Quality?,” *Zhiyun-tech.com*, 2025. <https://www.zhiyun-tech.com/en/newsroom/1422> (accessed Dec. 02, 2025).

- [19] “Robot Mounting — ZIVID KNOWLEDGE BASE documentation,” *Zivid.com*, 2015. <https://support.zivid.com/getting-started/user-guide/mechanical-installation/available-mounts/robot-mounting.html> (accessed Dec. 02, 2025).
- [20] “Robotic Arm Design: Types & Components of Robotic Arms,” *www.universal-robots.com*. <https://www.universal-robots.com/in/blog/robotic-arm-design/>
- [21] ISO, “ISO - International Organization for Standardization,” *iso.org*, 2025. <https://www.iso.org/home.html>
- [22] “safety-functions,” *Universal Robots*. <https://www.universal-robots.com/media/1801971/ur-g3-safety-functions-20180418.pdf> (accessed Dec. 02, 2025).
- [23] “Documents,” *franka.de*. <https://franka.de/documents>
- [24] “Humans should work together with industrial robots, is that possible?,” *KUKA*, Mar. 23, 2022. <https://www.kuka.com/en-ca/industries/solutions-database/2021/02/airskin-sick-und-kuka> (accessed Dec. 02, 2025).
- [25] ISO - International Organization for Standardization, “ISO/TS 15066:2016,” *ISO*, Mar. 08, 2016. <https://www.iso.org/standard/62996.html>
- [26] “Sony ILCE-7M3K Alpha Camera with Full-Frame 35mm Image Sensor + 28-70mm Zoom Lens,” *Amazon*. https://www.amazon.ca/Sony-ILCE-7M3K-Camera-Full-Frame-28-70mm/dp/B07FYDLVX3?utm_source=undefined&th=1 (accessed Dec. 02, 2025).
- [27] D. Sachs, S. Nasiri, and D. Goehl, “Image Stabilization Technology Overview,” p. 18.
- [28] <https://www.facebook.com/JeffPicoultPhotography>, “Camera Tripod Screw Size: The Standard Dimensions,” *MeFOTO*, May 12, 2024. <https://www.mefoto.com/camera-tripod-screw-size/>
- [29] “Robotics - total control on repeatability and accuracy,” *Renishaw.com*, 2024. <https://info.renishaw.com/Encoders-Robotics>
- [30] “How to Assess Camera Tripod Stability | Tripod Buying Guide – Part 4,” *scg-pro*, 2024. https://www.scg-pro.com/blogs/camera-tripod-school/buying-guide-4-tripod-stability?srsltid=AfmBOoqQ1O-MUeOi45kqaMPDHI3jkD_rFPIUc_GR-Sv980Pw8Qn-7wc1ocy=USD (accessed Dec. 02, 2025).

[31] K. Deguzman, “Types of Camera Movements in Film Explained: Definitive Guide,” *StudioBinder*, Feb. 02, 2025.

<https://www.studiobinder.com/blog/different-types-of-camera-movements-in-film/>

[32] <https://www.facebook.com/studiobinderapp>, “The Dutch Angle Shot in Film — Ultimate Guide,” *StudioBinder*, Jul. 02, 2025.

<https://www.studiobinder.com/camera-shots/camera-angles/dutch-angle-shot/>

[33]

First in Architecture, “Metric Data 01 Average dimensions of person standing,” www.firstinarchitecture.co.uk, 2019.

<https://www.firstinarchitecture.co.uk/metric-data-01-average-dimensions-of-person-standing/>

[34] StudioBinder, “50+ Types of Camera Shots & Angles,” *StudioBinder*, Jan. 13, 2025.

<https://www.studiobinder.com/blog/ultimate-guide-to-camera-shots/>

[35] C. C. for O. H. and S. Government of Canada, “Assessing Relevant Handling Factors : OSH Answers,” www.ccohs.ca, Aug. 12, 2021.

<https://www.ccohs.ca/oshanswers/ergonomics/niosh/assessing.html>

[36] E. M. Murtagh, J. L. Mair, E. Aguiar, C. Tudor-Locke, and M. H. Murphy, “Outdoor Walking Speeds of Apparently Healthy Adults: A Systematic Review and Meta-analysis,” *Sports Medicine (Auckland, N.z.)*, vol. 51, no. 1, pp. 125–141, 2021, doi:

<https://doi.org/10.1007/s40279-020-01351-3>.

[37] “Ronin-S - Product Information - DJI,” *DJI Official*, 2018.

<https://www.dji.com/ca/ronin-s/info#specs> (accessed Dec. 02, 2025).

[38] “mBot Ranger 3-in-1 Robot Building and Coding Robtics for Kids with App Remote Control | Makeblock,” *Makeblock*.

<https://www.makeblock.com/pages/mbot-ranger-robot-building-kit>

[39] “Hi-Spec 24pc Yellow Household DIY Tool Kit Set. Small Mini Tool Box Set of Starter Basic Tools for Home & Office.”

https://www.amazon.ca/Hi-Spec-Yellow-Household-Starter-Office/dp/B0CL68YYDT/ref%3Dsr_1_2_sspa?crid=3CMC971SP7JK1&dib=eyJ2IjoiMSJ9.oSoxAE0RNImq69Y-fFq4-xb_OFoaGlbsgqnMTrESO-VmxV13-1dbPhh8j26JaO9SNQ7LIS6FfgaUoBqcKwJGoIYlGMdG9NIKfHoft8Xi03sD_BiTJvpvgk2vP6IpgF6CHmGKVfSan9uM0lbidSXEYHP7o4tuggF3GSIaL_f2ZqsZbiyqKmbjalc7eV6eNhEw_L-czShObgqsosohyGHFYl1zsVsn1jgP_zXbvLBPVVV7zf1z5SOywE9RWw5RKLJyzRjuKmlbfa3SGCx3Tv4dfg4b8pDyaaHUtKA_fZvSk.XmOOqBccKrYGRaf5VB_YAKUqPPI4Hzd1nVyoj4I0UQg&dib_tag=se&keywords=amazon%2Bbasics%2Btoolbox&qid=1759112097&sp_csd=d2lkZ2V0TmFtZT1zcF9hdGY&sprefix=to olbox%2Bamazon%2B%2Caps%2C159&sr=8-2-spons&th=1 (accessed Dec. 02, 2025).

[40] admin, “myCobot Pro 600 - Elephant Robotics,” *Elephant Robotics - Enjoy Robots World*, Jul. 21, 2021. <https://www.elephantrobotics.com/mycobot-pro-600/> (accessed Dec. 03, 2025).

[41] “Robotic Arm Manufacturer - Collaborative Robots | UFACTORY,” *UFACTORY Official Website*, Feb. 15, 2023. <https://www.ufactory.cc/>

[42] “3. Technical specifications — Meca500 - User manual,” *Mecademic.com*, 2025. <https://resources.mecademic.com/en/doc/MC-UM-MECA500/latest/manual/technical-specifications.html> (accessed Dec. 03, 2025).

[43] “Dimensions: mm (in).” Available: <https://media.pbclinear.com/pdfs/pbc-linear-data-sheets/data-sheet-stepper-motor-support.pdf>

[44] O. for, “ISO 10218-1:2025,” *ISO*, 2025. <https://www.iso.org/standard/73933.html>

[45] 14:00-17:00, “ISO/FDIS 10218-2,” *ISO*. <https://www.iso.org/standard/73934.html>

[46] ISO - International Organization for Standardization, “ISO/TS 15066:2016,” *ISO*, Mar. 08, 2016. <https://www.iso.org/standard/62996.html>

[47] R. F. M. Ameen and M. Mourshed, “Urban sustainability assessment framework development: The ranking and weighting of sustainability indicators using analytic hierarchy process,” *Sustainable Cities and Society*, vol. 44, pp. 356–366, Jan. 2019, doi: <https://doi.org/10.1016/j.scs.2018.10.020>.

[48] O. for, “ISO 1222:2010,” *ISO*, 2025. <https://www.iso.org/standard/55918.html> (accessed Dec. 03, 2025).

[49] “ASM Material Data Sheet,” *Matweb.com*, 2025. https://asm.matweb.com/search/specifymaterial.asp?bassnum=ma6061t6&utm_

[50] G. Team, “6061 Aluminum: Get to Know its Properties and Uses - Gabrian,” *Gabrian*, Dec. 02, 2018. https://www.gabrian.com/6061-aluminum-properties/?utm_ (accessed Dec. 03, 2025).

[51] R. Media, “What are the Differences Between 6061 and 7075 Aluminum?,” *Metal Supermarkets - Steel, Aluminum, Stainless, Hot-Rolled, Cold-Rolled, Alloy, Carbon, Galvanized, Brass, Bronze, Copper*, May 23, 2019. <https://www.metalsupermarkets.com/differences-6061-and-7075-aluminum/>

[52] Protolabs, “ABS Plastic: Advantages, Disadvantages, and Applications,” *www.protolabs.com*, 2024. <https://www.protolabs.com/materials/abs/>

[53] “ABS,” *Curbell Plastics*, Sep. 16, 2025.
https://www.curbellplastics.com/materials/plastics/abs/?srsltid=AfmBOopKXctMoHDyjnNXcII9o8uo7t1pF52OWEv7vuSBB_oC4CA7gOKk (accessed Dec. 03, 2025).

[54] “ABS Plastic: Definition, Composition, Properties and Uses,” *Ruitai Mould*.
<https://www.rtprototype.com/what-is-abs-plastic/>

11.0 Appendices

Appendix A: Idea generation methods

Figure 78. Black Box Method

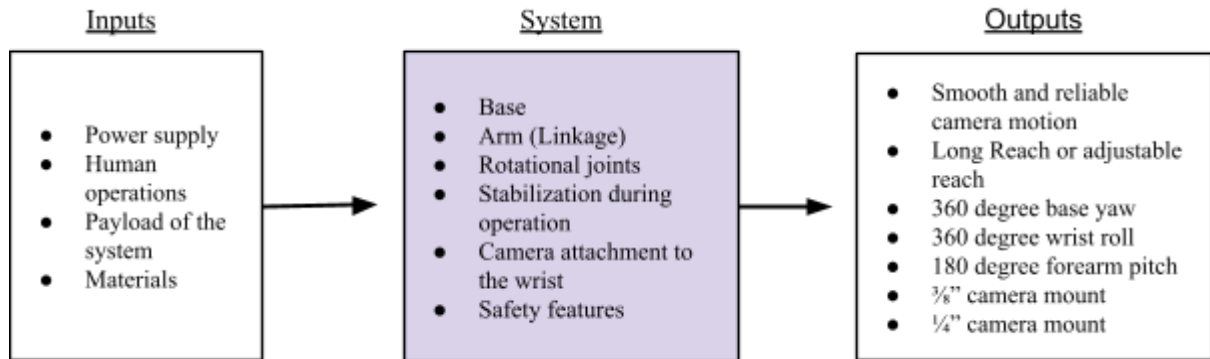


Table 11. Blue Sky Thinking

#	Idea	Feasibility [Yes/No]
1	Robotic arm that floats	No (not a static base during operation)
2	Infinite rotation gimbal wrist	Yes
3	Overhead camera arm with two rails (utilizing rail systems like trains)	No (not a moveable base)
4	A-frame that self-deploys	Yes
5	Gyroscopic support	No (weight restrictions)
6	Shoulder joint with clutch integration	Yes
7	3-link articulated arm design	Yes
8	Telescopic extension of robot arms	Yes
9	Lift with drone assistance	No (safety restrictions)
10	Tension-based cable stabilization	Yes
11	Dual-pivot articulated arm	Yes
12	Low center of gravity base	Yes

Table 12. Free Brainstorming

#	Idea	Feasibility [Yes/No]
1	Flywheel-driven stabilization	Yes
2	Snake-arm design that is overly flexible	No (safety regulations/restrictions)
3	Arm that has a counterweight block	Yes
4	A turntable base that can move 360°	Yes
5	Emergency stop button attached to the base of the robot	Yes
6	A camera plate that can be replaceable quickly	Yes
7	Using lockable wheels for moveable base (static during operation since lockable)	Yes
8	Castor wheels	Yes
9	String attachments to reduce payload	Yes
10	Adjustable vertical mast height	Yes

Table 13. Morph chart

	Functions					
	Base	Arm (Linkage)	Shoulder (Joint)	Stabilization during Operation	Camera Attachment to the Wrist	Safety Features
Design 1	Castor Wheels	3-link articulated arm	180 degree pivot	Low center of gravity base	Standard camera attachment with screws	Emergency stop button attached to the robot with a long cable
Design 2	A-frame mounted on base with lockable wheels	Dual pivot arm with string attachments	180 degree pivot	Tension based cable stabilization	Standard camera attachment with screws	Emergency stop button attached to the robot with a long cable
Design 3	Lockable wheels	Dual pivot articulated arm	Shoulder joint with clutch integration	Flywheel driven stabilization	Camera attached to a Gimbal wrist	Emergency stop button attached to the robot with a long cable

Table 14. SCAMPER method for Design 1

Steps	Application
S – Substitute	The clutch shoulder was replaced with linear actuators and lead screws.
A – Adapt	The tripod-like stability geometry was adapted into a triangular mechanical base.
M – Modify	The DOF approach was modified so that the base moves the head instead of the arm joints.
E – Eliminate	The clutch was eliminated from the design.
R – Reverse	The motion generation was reversed, now the camera platform stays rigid and the base provides more degrees of freedom.

Table 15. SCAMPER method for Design 2

Steps	Application
S – Substitute	The clutch mechanism was substituted with a spherical parallel manipulator.
C – Combine	The 3 DOF spherical end-effector was combined with a 3 DOF arm.
A – Adapt	The industrial parallel manipulator geometry was adapted to the motion of the camera.
M – Modify	The elbow and shoulder drives were modified to a belt-drive system.
R – Reverse	The typical wrist was revered so that the spherical manipulator is now the primary orientation system.

Table 16. SCAMPER method for Design 3

Steps	Application
S – Substitute	The large stabilizing cables were substituted for string-tension supports
M – Modify	The arm geometry was modified to allow for there to be greater than 1m reachable span.
P – Put to another use	Strings are now used for both tension and motion stability.

E – Eliminate	Complex pivot mechanisms were eliminated.
R – Reverse	The direction of support loads were reversed using tension.

Table 17. SCAMPER method for Design 4

Steps	Application
S – Substitute	Cable tension was substituted with a parallelogram four bar.
C – Combine	The belt driven yaw was combined with a 4 bar vertical lift.
A – Adapt	The four bar crane was adapted to allow for vertical movement principles.
M – Modify	The rigid arm was modified to allow for there to be triangular linkage.
E – Eliminate	String tension that reversed the direction of support loads were removed.

Table 18. SCAMPER method for Design 5

Step	Application
S – Substitute	The wheeled base was replaced with tank tracks.
C – Combine	The telescoping arms were combined with multi link joints.
A – Adapt	The excavator style boom was adapted to ensure articulation in the robotic arm.
M – Modify	The arm segments were modified to extrude rather than stay at a fixed length.
E – Eliminate	The overextended base was removed.

Table 19. SCAMPER method for Design 6

Step	Application
S – Substitute	The wheel base was replaced with a tripod.
C – Combine	The curvature was combined with multi link bending.

A – Adapt	The cinematography tripod was adapted to a higher standard.
M – Modify	The arms were modified to create an “S” shaped path.
P – Put to another use	The tripod is now used for both support and elevation.

Table 20. SCAMPER method for Design 7

Step	Application
S – Substitute	The complex arm was replaced with a simple 2 link arm.
C – Combine	Aspects of the design such as the complex arm were combined for simplicity and mobility.
A – Adapt	The industrial robot arm shape was adapted for better mobility.
P – Put to another use	The wheels are now used for transport and positioning.

Appendix B: Candidate Designs

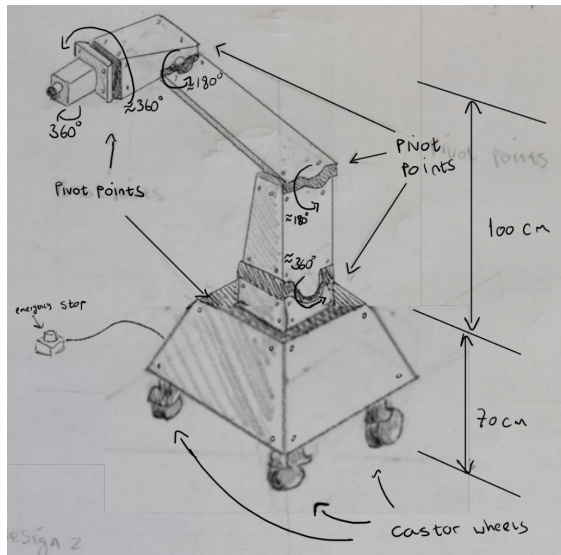


Figure 79. Initial candidate design 1

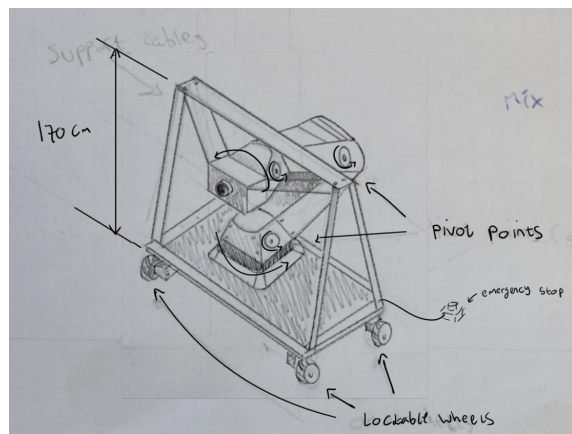


Figure 81.a Initial candidate design 2

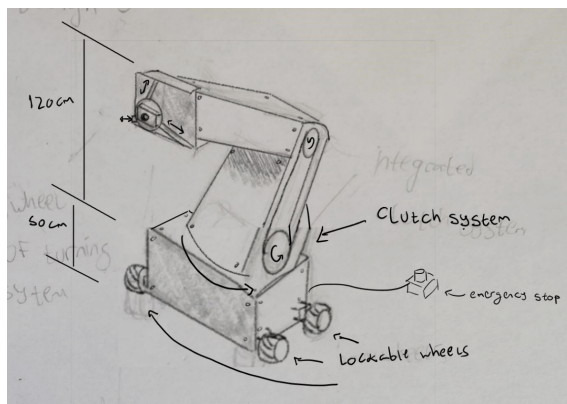


Figure 80.a Initial candidate design 3 platform

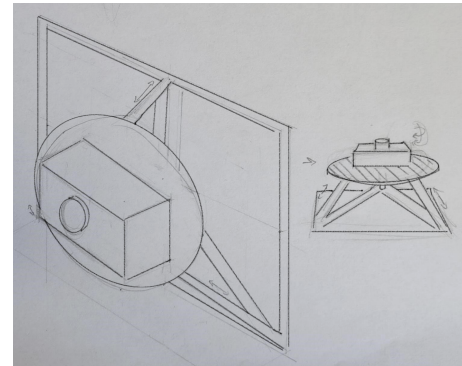


Figure 81.b Design 3 - Gimbal rotating

Appendix C: Idea and Final Design selection and reiteration

This appendix outlines the multi-voting tool results used in the idea selection of the design process detailed in Figure 82 in addition to the initial sketch of the final design illustrated in Figure 82.

Which designs do you believe better meet the projects objectives? (Vote for 3 designs)

4 respostas



Figure 82. Multi-voting results.

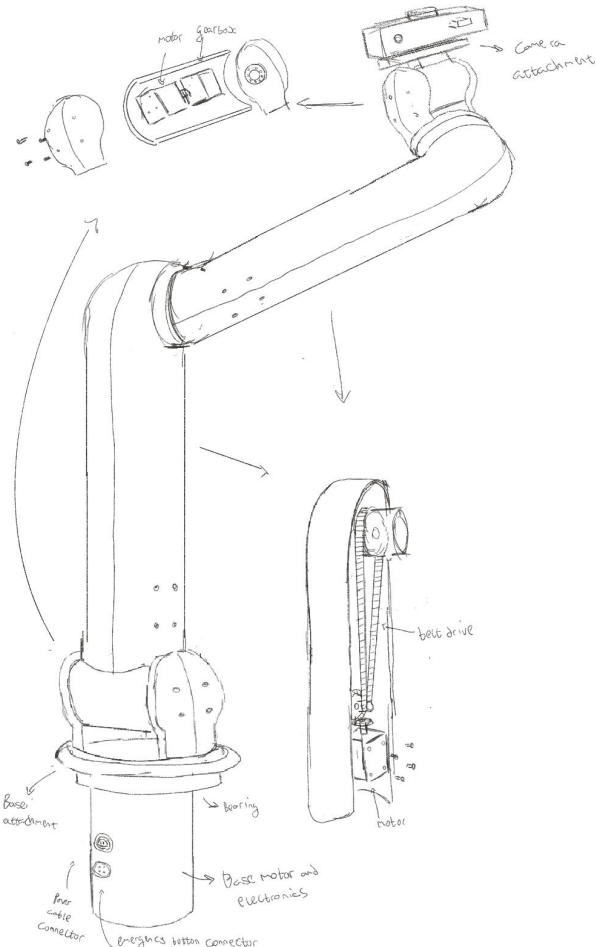


Figure 83. Final Design reiteration sketch

Appendix D: Python Calculations

This appendix demonstrates the code used to calculate the complete kinematic and dynamic model. The code is illustrated in Figures 84. a - h

```

45     R = matrix_exp3(w, theta)
46     w_hat = skew3(w)
47     V = (np.eye(3) * theta
48           | + (1.0 - np.cos(wn * theta)) / (wn**2) * w_hat
49           | + (wn * theta - np.sin(wn * theta)) / (wn**3) * (w_hat @ w_hat))
50     p = V @ v
51     T = np.eye(4)
52     T[0:3, 0:3] = R
53     T[0:3, 3] = p
54     return T
55
56     def screw_axis(w, q):
57         """Screw axis for S = [W v]"""
58         w = np.asarray(w, dtype=float)
59         q = np.asarray(q, dtype=float)
60         v = -np.cross(w, q)
61         return np.hstack((w, v))
62
63     # =====
64     # Arm calucaltions for our robot We used 5 DOFs
65     # =====
66
67     class FiveDOFArm:
68         def __init__(self):
69             #Geometry from CAD
70             z_shoulder = 0.13875 #Shouldder offset
71             z_wrist = 0.69510 #wrist offset
72
73             # J1
74             q1 = np.array([0.0, 0.0, 0.0])
75             w1 = np.array([0.0, 0.0, 1.0])
76
77             # J2
78             q2 = np.array([0.0, 0.0, z_shoulder])
79             w2 = np.array([1.0, 0.0, 0.0])
80
81             # J3
82             q3 = np.array([0.125, 0.0, z_wrist])      # 125 mm, 0, 695.10 mm from above
83             w3 = np.array([1.0, 0.0, 0.0])
84
85             # J4
86             q4 = np.array([0.180, 0.32021, z_wrist])
87             w4 = np.array([-1.0, 0.0, 0.0])
88

```

Figure 84.a Python Code

```

88
89     # J5
90     q5 = np.array([0.125, 0.32021, z_wrist])
91     w5 = np.array([0.0, 1.0, 0.0])
92
93     S1 = screw_axis(w1, q1)
94     S2 = screw_axis(w2, q2)
95     S3 = screw_axis(w3, q3)
96     S4 = screw_axis(w4, q4)
97     S5 = screw_axis(w5, q5)
98
99     self.Slist = np.column_stack((S1, S2, S3, S4, S5))
100
101     # Home conf end-if
102     self.M = np.eye(4)
103     self.M[0:3, 3] = np.array([0.180, 0.32021, z_wrist])
104
105     self.g = 9.81
106
107     # Kinematics (horror movie)
108
109     def fkine(self, q):
110         """Forward kinematics T(q)"""
111         T = np.eye(4)
112         for i in range(len(q)):
113             Si = self.Slist[:, i]
114             T = T @ matrix_exp6(Si, q[i])
115         return T @ self.M
116
117     def jacobian_space(self, q):
118         """Space Jacobian J_s(q). 6x5 bcs 5 dof"""
119         n = self.Slist.shape[1]
120         J = np.zeros((6, n))
121         T = np.eye(4)
122         for i in range(n):
123             if i == 0:
124                 J[:, 0] = self.Slist[:, 0]
125             else:
126                 Ad_T = adjoint(T)
127                 J[:, i] = Ad_T @ self.Slist[:, i, q[i]]
128                 T = T @ matrix_exp6(self.Slist[:, i], q[i])
129         return J
130

```

Figure 84.b Python Code

Figure 84.c Python Code

Figure 84.d Python Code

```

222
223
224     def sample_joint_space(joint_limits, samples_per_joint=3):
225         """
226             Generate a coarse grid of joint configurations for analysis.
227             joint_limits: list of (min, max) for each joint [rad]
228
229             samples_per_joint: how many samples per joint dimension
230
231             Return: array of shape (N, 5)
232             """
233
234     grids = [
235         np.linspace(lim[0], lim[1], samples_per_joint)
236         for lim in joint_limits
237     ]
238
239     # Cartesian product
240     mesh = np.meshgrid(*grids, indexing="ij")
241     qs = np.stack([m.reshape(-1) for m in mesh], axis=-1)
242     return qs
243
244
245     def analyze_gravity_over_workspace(arm, m_payload, m_arm_est, joint_limits,
246                                         | | | | | samples_per_joint=3, gravity_margin=1.5):
247         """
248             Scan a grid of joint angles and compute worst-case gravity torques
249             for payload and payload+arm with margin.
250             """
251
252     qs = sample_joint_space(joint_limits, samples_per_joint)
253     nJ = arm.Slist.shape[1]
254
255     tau_max_payload = np.zeros(nJ)
256     tau_max_eff = np.zeros(nJ)
257
258     m_eff = m_payload + m_arm_est
259
260     for q in qs:
261         tau_p = arm.gravity_torque_payload(q, m_payload)
262         tau_e = arm.gravity_torque_effective_mass(q, m_eff)
263
264         tau_max_payload = np.maximum(tau_max_payload, np.abs(tau_p))
265         tau_max_eff = np.maximum(tau_max_eff, np.abs(tau_e))
266
267     tau_design_payload = gravity_margin * tau_max_payload
268     tau_design_eff = gravity_margin * tau_max_eff
269
270     return {
271         "tau_max_payload": tau_max_payload,
272         "tau_design_payload": tau_design_payload,

```

Figure 84.e Python Code

```

269         "tau_max_eff": tau_max_eff,
270         "tau_design_eff": tau_design_eff,
271         "m_eff": m_eff,
272     }
273
274     def analyze_speed_requirement_over_workspace(arm, speed_des,
275                                                 | | | | | | | joint_limits,
276                                                 | | | | | | | samples_per_joint=3):
277
278         """
279             For a given desiredd Cartersian speed msagnitude, scan workspace and directions
280             and compute worst-case required joint speeds.
281             In x,y,z cord sys
282             Returns: dict with max |qdot| per joint.
283             """
284
285     qs = sample_joint_space(joint_limits, samples_per_joint)
286     nJ = arm.Slist.shape[1]
287
288     directions = [
289         np.array([1.0, 0.0, 0.0]),
290         np.array([-1.0, 0.0, 0.0]),
291         np.array([0.0, 1.0, 0.0]),
292         np.array([0.0, -1.0, 0.0]),
293         np.array([0.0, 0.0, 1.0]),
294         np.array([0.0, 0.0, -1.0]),
295     ]
296
297     qdot_max = np.zeros(nJ)
298
299     for q in qs:
300         for d in directions:
301             d_unit = d / np.linalg.norm(d)
302             v_des = speed_des * d_unit
303             qdot = arm.required_joint_speeds_for_cartesian_velocity(q, v_des)
304
305             if qdot is None:
306                 # Singularity or not full rank; skip
307                 continue
308             qdot_max = np.maximum(qdot_max, np.abs(qdot))
309
310     return {"qdot_max": qdot_max}
311
312     def analyze_dynamic_over_workspace(arm, a_des, m_eff,
313                                         | | | | | joint_limits,
314                                         | | | | | samples_per_joint=3):
315
316         """
317             Approx dyn torque req over the workspace for a desired
318             ee linear acceleration magnitude a_des [m/s^2].

```

Figure 84.f Python Code

```

315     Use an effective mass m_eff lumped at the end-effector.
316     Tests directions: tx, ty, tz (space frame).
317     Returns: dict with max |tau_dynamic| per joint.
318     """
319
320     qs = sample_joint_space(joint_limits, samples_per_joint)
321     nJ = arm.Slist.shape[1]
322
323     directions = [
324         np.array([1.0, 0.0, 0.0]),
325         np.array([-1.0, 0.0, 0.0]),
326         np.array([0.0, 1.0, 0.0]),
327         np.array([0.0, -1.0, 0.0]),
328         np.array([0.0, 0.0, 1.0]),
329         np.array([0.0, 0.0, -1.0]),
330     ]
331
332     tau_dyn_max = np.zeros(nJ)
333
334     for q in qs:
335         for d in directions:
336             d_unit = d / np.linalg.norm(d)
337             a_ee = a_des * d_unit
338             tau_dyn = arm.inertial_torque_effective_mass(q, a_ee, m_eff)
339             tau_dyn_max = np.maximum(tau_dyn_max, np.abs(tau_dyn))
340
341     return {"tau_dyn_max": tau_dyn_max}
342
343
344
345
346
347
348
349
350
351     # =====
352     # Main
353     # =====
354
355     if __name__ == "__main__":
356         arm = FiveDOFArm()
357
358         # Def. joint lints (rad please)
359         # J1: base yaw, ±180°
360         # J2: shoulder pitch, [-90°, +90°]
361

```

Figure 84.g Python Code

```

361     # J2: shoulder pitch, [-90°, +90°]
362     # J3: elbow pitch, [-120°, +120°]
363     # J4: wrist pitch, [-120°, +120°]
364     # J5: wrist roll, ±180°
365     joint_limits = [
366         (-np.pi, np.pi),           # J1
367         (-np.pi/2.0, np.pi/2.0),   # J2
368         (-2.0*np.pi/3.0, 2.0*np.pi/3.0), # J3
369         (-2.0*np.pi/3.0, 2.0*np.pi/3.0), # J4
370         (-np.pi, np.pi),          # J5
371     ]
372
373     # Payload and arm mass assump
374     m_payload = 1.35 # kg (camera)
375     m_arm_est = 17.0 # kg (rough estimate of all links + wrist etc.)
376     gravity_margin = 1.5
377
378     print("== Gravity torque analysis over workspace ==")
379     grav_results = analyze_gravity_over_workspace(
380         arm,
381         m_payload=m_payload,
382         m_arm_est=m_arm_est,
383         joint_limits=joint_limits,
384         samples_per_joints=3,
385         gravity_margin=gravity_margin,
386     )
387
388     print("Effective mass (payload + arm) [kg]:", grav_results["m_eff"])
389     print("Max |tau| from payload only [N·m]:", grav_results["tau_max_payload"])
390     print("Design tau (1.5x payload gravity) [N·m]:", grav_results["tau_design_payload"])
391     print("Max |tau| from effective mass [N·m]:", grav_results["tau_max_eff"])
392     print("Design tau (1.5x effective gravity) [N·m]:", grav_results["tau_design_eff"])
393
394     # Speed req analys
395     speed_des = 1.5 # m/s (end-effector linear speed)
396     print("\n== Speed requirement analysis over workspace ==")
397     speed_results = analyze_speed_requirement_over_workspace(
398         arm,
399         speed_des=speed_des,
400         joint_limits=joint_limits,
401         samples_per_joints=3,
402     )
403
404     qdot_max = speed_results["qdot_max"]
405     qdot_max_deg = qdot_max * 180.0 / np.pi
406
407     print(f"Max |qdot| to achieve {speed_des} m/s in tx, ty, tz [rad/s]:", qdot_max)

```

Figure 84.a Python Code

```

407     print(f"Max |qdot| to achieve {speed_des} m/s in tx, ty, tz [rad/s]:", qdot_max)
408     print(f"Max |qdot| to achieve {speed_des} m/s in tx, ty, tz [deg/s]:", qdot_max_deg)
409
410     # Dynamic torque requirement analysis (approx)
411     m_eff = m_payload + m_arm_est
412     a_des = 3.0 # m/s^2, e.g. to go 0 -> 1.5 m/s in ~0.5 s
413
414     print("\n==== Dynamic torque analysis over workspace (lumped mass) ===")
415     dyn_results = analyze_dynamic_over_workspace(
416         arm,
417         a_des=a_des,
418         m_eff=m_eff,
419         joint_limits=joint_limits,
420         samples_per_joint=3,
421     )
422
423     print(f"Max |\tau_{dynamic}| for a_des = {a_des} m/s^2 [N·m]:",
424         | | dyn_results["tau_dyn_max"])
425

```

Figure 84.h Python Code

Appendix E: Load Analysis

This appendix outlines the load analysis visualization using the SolidWorks Simulation Add-in. The screenshots of the load analysis results are illustrated in Figures 85. a - c

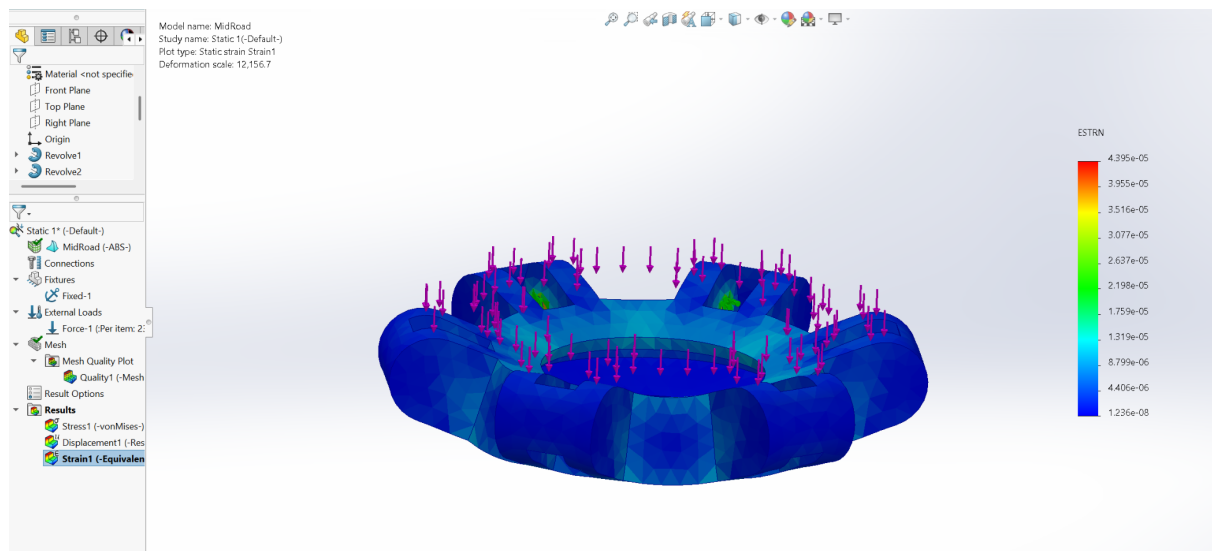


Figure 85.a Load Analysis

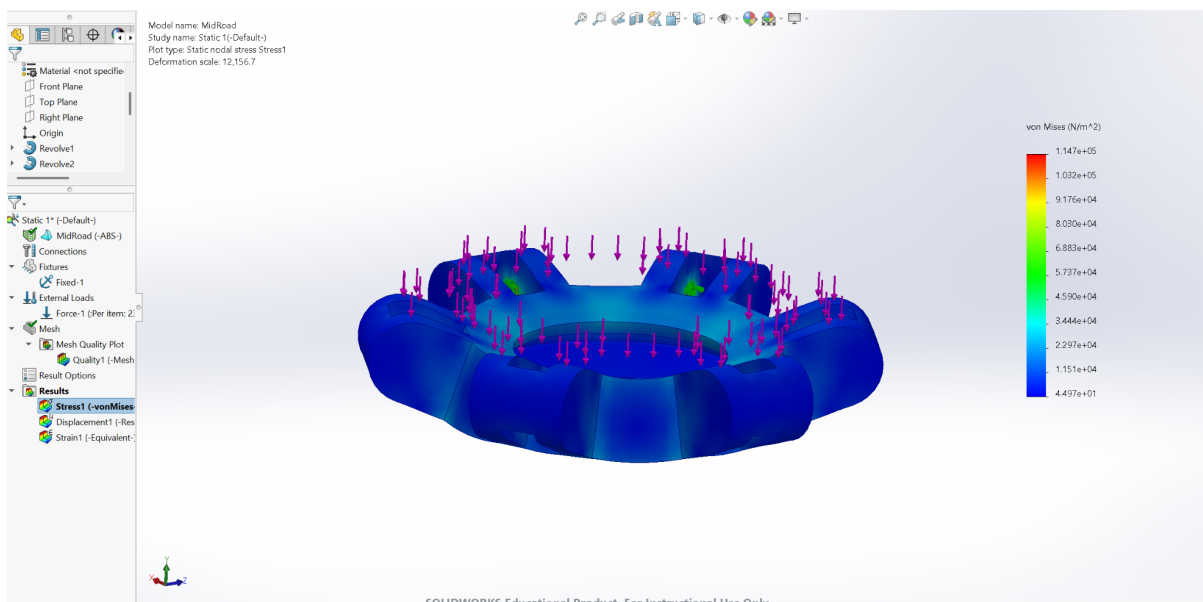


Figure 85.b Load Analysis

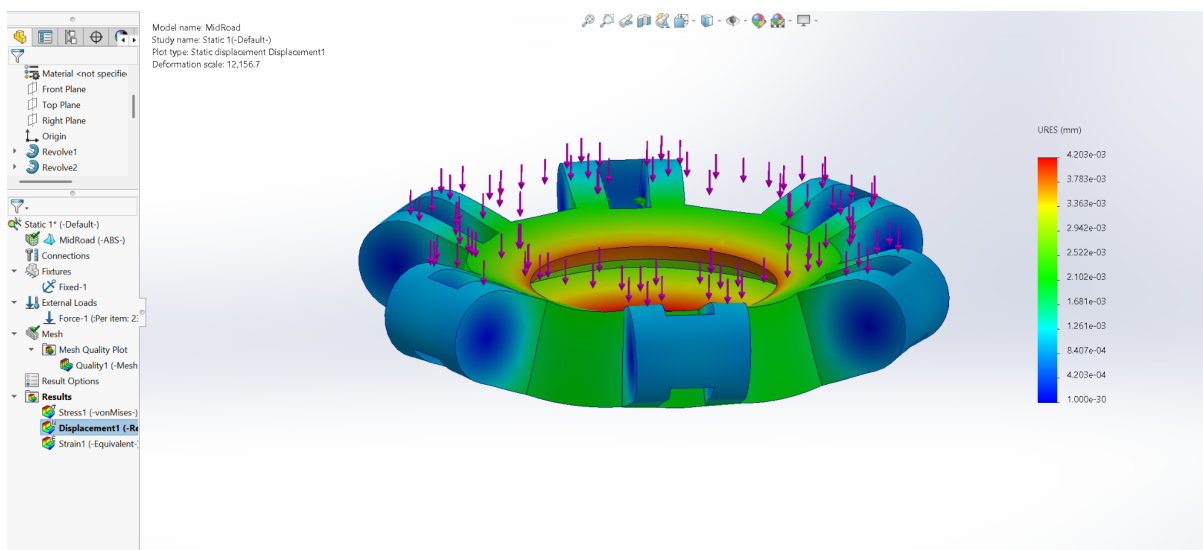


Figure 85.c Load Analysis